The role of bathymetry, wave obliquity and coastal curvature in dune erosion prediction

This page intentionally left blank

The role of bathymetry, wave obliquity and coastal curvature in dune erosion prediction

Proefschrift

ter verkrijging van de graad van doctor
aan de Technische Universiteit Delft,
op gezag van de Rector Magnificus prof.ir. K. C. A. M. Luyben,
voorzitter van het College voor Promoties,
in het openbaar te verdedigen

op dinsdag 7 mei 2013 om 12.30 uur

door

Cornelis DEN HEIJER
civiel ingenieur
geboren te 's-Gravenhage

Dit manuscript is goedgekeurd door de promotoren:
Prof.dr.ir. M. J. F. Stive
Prof.dr.ir. A. J. H. M. Reniers
Copromotor:
Dr.ir. P. H. A. J. M. van Gelder

Samenstelling promotiecommissie:

Rector Magnificus	voorzitter
Prof.dr.ir. M.J.F. Stive	Technische Universiteit Delft, promotor
Prof.dr.ir. A.J.H.M. Reniers	University of Miami (Verenigde Staten), promotor
Dr.ir. P.H.A.J.M. van Gelder	Technische Universiteit Delft, copromotor
Prof.dr.ir. A.W. Heemink	Technische Universiteit Delft
Prof.dr.ir. J.A. Roelvink	UNESCO-IHE Institute for Water Education en Technische Universiteit Delft
Prof.dr. P. Hoekstra	Universiteit Utrecht
Dr.ir. J.S.M. van Thiel de Vries	Deltares
Prof.dr.ir. M. Kok	Technische Universiteit Delft, reservelid

This research was financially supported by the Dutch Technology Foundation STW (10196). Additional financial support was provided by Rijkswaterstaat Waterdienst (WD-4886).

The electronic version of this thesis can be found at `http://repository.tudelft.nl`

Source cover photo: https://beeldbank.rws.nl, Rijkswaterstaat / Joop van Houdt

ISBN 978-1-61499-245-5 (print) ISBN 978-1-61499-246-2 (online)

Publisher
IOS Press BV
Nieuwe Hemweg 6B
1013 BG Amsterdam
The Netherlands
fax: +31 20 687 0019
e-mail: order@iospress.nl

Distributor in the USA and Canada
IOS Press, Inc.
4502 Rachael Manor Drive
Fairfax, VA 22032
USA
fax: +1 703 323 3668
e-mail: iosbooks@iospress.com

Abstract

Low lying coastal areas have always been attractive for people to live, but are also prone to flooding. In The Netherlands, half of the population lives in the coastal area below mean sea level where two-thirds of the economic value is located. Coastal dunes protect the hinterland from flooding as a primary sea defence along the major part of the Dutch coastline. The envisaged protection level of the densely populated and economically valuable areas is one of the world's highest, with a normative failure probability of $\mathcal{O}(1 \times 10^{-5}\,\text{year}^{-1})$. The extreme storm events of this order of magnitude are not observed in (known) recent history. Hence, design, evaluation and maintenance of flood defence systems that can resist these extreme normative conditions rely on models and data extrapolations.

The safety assessment method for the Dutch dune coast includes an empirical dune erosion model (DUROS+) and boundary conditions that represent the normative loading (semi-probabilistic). Every six years, a safety assessment is performed for a series of cross-shore dune profiles along the coast. The prediction skill of the DUROS+ model is limited due to its empirical nature and the omission of the alongshore dimension. The model only takes the upper part of the cross-shore profile explicitly into account and does not account for effects of wave obliquity and coastal curvature. Several dune erosion models have been developed over the last two decades that provide the means to model the dune erosion process in a more comprehensive way. In addition, probabilistic methods have improved and computational power has increased, potentially allowinga probabilistic safety assessment of complex dune areas to be performed.

The aim of this thesis is the reduction of uncertainty in dune erosion prediction, in particular at complex dune coasts, in order to improve dune safety

assessment methods. To that end, state-of-the-art process-based models are employed to study the influence of the cross-shore bathymetry, wave obliquity and coastline curvature on dune erosion. In addition, a Bayesian Network is introduced as a probabilistic method to account for their uncertainties.

Reducing uncertainty in dune erosion prediction is envisaged by deploying a more comprehensive dune erosion modelling approach and by using a tailored probabilistic approach. The development of the dune erosion modelling capabilities concerns the improvement of the 1D cross-shore modelling skills and the expansion of the coverage by providing a 2DH modelling approach for complex areas. The introduction of a more advanced and computationally expensive dune erosion model leads to other requirements for the probabilistic approach. The probabilistic methods presently applied require either relatively large numbers of simulations (Monte Carlo) or continuous limit state functions (FORM). These requirements inhibit the comprehensive process-based modelling of complex dune areas as considered in this thesis. The use of a Bayesian Network model provides a flexible way to overcome the limitations of the probabilistic methods and allows model, field and laboratory data to be combined as well as experts' opinions to estimate the dune erosion rate.

The process-based XBEACH model is deployed in 1D mode to investigate the influence of distinct parts of the cross-shore profile. Intercomparison of model simulations of different cross-shore profiles led to the conclusion that the upper profile part is of major importance for the dune erosion volume under extreme conditions, while the lower profile part only has marginal influence. The DUROS+ model, utilized in the current Dutch dune safety assessment method, takes the upper profile part explicitly into account, but the lower part implicitly. Hence, it is not strictly needed to modify the safety assessment method regarding the cross-shore bathymetry influence, provided that the offshore profile part does not influence the forcing significantly.

The influence of wave obliquity on dune erosion is studied by XBEACH simulations in 2DH for a simplified alongshore uniform coastal stretch with time invariant hydraulic loading. For an incident wave angle of 40°, 30 % more erosion is found with respect to the reference case with shore normal wave direction. The 2DH model shows additional stirring of the sediment, which is related to the wave driven alongshore current enhancing the cross-shore transport.

A 2DH curvilinear XBEACH model is used to investigate the governing phenomena that play a role in dune erosion on a curved coastline. The series of

model simulations with an alongshore uniform bathymetry and time invariant hydraulic loading shows a strong relation between the dune erosion volume and the coastal orientation with respect to the (incident) wave angle. Only a marginal dependency on the coastal radius is found for approximately shore normal waves. At the area along the curved coast where the incident wave angle is 45° with respect to the local coastal orientation, 30 to 50 % more erosion is found relative to the reference case with a straight coast and shore normal wave direction. The alongshore variation in alongshore current, relative wave obliquity, wave height and wave set-up as well as their interactions make the erosion rate primarily spatially varying rather than coastal radius dependent.

A fully probabilistic evaluation (Monte Carlo) of the failure probability of the first dune row is carried out for the major part of the Dutch dune coast where a 1D dune erosion model (DUROS+) is applicable. In nearly the full study area, the first dune row meets the normative safety level. At the limited number of locations where first dune row's failure probability exceeds the normative safety level, either these areas are not part of the primary sea defence or secondary dune bodies are present landward.

As an alternative to the probabilistic methods Monte Carlo and First Order Reliability Method (FORM), a Bayesian Network is introduced that estimates the relative dune erosion due to the effects of wave obliquity and coastal curvature, with respect to a reference case with a straight coast and shore normal wave direction. The Bayesian Network uses the XBEACH model results concerning wave obliquity and coastal curvature. The Bayesian Network has been utilised to evaluate the failure probability of the first dune row, of the major part of the Dutch dune coast, with the effects of wave obliquity and coastal curvature included. The failure probabilities are a factor $\mathcal{O}(10)$ higher for the major part of the study area, with respect to the reference without wave obliquity and coastal curvature effects.

This thesis stresses the importance of wave obliquity and coastal curvature for the assessment of dune safety against flooding. The effects of these phenomena are investigated based on 2DH XBEACH model simulations in a schematised configuration and show that wave obliquity and coastal curvature can lead to significantly larger dune erosion volumes and thus larger dune failure probabilities. Hence, there is a need to include the effects of wave obliquity and coastal curvature into future versions of the dune safety assessment method, combined with proper validation and a tailored probabilistic method.

Samenvatting

Titel: *De rol van bodemligging, scheve golfinval en kustkromming in duinafslag voorspelling*

Laaggelegen kustgebieden zijn altijd aantrekkelijk voor mensen om te wonen, maar zijn ook gevoelig voor overstromingen. In Nederland woont de helft van de bevolking in het kustgebied onder gemiddeld zeeniveau, waar tweederde van de economische waarde zich bevindt. Duinen beschermen als een primaire zeewering het achterland tegen overstromingen langs het grootste deel van de Nederlandse kust. Het beoogde beschermingsniveau van de dichtbevolkte en economisch waardevolle gebieden is een van de hoogste in de wereld, met een normatieve faalkans van $\mathcal{O}(1 \times 10^{-5}\,\text{jaar}^{-1})$. De extreme stormen van deze orde van grootte zijn niet waargenomen in de (bekende) recente geschiedenis. Daarom moet in het ontwerp, de toetsing en het onderhoud van waterkeringen, die bestand moeten zijn tegen deze extreme maatgevende omstandigheden, vertrouwd worden op modellen en extrapolaties.

De toetsingsmethode voor de Nederlandse duinenkust omvat een empirisch duinafslag model (DUROS+) en randvoorwaarden die de normatieve condities (semi-probabilistische) representeren. Om de zes jaar wordt een veiligheidstoetsing uitgevoerd voor een reeks van duin dwarsprofielen langs de kust. De betrouwbaarheid van het DUROS+ model is beperkt, als gevolg van het empirische karakter en het ontbreken van de kustlangse dimensie. Het model neemt alleen het bovenste deel van het dwarsprofiel expliciet mee en houdt geen rekening met effecten van golfhoek en kustkromming. In de afgelopen twee decennia zijn verschillende duinafslag modellen ontwikkeld die de mogelijkheid bieden om de duin processen op een vollediger manier te modelleren. Daarnaast zijn probabilistische methoden verbeterd en is de rekencapaciteit toegenomen, waardoor het mogelijk wordt om een probabilis-

tische veiligheidsbeoordeling van complexe duingebieden uit te voeren.

Het doel van dit proefschrift is om de onzekerheden in duinafslag voorspelling te reduceren, in het bijzonder bij complexe duinenkusten, om daarmee duinveiligheidstoetsing te kunnen verbeteren. Hiervoor zijn state-of-the-art proces-gebaseerde modellen gebruikt om de invloed van het dwarsprofiel, de golfhoek en kustkromming op duinafslag te bestuderen. Daarnaast wordt een Bayesiaans Netwerk geïntroduceerd als probabilistische methode om de bijbehorende onzekerheden in rekening te brengen.

Het verkleinen van onzekerheden in duinafslagvoorspelling wordt nagestreefd door het inzetten van een meer omvattende duinafslag model en door gebruik te maken van een daarop toegesneden probabilistische aanpak. De ontwikkeling van de duinafslag modellering betreft de verbetering van de nauwkeurigheid van 1D kustdwarse modellering en de uitbreiding van het toepassingsgebied door middel van een 2DH model aanpak voor complexe gebieden. De introductie van een meer geavanceerd en rekenintensief duinafslagmodel stelt andere eisen aan de probabilistische aanpak. De probabilistische methoden die momenteel worden toegepast vereisen ofwel relatief grote aantallen simulaties (Monte Carlo) of continue grenstoestand functies (FORM). Deze eisen bemoeilijken de uitgebreide procesmatige modellering van complexe duingebieden, zoals deze in dit proefschrift wordt toegepast. Het gebruik van een Bayesiaans Netwerk model biedt een flexibele manier om de beperkingen van de eerder genoemde probabilistische methoden op te lossen en maakt het mogelijk om model-, veld- en laboratoriumdata, alsmede inzichten van deskundigen, te combineren om de mate van duinafslag te schatten.

Het proces-gebaseerde XBEACH model is gebruikt in 1D modus om de invloed van verschillende delen van het dwarsprofiel te onderzoeken. Onderlinge vergelijking van modelsimulaties van verschillende dwarsprofielen leidde tot de conclusie dat het bovenste profieldeel van groot belang is voor het duinafslag volume onder extreme omstandigheden, terwijl het onderste profieldeel slechts marginale invloed heeft. Het DUROS+ model, gebruikt in de huidige Nederlandse duin veiligheidstoetsingsmethode, brengt het bovenste profieldeel expliciet in rekening, maar het onderste gedeelte impliciet. Daarom is het niet strikt nodig om de veiligheidstoetsingsmethode aan te passen betreffende de dwarsprofielinvloed, mits het offshore profieldeel de hydraulische forcering niet significant beïnvloedt.

De invloed van golfhoek op duinafslag is bestudeerd door XBEACH simulaties

in 2DH voor een vereenvoudigde kustlangs uniforme kust met tijdsinvariante hydraulische belasting. Voor een golfinvalshoek van 40°, wordt 30 procent meer erosie gevonden ten opzichte van het referentie geval met de kustnormale golfrichting. Het 2DH model toont extra opwoeling van sediment, die gerelateerd is aan de golfgedreven kustlangse stroming, waardoor het dwarstransport versterkt wordt.

Een 2DH curvilineair XBEACH model is gebruikt om de maatgevende fenomenen die een rol spelen bij duinafslag langs een gekromde kustlijn te onderzoeken. De reeks modelsimulaties met een kustlangs uniforme bodem en tijdsinvariante hydraulische belasting toont een sterke relatie tussen het duinafslagvolume en de kust oriëntatie ten opzichte van de (invallende) golfhoek. Slechts een marginale afhankelijkheid van de kustboogstraal wordt gevonden voor ongeveer loodrecht invallende golven. In het gebied langs de gebogen kust waar de invallende golfhoek 45° ten opzichte van de lokale kust oriëntatie is, wordt 30 tot 50 procent meer erosie gevonden ten opzichte van het referentiegeval met een rechte kust en loodrecht invallende golven. De variatie van kustlangse stroming in langsrichting, relatieve golfhoek, golfhoogte en golf opzet alsmede interacties daartussen, maken de mate van duinafslag voornamelijk ruimtelijk variërend in plaats van boogstraal afhankelijk.

Een volledig probabilistische evaluatie (Monte Carlo) van de faalkans van de eerste duinenrij is uitgevoerd voor het grootste deel van de Nederlandse duinenkust, waar een 1D duinafslag model (DUROS+) toepasbaar is. In bijna het volledige studiegebied voldoet de eerste duinenrij aan het normatieve veiligheidsniveau. Op het beperkte aantal locaties waar de faalkans van de eerste duinenrij groter is dan het normatieve veiligheidsniveau, is er ofwel sprake van een gebied dat geen deel uitmaakt van de primaire zeewering of zijn er landwaarts secundaire duinenrijen aanwezig.

Als alternatief voor de probabilistische methoden Monte Carlo en FORM wordt een Bayesiaans Netwerk geïntroduceerd dat de relatieve duinafslag schat als gevolg van scheve golfinval en kustkromming, ten opzichte van een referentie geval met een rechte kust en loodrechte golfrichting. Het Bayesiaanse Netwerk maakt gebruik van de XBEACH modelresultaten met betrekking tot golfhoek en kustkromming. Het Bayesiaanse Netwerk is gebruikt om de faalkans van de eerste duinenrij te evalueren, van het grootste deel van de Nederlandse duinenkust, met inbegrip van de effecten van de golfhoek en kustkromming. De faalkansen zijn een factor $\mathcal{O}(10)$ hoger voor het grootste deel van het studiegebied, ten opzichte van de referentie, zonder

golfhoek- en kustkrommingseffecten.

Dit proefschrift benadrukt het belang van golfhoek en kustkromming voor de beoordeling van duinveiligheid tegen overstromingen. De effecten van deze verschijnselen zijn onderzocht op basis van 2DH XBEACH modelsimulaties in een geschematiseerde configuratie en laten zien dat golfhoek en kustkromming kunnen leiden tot aanzienlijk grotere duinafslag volumes en dus grotere duin faalkansen. Het is daarom noodzakelijk om de effecten van golfhoek en kustkromming in toekomstige versies van de toetsmethode van de veiligheid van duinen mee te nemen, in combinatie met goede validatie en een toegesneden probabilistische methode.

Contents

Chapter 1

Introduction

1.1 Background

Coastal areas have always been attractive to live in, because of the soil fertility and the easy accessibility of the ocean for transport and fishing purposes. On the other hand, coastal waters are a serious threat for flooding, especially when the hinterland is below sea level. In The Netherlands, half of the population and over two-third of the economic value is in coastal areas below mean sea level. Along a large part of the Dutch coast (254 km; Min V&W, 1989), dunes act as a primary defence against flooding of the hinterland. The remaining primary defences are mainly dikes, dams and storm surge barriers. To ensure the protection of the densely populated and economic valuable hinterland, one of the world's smallest failure probabilities ($\mathcal{O}(1 \times 10^{-4}\,\text{year}^{-1})$)[1] are prescribed by law (Figure 1.1). These small probabilities correspond to extreme storm events which have not been observed in (known) recent history (Baart et al., 2011). Therefore, design and maintenance of flood defence systems that can withstand these extreme storm conditions mainly rely on models and data extrapolations. To control the safety of the hinterland, a periodic (six yearly) safety assessment for all primary flood defences is prescribed by law.

The Dutch safety assessment method for dunes (ENW, 2007), currently in

[1] For dunes, a failure probability of $1 \times 10^{-5}\,\text{year}^{-1}$ is used, in order to end up with a similar safety level as dikes. Dikes are supposed to have some 'rest strength' after breaching whereas dunes are expected to either withstand the loading or totally fail.

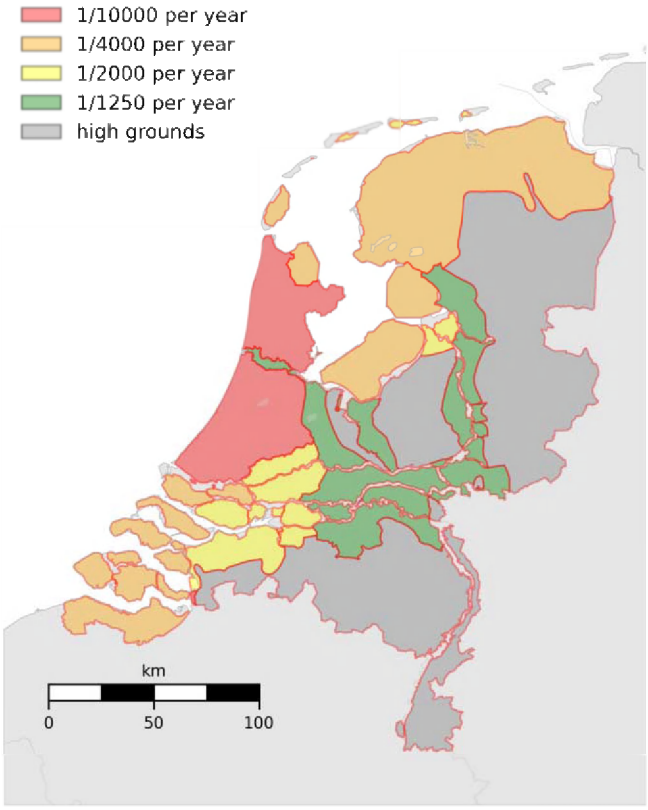

Figure 1.1: Safety standards for dike ring areas in The Netherlands

force, consists of hydraulic boundary conditions (surge level and waves) and a dune erosion model. The hydraulic boundary conditions represent the normative loading. The dune erosion model evaluates the strength of a dune and estimates its response to the normative hydraulic loading conditions. A dune cross-section is considered sufficiently safe if the estimated response does not result in failure of the water defence function of the dune. The safety assessment method is a simplification of an extensive probabilistic investigation that has been carried out at a number of locations along the coast.

This fully probabilistic approach consists of three components: 1) a hydraulic loading model, 2) a probabilistic method and 3) a dune erosion model. The hydraulic loading model derives probability distributions of waves and surge using statistical methods and time series of measurement data. The probabilistic method serves as an interface, by converting the probability distributions into boundary conditions for individual storm events that can be handled by the dune erosion model. The dune erosion model simulates individual storm events, based on pre-storm bathymetry information, grain size distributions and hydraulic boundary conditions, resulting in a post-storm bathymetry.

1.2 Dune erosion

Dune erosion is the relatively dynamic process of cross-shore sediment transport of dune sand to the beach and foreshore on the time scale of a storm ($\mathcal{O}(hours)$). The dune erosion process is driven by storm conditions that are mainly described by surge and severe wave attack. The cross-shore profile changes rapidly during a storm event, because storm conditions are striving for a cross-shore profile that dynamically adapts to the forcing conditions such that energy dissipation per unit volume in the surfzone becomes spatially more uniform and significantly differs from the pre-storm profile. The eroded sediment is deposited on the beach and foreshore (Figure 1.2), presuming that no significant losses occur in offshore or lateral direction. As the profile adapts to the storm conditions, the response rate decreases towards a new equilibrium, but the time scale of a storm is usually too short to reach this equilibrium.

In stable coastal sections, eroded dunes completely recover due to wave and wind action during normal conditions. The sediment from the foreshore is

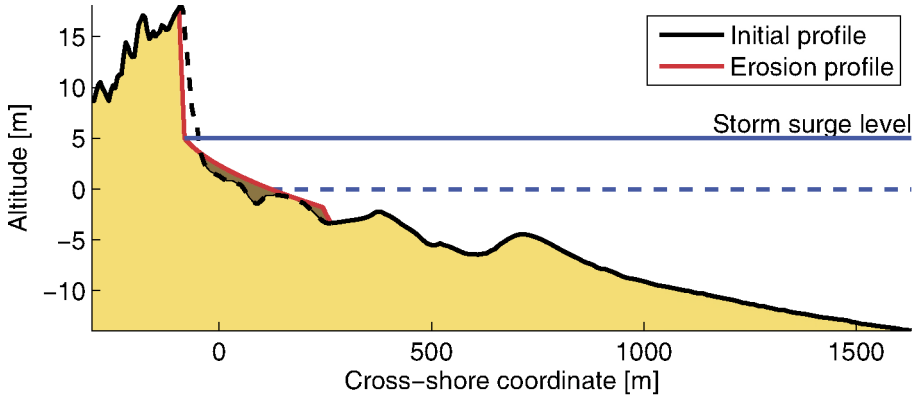

Figure 1.2: Principle of dune erosion.

transported by waves towards the intertidal beach. Subsequently, aeolian transport picks up the sand from the beach and moves it towards the dunes, leading to dune recovery. By this mechanism the dune erosion process is reversible and is part of the natural dynamics of a dune coast.

Structural erosion is a gradual retreat of the coastline due to alongshore gradients in sediment transport[2]. Although dune erosion in itself is not structural, a dune erosion event can cause a temporarily amplification of the structural erosion. The sediment eroded from the dune and deposited on the beach and foreshore feeds the permanent loss from the profile by alongshore transport gradients. By this mechanism, dune erosion is turned into a (partially) irreversible process, at structural eroding coastal sections.

The process of dune erosion gets particularly complicated when cross-shore processes are influenced by an alongshore flow and/or water level gradient. The alongshore flow can be generated by the tide, oblique incoming waves and an alongshore water level gradient. An alternating alongshore flow is generated by the tide. At inlets this can be amplified due to flow contraction and filling and emptying of the tidal basin. Inlets generally coincide with curved coastlines at both sides, leading to even more complexity. The curvature leads to an alongshore sediment transport gradient, acting as a sink to the cross-shore sediment balance. The alongshore flow can influence the

[2]It is assumed that the type of coast considered in this thesis has a negligible net sediment loss or gain due to cross-shore sinks or sources.

stirring of the sediment. A water level gradient can originate during storm conditions at areas where a dike section is adjacent to dune area. Alongshore difference in beach and foreshore development can locally generate alongshore flow, influencing the dune erosion process (De Vries, 2011).

1.3 Problem definition

The prediction skill of the current Dutch dune safety assessment method (ENW, 2007) is limited, due to both the empirical nature of the dune erosion model and the application in the extreme range, relying on extreme value statistics. In addition, the applied dune erosion model (DUROS+; Vellinga, 1984; Van Gent et al., 2008) only takes the cross-shore dimension into account, which means that the model is actually only valid for alongshore uniform sandy dune coasts. New developments in dune erosion models allow for more accurate process-based modelling (Van Thiel de Vries, 2009) and including the alongshore dimension (Roelvink et al., 2009). However, to effectively apply these computationally more expensive dune erosion model approaches in the safety assessment, the underlying probabilistic representation has to be reconsidered.

Over the last three decades several dune erosion models have been developed. The first safety assessment guideline (TAW, 1984) prescribed the empirical DUROS model (Vellinga, 1984). Later on, when the importance of the wave period for dune erosion was recognised, Van Gent et al. (2008) extended this model with the wave period effect (DUROS+). D++ (Deltares, 2010) is a recently developed empirical model, closely related to DUROS+, which allows for hydraulic boundary conditions at shallower water. The latter model thus also covers areas with shoals in front of the coast, which cannot be assessed with DUROS+. DUROSTA (Steetzel, 1993) is developed in the early 1990s with the purpose to investigate the effect of alongshore currents and current gradients on the amount of dune erosion. It is a 2DV (cross-shore) time-dependent model that has capabilities to approximate some alongshore phenomena such as alongshore currents, wave obliquity and coastal curvature (quasi 3D). These capabilities make DUROSTA potentially useful to cover the major part of the Dutch dune coast. XBEACH (Roelvink et al., 2009) is a 2DH numerical modelling approach to assess the natural coastal response during time-varying storm and hurricane conditions. It aims at describing the processes relevant for the different storm regimes as defined by Sallenger

(2000): swash, collision (dune erosion), overwash and inundation. The wide ranging capabilities including complex 2DH cases make XBEACH potentially applicable to the whole Dutch dune coast.

To effectively benefit from a more comprehensive dune erosion model in the next generation dune safety assessment methodology, the probabilistic methods and the stochastic variables need to be reconsidered. The selection of the probabilistic method should depend on the computational cost and stability of the dune erosion simulations. Straightforward methods like Monte Carlo require relatively large numbers of simulations, especially for small failure probabilities. Various smart Monte Carlo variants are available that allow for significant reduction of the number of required simulations (Fishman, 1996). Apart from the Monte Carlo methods, the first-order reliability method (FORM; Hasofer and Lind, 1974) is an efficient alternative, provided that the limit state function is continuous. Discontinuity can occur when shifting from one regime (Sallenger, 2000) to another, e.g. from collision to overwash, or when the model contains processes that behave irregular. As an alternative to these model driven methods, a Bayesian Network can combine simulation and observation data (both field and laboratory) to make predictions in terms of a probability distribution. The amount of underlying data and the available evidence is, among others, determining the confidence bounds of the resulting probability distribution. When having a sufficiently large dataset available, consisting of measurements and/or simulations, a Bayesian Network approach can be beneficial. The governing processes, their uncertainty and their sensitivity must be guiding in the selection of the stochastic variables. These properties are related to the dune erosion model under concern.

1.4 Aim

This thesis aims at reducing uncertainty in dune erosion predictions, in particular at complex dune coasts, in order to improve the assessment method for dune safety against flooding. To that end, state-of-the-art process-based dune erosion models are employed to further investigate issues insufficiently covered by the current Dutch safety assessment method. The influence of cross-shore bathymetry, coastal curvature and incident wave angle are the main focus in this thesis. In addition, a Bayesian Network approach is introduced to create a practical framework for the inclusion of additional aspects and uncertainties to the safety assessment method for complex coasts.

1.5 Approach

This section outlines the approach of this thesis following the structure as presented in Figure 1.3.

Chapter 2 elaborates on the problem definition by discussing the current Dutch safety assessment method for dunes. In addition, an inventory of the relevant processes for dune erosion is made. The dune erosion model in the current safety assessment method includes some of these processes. A number of other processes can be accounted for by alternative models. Chapter 2 compares the relevant dune erosion models, in terms of their theoretical capabilities. Related to their capabilities, the applicability (coverage) of the models along the Dutch coast is compared. Finally, the chapter discusses various probabilistic methods that are potentially useful for dune safety assessment.

In Chapter 3, the selected dune erosion models are evaluated, inter-compared and limitations are explored based on sensitivity to determining variables and practical capability of modelling complex coasts. The consistency between the models is discussed for the main variables which they have in common. In addition, special attention is paid to the influences of bathymetry, coastal curvature and wave obliquity.

Chapter 4 describes in a probabilistic analysis for a reference case, the implication of including wave obliquity and coastal curvature. As a first step the present Dutch approach is adopted, which is based on the DUROS+ model and the FORM method, as a reference. Next, a Bayesian Network is introduced that aims at reproduction of the DUROS+ dune erosion estimates with comparable performance to illustrate the capabilities of this alternative approach. Finally, the additional effects of wave obliquity and coastal curvature are included, in both the FORM and Bayesian Network approach, based on estimates by process-based dune erosion models. The updated insights are compared to the reference framework.

A practical application is presented in Chapter 5. A reference framework is created by applying the 'present approach' to the major part of the Dutch sandy coast, to estimate the probability of failure of the first dune row. The failure probability of this first line of defence is an upper boundary for the inundation probability of the hinterland. The present approach is defined here as the stochastic variables as presently established combined with the DUROS+ dune erosion model. The Monte Carlo method is adopted here as a reliability method. As an alternative, the additional influences of wave obliquity and

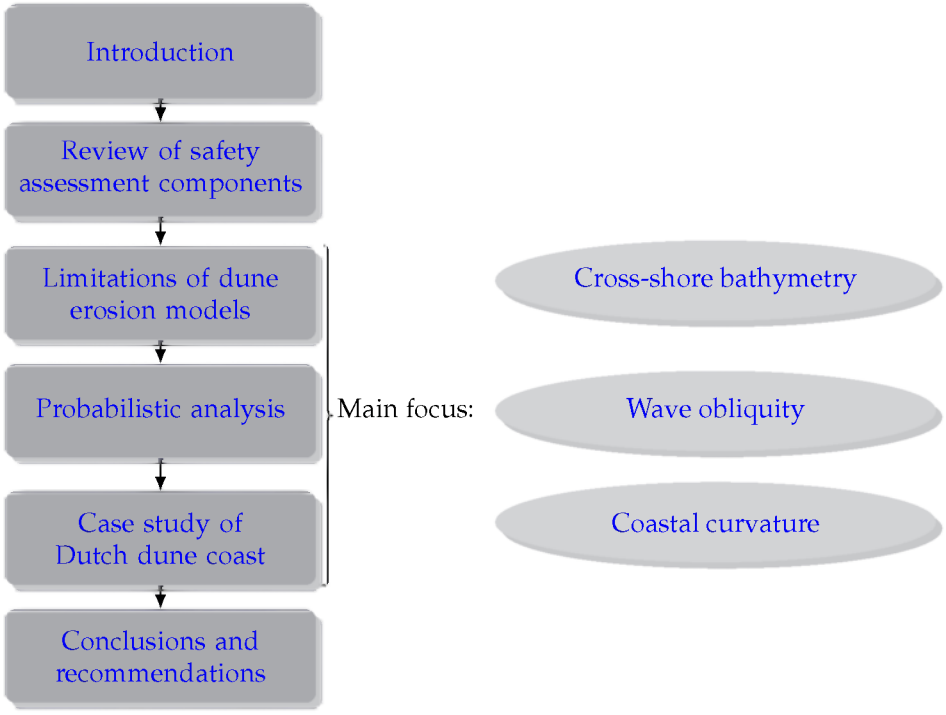

Figure 1.3: Structure of the thesis.

coastal curvature are included. Here a combination of the Monte Carlo method and the Bayesian Network is used to again estimate the failure probability of the first dune row. Comparison with the reference provides insight in the potential impact of wave obliquity and coastal curvature on the anticipated safety level.

The thesis ends with conclusions and recommendations from this study in Chapter 6.

Chapter 2

Review of safety assessment components

This chapter discusses the Dutch dune safety assessment procedure and the underlying models, in order to identify its possibilities but also its limitations. The procedure and the various components of dune safety assessment are described. Relevant aspects and issues when modelling dune erosion as well as an inventory of the governing processes and quantities are given. This facilitates the comparison of dune erosion models by considering whether specific processes are covered by a model and in what way. A number of relevant dune erosion models, their intercomparison and applicability (coverage) along the Dutch coast is evaluated based on their theoretical capabilities. Finally, this chapter discusses a number of relevant probabilistic methods.

2.1 Safety assessment

2.1.1 Strategy

Management of coastal dunes involves balancing the interests of multiple user functions provided by dune areas. A dune area provides valuable ecological

habitat for a wide range of flora and fauna, it is a popular area for recreation and it provides flood protection for the hinterland. Clearly a dune area preferably provides all of the above-mentioned services simultaneously. Especially for low lying countries (such as The Netherlands), the flood protection function is usually treated with priority.

An economically optimised flood defence system provides a maximal safety level at minimal costs (Starr, 1969; Vrijling, 2001). In order to find this optimum, three issues need to be addressed. First of all, the failure probability of the flood protection system needs to be assessable. In terms of dunes, this means that a method to quantitatively assess the resilience of a dune area is required. Second, the expected damage in case of failure should be estimated. This could be approximated, in a worst case scenario, by the total economic value of the dune area and the hinterland protected by it. The reasoning behind it is that if the dunes fail, serious flooding is assumed to totally destroy the hinterland. Third, insight is required in the investment costs associated with enhancing the level of safety locally as well as regionally (construction as well as maintenance costs). Combining these in a cost-benefit analysis provides a rational desired level of safety. The actual decision on the desired safety level is a political issue, since costs and benefits may be valued differently by different stakeholders (Vrijling, 2001).

A practical application of the above described approach is the development of the normative safety level presently used for the Dutch coast. It is based on the evaluation of the probability of failure, the cost of maintenance and the cost of failure in terms of damage to economic value present in the hinterland (Van Dantzig, 1956). This normative safety level was proposed by the Delta Committee (1960) following the 1953 storm surge disaster (Rijkswaterstaat and KNMI, 1961). An overview of the safety levels for the The Netherlands is given in Figure 1.1. The densely populated Holland coast should be able to withstand hydraulic boundary conditions with an exceedance probability of $1 \times 10^{-4}\,\text{year}^{-1}$; the Wadden area $5 \times 10^{-4}\,\text{year}^{-1}$ with the exception of the island Texel ($2.5 \times 10^{-4}\,\text{year}^{-1}$); the Delta area $2.5 \times 10^{-4}\,\text{year}^{-1}$. These safety standards are based on an econometric analysis. Inundation of the hinterland is assumed to result in total loss of properties, but fatalities and social disruption are not taken into account. The Delta Committee (1960) explicitly intended the flood defences to be able to (just) withstand the design conditions. The exceedance probabilities of the design conditions are therefore not the failure probabilities of the defence. Working Group 10; Delta Committee (1954) recommended to set the maximum failure probability at a

factor of 10 smaller than the exceedance probability of the design level. In line with this recommendation, we use a failure probability of 1×10^{-5} year^{-1}, for the Holland coast, in this thesis.

The management of the safety against flooding is implemented in The Netherlands by a periodic safety evaluation. The results of that evaluation are decisive in strengthening measures to be taken.

2.1.2 Implementation

As mentioned in Section 1.1, a probabilistic dune safety assessment includes three components: 1) a hydraulic loading model, 2) a probabilistic method and 3) a dune erosion model. To provide and maintain the stringent safety levels against flooding, in The Netherlands a six-yearly safety assessment is established and prescribed by law. For each periodic safety assessment, guidelines (VTV2006, 2007) and hydraulic boundary conditions (HR2006, 2007) are provided. More extensive guidelines, specifically focussed on dunes are provided by ENW (2007). This section describes the main features of the Dutch dune safety assessment.

Both the hydraulic loading model and the probabilistic method are captured by the guidelines (VTV2006, 2007) and hydraulic boundary conditions (HR2006, 2007). Practically, the actual assessment is a deterministic evaluation to check whether a coastal cross-section is able to withstand the pre-defined boundary conditions. The DUROS+ model plays a major role in the dune safety assessment. The model estimates the cross-shore profile change by a storm event and assumes alongshore uniformity. In addition, the model is only applicable to sandy areas, excluding structures like dune revetments and seawalls. Dune erosion calculations are performed for cross-shore transects along the coast, with an alongshore spacing of about 250 m, based on the annual bathymetries over the last 15 years. The position of the dune face is the key figure from the resulting post-storm profile in the safety assessment. Based on the linear trend through the set of 15 dune face positions, the judgement is established. If the trend line exceeds the landward threshold within the evaluation period of six year, the transect is labelled as non-save.

While the standard evaluation procedure is rather straightforward, the assumptions underlying the DUROS+ model limit the validity of the method along the coast. Hence, specific procedures are prescribed, or at least special attention is paid, to complex dune areas with the following features:

- Alongshore transport gradients, i.e. curved coastlines
- Hard (structural) elements in the cross-shore profile
- Alongshore transitions from hard structures to sandy dunes
- Deep channels relatively close to the shoreline
- More than one dune row, in the sense that the first dune row is not sufficient to withstand the design conditions

The 1D approach in DUROS+ and the separate treatment of the complex dune areas leads to alongshore discontinuities in the anticipated dune failure probability. In order to come to a more integrated approach, covering a variety of dune areas, a clear picture of all features that potentially play a role is required.

2.2 Inventory of relevant factors controlling dune erosion

Proper assessment of dune safety against flooding requires a suitable dune erosion model that includes all relevant features of the processes involved. Dune erosion is basically considered as a purely cross-shore process. Complex areas can however turn the alongshore processes into additional non-negligible contributions. Thus, the local situation and the processes involved determine the requirements for the dune erosion model to be applied. This section gives an overview of factors that potentially play a role. Each of these factors is briefly discussed.

Water level / storm surge The water level is the combination of astronomical tide and storm surge. A sufficiently high water level is a prerequisite for wave impact on dunes. Provided that the water level is sufficient to cause dune erosion, it has a major influence on the rate of dune erosion (Van de Graaff, 1986).

Wave height In addition to a sufficiently high water level, the waves are another prerequisite for dune erosion. The wave height determines the wave energy. Near the shore, the energy is dissipated due to wave breaking. Wave dissipation leads to wave set-up and subsequently a cross-shore return current (undertow). Sediment is stirred up by the orbital motion, breaking induced

turbulence and the undertow. The undertow is responsible for sediment transport in offshore direction.

Wave obliquity In case of wave obliquity, a wave driven alongshore current is generated. The magnitude of the alongshore current is dependent on the wave height, period and angle. In addition, the wave energy per running meter coastline becomes smaller for larger off normal wave angles. Assuming a straight coast, no alongshore transport gradient is present. The alongshore current can facilitate the stirring of the sediment, but at the same time the undertow becomes weaker because of the reduced mass flux per running meter coastline. The resulting influence of wave obliquity on dune erosion is not clear beforehand, but the relevance of the alongshore dimension is obvious. Falqués (2006) shows that the wave angles along the Dutch coast are mostly oblique.

Alongshore current Alongshore currents can be tide and/or wave driven. When alongshore and cross-shore are considered separately, the alongshore current is supposed to not influence the dune response as long as no gradients are involved. However, the alongshore flow can facilitate stirring of the sediment and consequently lead to higher suspended sediment concentrations. These higher sediment concentrations can increase the offshore transport by the undertow. In case of a combination of tide and wave driven alongshore currents, a periodic amplification and (partly) cancelling out can play a role.

Directional spreading Dune erosion, being schematised as a purely cross-shore process, has been mainly investigated based on flume experiments. In nature, however, waves are directionally spread. Hence, dune erosion rates are hypothesised to be reduced. Refraction of the short waves will reduce the energy over a wave crest. In addition, the short to long wave energy transfer is expected to be reduced (Reniers et al., 2002).

Wave period Analysis of wave data from historic storms by De Ronde et al. (1995) and Roskam and Hoekema (1996) indicated that the wave period during normative conditions would be larger than the previously assumed maximum peak wave period of 12 s. Small-scale ($n_d = 30$ and $n_d = 40$) and large-scale ($n_d = 6$) dune erosion experiments conducted afterwards, showed a significant increase in dune erosion for larger peak wave periods in the range of 10 s to 18 s

(Coeveld and de Vroeg, 2004; Den Heijer, 2005; Van Gent et al., 2008). Large scale dune experiments, performed by Van Gent et al. (2008), showed that a larger wave period allows more wave energy to reach the dune and results in significantly larger near-bed sediment concentrations in the shallow area (Van Thiel de Vries et al., 2008). Based on these experimental results, Van Gent et al. (2008) updated the empirical dune erosion model of Vellinga (1986) to account for the wave period.

Long waves Large scale dune erosion experiments and field observations indicated that near dune hydrodynamics during dissipative storm conditions are dominated by wave group generated long waves (Van Thiel de Vries et al., 2008). Applying the surf beat modelling concept (Roelvink, 1993), measured time series of hydrodynamics could be accurately reproduced and explained by simulated long-wave hydrodynamics (Van Thiel de Vries, 2009; Van Thiel de Vries et al., 2006).

Bathymetry The bathymetry is determinant for wave propagation, dissipation and consequently wave driven currents. In this way the bathymetry influences the wave attack that the dune experiences and transport capacity of the water. Alongshore variability and coastline curvature, being a separate topic, are also important in this respect.

Topography The topography describes the dune shape and with that the dune volume. The available dune volume, above a certain level and per running meter of coast, can be considered as an important resilience indicator. In addition to the volume, the presence of one or more alongshore closed lines of defence is relevant. In case of two dune rows where in the landward row one or more gaps occur, failure of the first dune row can lead to inundation of the hinterland via a neighbouring gap in the second dune row.

Grain size The grain size plays an important role for sediment transport, and consequently for dune erosion. Smaller grain sizes lead to higher concentrations of suspended sediment (Van Rijn, 2007) and thus a larger offshore transport capacity which increases dune erosion. In addition, there is a relation between the grain size and the coastal profile steepness. Finer grains will allow

milder slopes whereas coarser grains allow steeper slopes. The steepness of the profile influences the wave transformation and so the dune erosion.

Dune face slumping One of the key phenomena of the dune erosion processes is the episodic slumping of the dune face. The wave attack on the dune face and the alternating flooding and drying of the zone around the waterline lead to geotechnical instability. A slump event will instantaneously provide a hump of sediment to the shallow water zone just in front of the dune. The long wave swash will then gradually transport the sediment in offshore direction and distribute it over the cross-shore profile. The slumping process is closely related to the geotechnical properties of the dune face and its response to the dynamic flooding and drying on a long wave time scale, but is not fully understood yet. Note that the slumping process, due to its episodic nature, is by definition not continuous in time (Palmsten and Holman, 2012).

Storm duration Storms are the common cause of energetic hydrodynamic conditions, extreme water levels and waves, potentially leading to dune erosion. The storm characteristics, such as duration, wind speed and direction, together define the magnitude of the storm. The duration of the storm and the phase with respect to the tide largely determine the surge and with that the water level hydrograph and so the dune response.

Coastal curvature Coastal curvature implies an alongshore varying sediment transport i.e. an alongshore transport gradient. Interaction between cross-shore and alongshore processes is not negligible in this case. If the cross-shore and alongshore components are considered separately, at least a sink (or source) term should be added in the cross-shore sediment load. More likely, the interactions between these components should be taken into account explicitly, requiring a 2DH approach. This thesis only considers convex curved coastlines, since those are likely to increase the dune erosion rate. Since strongly curved coastlines often occur near inlets, not only the wave driven alongshore current and its gradient but also tidal currents can be of importance. The residual effect of wave and tidal driven currents on dune erosion at curved coasts is not taken into account in this thesis.

Structures A distinction can be made between structures that mainly influence the cross-shore processes and those that also include the alongshore dimension. The first type includes dune revetments and seawalls. These types of structures limit or prevent the supply of sediment by the dune towards the subaqueous area. Since the transport capacity of the water is not significantly different, a scour hole will develop in front of the structure. As long as the scour hole does not reach the toe of the structure and the structure is able to withstand the wave attack, there is no serious problem. Dune-dike connections do typically include the alongshore dimension. Due to the alongshore variation in cross-shore profile, which initially exists or develops in time as a result of different response, wave set-up variation and alongshore current gradients influence the erosion process locally (De Vries, 2011).

2.3 Dune erosion models

This section introduces the dune erosion models that are applied in this thesis and highlights their theoretical capabilities and limitations. The nature of a dune erosion model largely determines the type of cases it can be used for. Distinctions can be made between empirical and process-based models on the one hand, and cross-shore (1D/2DV) and combined cross-shore/alongshore (2DH) models on the other hand.

For morphological modelling, the spatial dimensionality and scales as well as the time scales are important (De Vriend, 1991). In essence, dune erosion is a cross-shore process on a storm time scale, $\mathcal{O}(\text{hours})$. In areas where significant alongshore variations occur, such as curved coastlines, a 2DH modelling approach is recommended. The spatial extent of the model also depends on the nature of the model. A process-based model should have 'stable' boundaries (limited gradients), which are not likely to be close to the area where morphological changes occur. The offshore boundary of an equilibrium model is a bit more arbitrary, but commonly the hydraulic boundary conditions are defined offshore of the morphological active zone.

In the choice for a modelling approach, the required (or sufficient) level of detail is determining. An empirical model estimates the post-storm profile shape. A process-based model describes the profile's shape in more detail and including its development in time. For hind-casting purposes, when at least pre and post storm bathymetry as well as hydraulic conditions are available,

a process-based model gives detailed information about the development in time. For forecasting applications, when the initial bathymetry as well as realistic estimations of conditions are available, a process-based model can be worthwhile as well. In case of safety evaluations, in fact all model input is based on rough estimations, assumptions and extrapolations. A process-based model, that involves more (stochastic) input variables, might respond unexpectedly to unfavourable combinations of input that is not covered by the validation data. A related empirical model that reflects the major governing phenomena, but includes a limited number of input (stochastic) variables, can be very useful for safety evaluations since it is computationally cheap and leads to a more precise (smaller spreading) but less accurate (larger bias) result.

2.3.1 DUROS/DUROS+/D++

The empirical dune erosion models DUROS (Vellinga, 1986), DUROS+ (Van Gent et al., 2008) and D++ (Deltares, 2010) are related to each other in the sense that they are 1D equilibrium profile models sharing part of the formulae describing the post-storm dune profile. This section briefly introduces the three models, where after the model specific properties are discussed for each model separately.

The models estimate a post-storm cross-shore profile shape, based on pre-storm bathymetry, sediment fall velocity in water and offshore hydraulic boundary conditions. The 1D approach implicitly includes the assumption of an alongshore uniform and straight coast. Table 2.1 summarises the main properties of the models. The models do not simulate the profile development in time, they only approximate the post-storm profile shape.

The original DUROS model, and later also DUROS+ and D++, are based on a series of dune erosion experiments with different scales (Vellinga, 1986; Van Gent et al., 2008). Since all underlying experiments focussed on dune erosion, the models are not applicable for other storm regimes, such as overwash. In the physical laboratory experiments used for the development of the model, it was assumed that stationary conditions during 5 h with maximum intensity generate approximately the same erosion as a representative complete storm with time varying intensity (Vellinga, 1986; Steetzel, 1993). In line with that, comparisons between models in Chapter 3 are mainly based on 5 h stationary conditions.

Using the estimated post-storm profile shape, the cross-shore position of

property	symbol	unit	model DUROS	DUROS+	D++
offshore boundary depth		m	25 m	25 m	custom
water level		m	✓	✓	✓
significant wave height	H_s	m	✓	✓	✓
peak wave period	T_p	s	-	✓	✓
sediment fall velocity	w_s	$\mathrm{m\,s^{-1}}$	✓	✓	✓

Table 2.1: Comparative overview of dune erosion models DUROS, DUROS+ and D++

that profile is found by assuming conservation of volume in the cross-shore direction. The algorithms of the models presented in this section are available in OpenEarth[1] (Van Koningsveld et al., 2010).

The post-storm profile comprises three elements (Figure 2.1):

1. the dry dune front,
2. the parabolic equilibrium post-storm beach profile, and
3. the transition slope connecting the post-storm beach profile with the initial profile.

The dry dune front is described by a 1:1 slope, from the storm surge level upward to the intersection with the pre-storm profile. The representation of the parabolic profile differs in the three models, and will therefore be dealt with separately. The transition slope connects the parabolic profile at the seaward end with a 1:12.5 slope to the initial profile.

The total post-storm profile shape is shifted in the cross-shore such that sediment conservation between dune face erosion and foreshore deposition is achieved. The post-storm cross-shore profile depends on (1) significant wave height, (2) wave peak period and (3) sediment fall velocity; the latter primarily determined by grain size (Equation 2.1).

The fall velocity of the sediment in water w_s is defined as a function of the D_{50} grain size (for a water temperature of 5 °C), following (WL | Delft Hydraulics,

[1] http://oss.deltares.nl/

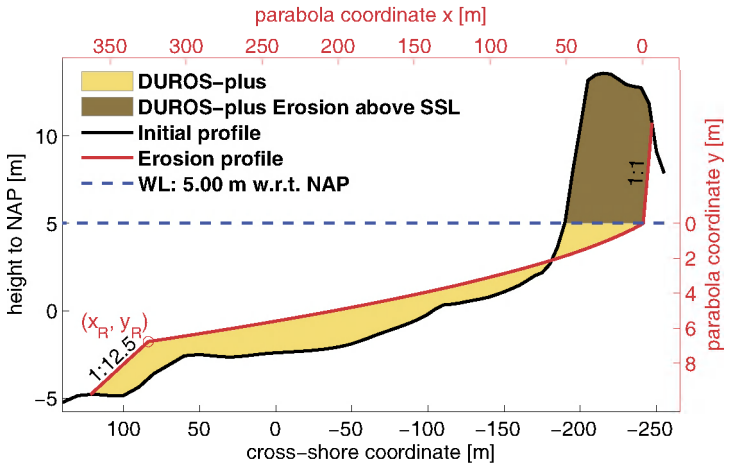

Figure 2.1: Example of a DUROS+ calculation and various sub elements of the method

1983):

$$^{10}\log\left(\frac{1}{w_s}\right) = 0.476\left(^{10}\log D_{50}\right)^2 + 2.180\,^{10}\log D_{50} + 3.226 \qquad (2.1)$$

DUROS+

The DUROS+ model is based on DUROS, but introduces an additional term to account for the wave period. The formulation for the parabolic profile in the DUROS+ model is given in Equation 2.2[2] (Van Gent et al., 2008).

$$\frac{7.6}{H_s}\cdot y = 0.4714\cdot\left[\left(\frac{7.6}{H_s}\right)^{1.28}\cdot\underbrace{\left(\frac{12}{T_p}\right)^{0.45}}_{T_p\text{ term}}\cdot\left(\frac{w_s}{0.0268}\right)^{0.56}\cdot x + 18\right]^{0.5} - 2 \qquad (2.2)$$

[2] All formulae are based on metric units

Herein y is the vertical coordinate, positive downward with $y = 0$ at the storm surge level and x is the cross-shore coordinate which is positive seaward (secondary axes in Figure 2.1). For the meaning of the other symbols see Table 2.1. The offshore extent of the parabolic profile is described by Equation 2.3 and 2.4.

$$x_R = 250 \cdot \left(\frac{H_s}{7.6}\right)^{1.28} \cdot \left(\frac{0.0268}{w_s}\right)^{0.56} \tag{2.3}$$

$$y_R = \left(\frac{H_s}{7.6}\right) \cdot \left[0.4714 \cdot \left(250 \cdot \underbrace{\left(\frac{12}{T_p}\right)^{0.45}}_{T_p \text{ term}} + 18\right)^{0.5} - 2\right] \tag{2.4}$$

DUROS

The DUROS and DUROS+ models are identical for a peak wave period of 12 s. The equations of the original DUROS model were derived for this peak period value. The parabolic profile is described by Equation 2.2 and 2.4, provided that $T_p = 12$ s, resulting in the T_p terms to become 1. In Equation 2.2, the T_p term simply falls out. Equation 2.4 can be simplified to:

$$y_R = 5.717 \cdot \left(\frac{H_s}{7.6}\right) \tag{2.5}$$

D++

The D++ model (Deltares, 2010) mainly differs from the related models, previously described, by its water depth at the offshore boundary where the hydraulic boundary conditions are imposed. Based on a comprehensive reanalysis of available dune erosion experiments, similar to WL | Delft Hydraulics (1982), new model formulations have been derived that account for the predicted wave propagation offshore of the surf zone. This implies in particular a different definition of the offshore extent of the parabolic profile (x_R, y_R). The parabolic shape is described in a similar way, but three

coefficients are different. It is described by:

$$\frac{7.6}{H_{0s}} \cdot y = 0.6 \cdot \left[\left(\frac{7.6}{H_s} \right)^{1.28} \cdot \left(\frac{12}{T_p} \right)^{0.45} \cdot \left(\frac{w_s}{0.0268} \right)^{0.56} \cdot x + 50 \right]^{0.5} - 4.2 \quad (2.6)$$

The cross-shore location to cut off the parabolic profile in this model, depends not only on the wave height and sediment fall velocity, but also on the water depth at the offshore boundary of the model:

$$x_R = x_{ref} \cdot cf_{depth} \cdot \left(\frac{H_s}{7.6} \right)^{1.28} \cdot \left(\frac{w_s}{0.0268} \right)^{-0.56} \quad (2.7)$$

Where x_{ref} is the x_R location for the reference conditions ($H_s = 7.6\,\mathrm{m}$, $w_s = 0.0268\,\mathrm{m\,s^{-1}}$), based on Equation 2.3, leading to $x_{ref} = 250\,\mathrm{m}$. The correction factor for the depth at the offshore boundary is described by:

$$cf_{depth} = \Delta \cdot max\left(\frac{15}{d} + 0.11; 1 \right) + (1 - \Delta) \quad (2.8)$$

Where transition function Δ is described by:

$$\Delta = \begin{cases} 0 & \frac{H_s}{d} \leq 0.4 \\ \left(\frac{\frac{H_s}{d} - 0.4}{0.06} \right) & 0.4 < \frac{H_s}{d} \leq 0.46 \\ 1 & \frac{H_s}{d} > 0.46 \end{cases} \quad (2.9)$$

2.3.2 DUROSTA

DUROSTA (Steetzel, 1993) is a numerical dune erosion model which is also known as UNIBEST-DE. It is a 2DV cross-shore model, solving the wave propagation, flow, sediment transport and bathymetry development for time-varying hydraulic conditions. Although the alongshore dimension is not explicitly taken into account by the model, it has the option to deal with wave obliquity, alongshore current gradients and coastal curvature.

DUROSTA simulates the cross-shore profile development in time, based on instantaneous sediment transport rates. The basic assumption is that the nett

local cross-shore sediment transport rate can be computed as the product of local flow velocity vertical and sediment concentration vertical according to:

$$S(x) = \frac{1}{nT} \int_{t=0}^{nT} \int_{z=0}^{\eta(x,t)} u(x,z,t)C(x,z,t)dzdt \tag{2.10}$$

in which:

S	nett transport	$[m^3\,m^{-1}\,s^{-1}]$
u	cross-shore velocity	$[m\,s^{-1}]$
C	sediment concentration	
x	cross-shore position	[m]
t	time	[s]
T	wave period	[s]
z	vertical coordinate with respect to the bed	[m]
η	instantaneous water level	[m]
n	sufficiently high number	

To elaborate Equation 2.10, the velocity and sediment concentration should be estimated in time and space. Due to the lack of a detailed description of the velocities and sediment concentrations including their variations, a number of simplifications had to be made. Figure 2.2 shows an overview of the various sub-models of DUROSTA and how they interact to simulate the profile evolution.

The model includes the ENDEC (Battjes and Janssen, 1978) wave model, that predicts the dissipation of energy in random waves breaking on a beach.

DUROSTA only includes the suspended sediment transport resulting from turbulence by breaking waves, meaning that bed-load transport is neglected. This assumption is considered valid because during storm conditions the majority of the sediment transport takes place as suspended transport.

The cross-shore flow is described as a time averaged velocity profile below the mean wave trough level and is based on the vertical distribution of the time averaged shear stress. The mass transport towards the coast is assumed to be concentrated in a narrow zone above the mean wave trough level. The mass flux in the upper part is compensated by a return current in the lower part of the water column.

The cross-shore transport model estimates the suspended sediment transport based on the cross-shore flow and the vertical distribution of the sediment concentration. This means that the wave related transport is neglected and

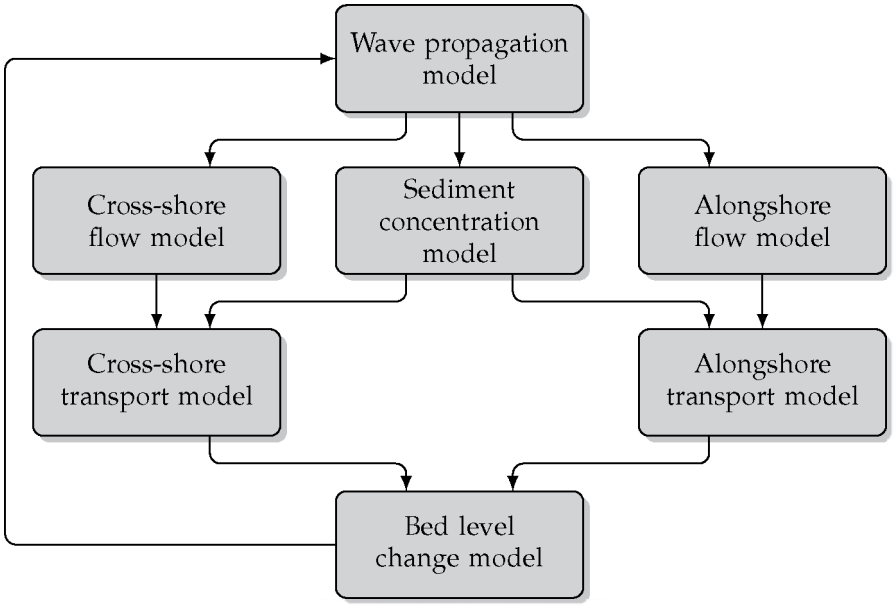

Figure 2.2: Overview of DUROSTA sub-models.

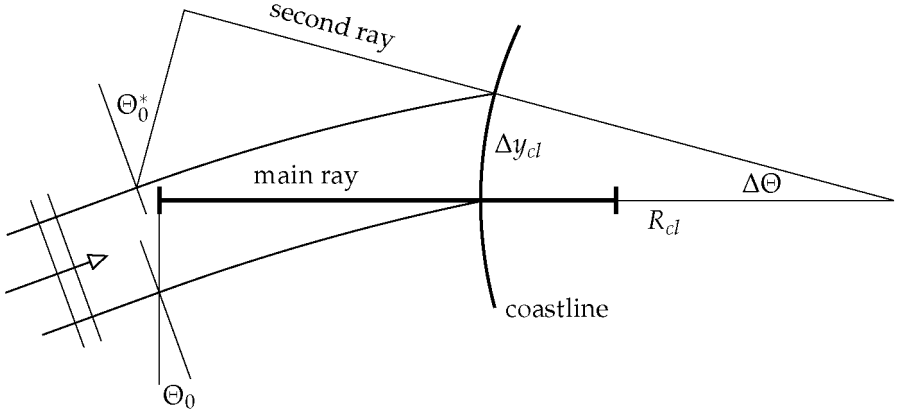

Figure 2.3: Schematic outline of DUROSTA's double-ray approach for a uniform curved coastline (source: Steetzel, 1993).

only the current related transport is included.

The alongshore flow model describes the cross-shore as well as the vertical distribution of the alongshore flow. The alongshore current is acting as a transport medium for the suspended sediment as generated by the breaking waves. This sub-model of DUROSTA includes the possibility to induce an alongshore current gradient, either directly (e.g. tide driven) or as a result of coastline curvature. Given the curvature, the model estimates the alongshore current gradient, which is a sink for the cross-shore sediment transport. The alongshore transport gradient is based on the alongshore flow gradient which in its turn is calculated from the difference between the flow velocities in the main ray and a virtual secondary ray at a distance Δy_{cl} along the coastline (Figure 2.3).

The alongshore transport model uses the alongshore current and the sediment concentration verticals as basis. The additional alongshore transport generated by alongshore current-induced bed shear stress is neglected.

The bed level change model combines the cross-shore and alongshore transport rates in order to estimate the bed level development in time. The model also has the optional feature of including hard layers, such as dune revetments.

This section only briefly discusses the main components of the DUROSTA

model. An extensive description of the model, including all the equations, can be found in Steetzel (1993). Related shorter descriptions can be found in Den Heijer (2005), Van Baaren (2007) and Hoonhout (2009) among others.

2.3.3 XBEACH

XBEACH (Roelvink et al., 2009) is an open source[3] numerical modelling approach to assess the natural coastal response during time-varying storm and hurricane conditions. It aims at describing the processes relevant for the different regimes defined by Sallenger (2000): swash, collision, overwash and inundation. The model solves 2DH equations for wave propagation, flow, sediment transport and bathymetry development, for time-varying wave and current boundary conditions. The model resolves the 'surf-beat', i.e. the long-wave motions created by the variation in wave height on a wave group time scale, that is responsible for most of the swash waves that actually attack the dune. Optionally, structural elements such as dune revetments or dune-dike transitions can be modelled as non-erodible layers.

A time dependent version of the wave-action balance equation transforms offshore wind waves to the near-shore and provides the wave forcing in the shallow water momentum equation, taking into account the directional distribution of the short wave action density (Holthuijsen et al., 1989).

A roller energy balance describes the transformation of surface rollers which uses the wave energy dissipation as a source term.

Shallow water equations are used to solve the low-frequency and mean flows. The wave-induced mass flux and the related (return) current are accounted for by a depth-averaged Generalized Lagrangian Mean formulation (Andrews and McIntyre, 1978; Walstra et al., 2000).

The sediment transport is described by a depth-averaged advection diffusion equation (Galappatti and Vreugdenhil, 1985). The model is capable of dealing with multiple sediment fractions.

Several formulations are available for the equilibrium sediment concentration. By default, the extended Van Rijn (Van Thiel de Vries et al., 2008) formulation is used. Alternatively, Soulsby–Van Rijn (Soulsby, 1997) can be chosen, including both bed load and suspended load transport.

[3] The source code is available via `http://oss.deltares.nl/`

Apart from the bed updating due to sediment transport directly related to the hydrodynamic conditions, the model also includes avalanching. This mechanism is activated in the model when a critical bed slope is exceeded. For the critical slope, separate values can be chosen for wet and dry points.

The wave energy density is prescribed at the offshore boundary as a function of the alongshore coordinate, wave angle and time.

Radiating flow boundary conditions are prescribed at the seaward and optionally, in case of a bay, also at the landward boundary.

This section only briefly discusses the main features of the XBEACH model. A comprehensive description of the model, including all equations, can be found in Roelvink et al. (2009).

2.3.4 Applicability of models along the Dutch coast

The Dutch coast has a length of 451 km (Central Intelligence Agency, 2008), of which 254 km is protected by dunes (Ruessink and Jeuken, 2002). Since 1965, cross-shore profiles along the complete North Sea coast of The Netherlands are measured yearly in the yearly Dutch coastal bathymetry survey "*JAaRlijkse KUStmeting*" (JARKUS) program (Rijkswaterstaat, 2008). This data gives a lot of information on the current status of the coast as well as the development over time. Three typical coastal areas can be distinguished:

1. The Wadden area in the north, consisting of a series of barrier islands with inlets in between;
2. the Holland coast, a closed coast in the middle part that mainly consists of dune areas and
3. the Delta area in the south with a series of river mouths, of which most have been closed by dams or protected by barriers.

The Wadden area is a rather complicated area when it comes to dune erosion modelling. First of all, strongly curved coastlines occur at the island heads. In addition, strong tide-driven currents occur in the inlets, leading locally to high alongshore flow velocities. Furthermore, the outer deltas of the inlets can significantly influence the local wave action near the coast. Thus, only limited parts of the coastline in that area can be considered as approximately alongshore uniform. The equilibrium models, DUROS, DUROS+ and D++, are more or less applicable to the relatively straight island bodies with a regular

foreshore. At the remaining straight parts of the island bodies, where the cross-shore profile contains deep channels and/or high shoals, D++ is the only applicable equilibrium model. Besides the straight parts, DUROSTA can also approximate the erosion for the curved island heads. However, the even more complex interactions of the 2DH phenomena and the alongshore varying curvature can only be covered by XBEACH.

The Holland coast is the least complex of the three areas. The coastline is slightly concave and the harbour entrance at IJmuiden is the only major interruption of the coast. At a few locations dune revetments are present and in the northern part there is a dike stretch of about 6 km (Hondsbossche and Pettemer Zeewering). A simplified representation of an average cross-shore profile of the Holland coast was the basis for the experiments underlying DUROS, DUROS+ and D++ (Vellinga, 1986; Van Gent et al., 2008). As a result, these equilibrium models, as well as the more advanced models DUROSTA and XBEACH, can be considered as applicable to the major part of this area. For the remaining areas, where structural elements are present, only DUROSTA and XBEACH are potentially applicable. More specifically, both models can be applied in the alongshore uniform stretches whereas only XBEACH is capable of modelling the non-uniform parts, such as dune-dike transitions.

For the Delta area similar model applicability considerations like for the Wadden area play a role. Moreover, in this area also storm surge barriers are present, which have an influence on the flow patterns and also lead to transition areas between the barrier and the adjacent dunes. At some straight parts of the coast, the equilibrium models can be used, but at many locations a more advanced approach is needed. Van Santen et al. (2012) show a practical application of both DUROSTA and XBEACH to a complex area, with both coastal curvature and alongshore non-uniformity, in the Delta region. Both 1D transect and 2DH area simulations have been performed. It is concluded that the 2DH approach gives a lot of additional information on the processes that play a role.

An indication of the applicability areas of the different models is presented in Figure 2.4.

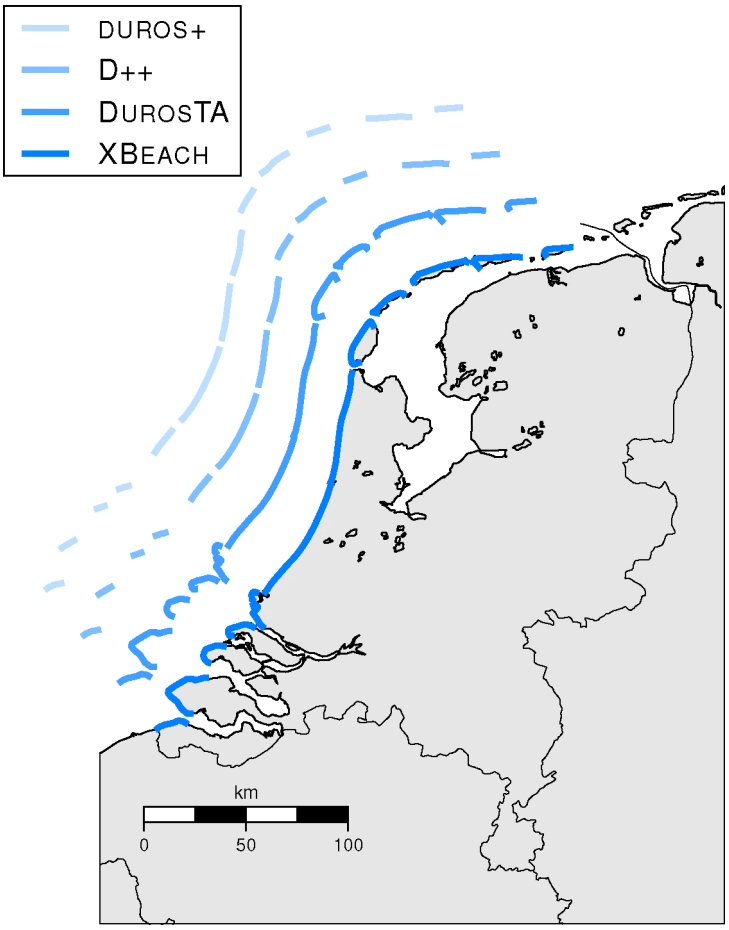

Figure 2.4: Indication of the applicability areas of dune erosion models along the Dutch coast.

2.4 Probabilistic methods

In order to be able to perform a dune safety evaluation, in addition to a suitable dune erosion model also a proper probabilistic method is required. The most suitable probabilistic method highly depends on the nature of the dune erosion model that is coupled to it. A straightforward probabilistic method like Monte Carlo is robust but requires relatively larger numbers of simulations, which limits its practical applicability to computationally cheap dune erosion models. The safety assessment of complex dune areas urges for computationally more expensive dune erosion modelling approaches which makes the selection of a suitable probabilistic method challenging. This section provides a brief description of a few methods that have been used in dune erosion applications or are considered potentially suitable.

2.4.1 Monte Carlo

Random numbers form the main basis for Monte Carlo methods. A fair roulette wheel can be considered as one of the first random number generators. The Monte Carlo methods are named after the eponymous Mediterranean coastal city, which was for a long time one of the best known venues for roulette.

A general limit state function, where Z is expressed as function of the physical variables in X, is used:

$$\begin{aligned} Z &= f(X) \\ \text{where: } X &= (x_1, x_2, \ldots, x_{n-1}, x_n) \end{aligned} \tag{2.11}$$

The Crude Monte Carlo method estimates the probability of failure P_f as:

$$P_f = \frac{N_f}{N} \tag{2.12}$$

Where N means the total number of samples and N_f the subset of N which leads to failure ($Z < 0$). Each sample represents a series of physical variables X that can be transferred to Z by a limit state function, generally described by Equation 2.11.

To get a sufficiently accurate result, the number of samples should be large enough. When aiming for 95% confidence, the minimum number of samples can according to CUR (1997) be estimated by:

$$N > 400 \left(\frac{1}{P_f} - 1 \right) \tag{2.13}$$

This means that for small probabilities relatively many samples are required. The probabilities relevant for the dune failure as discussed in this thesis are in the order of magnitude $\mathcal{O}(1 \times 10^{-5})$, leading to a required number of samples of at least $\mathcal{O}(1 \times 10^{7})$.

Importance sampling techniques are useful to reach the desired level of accuracy while using a reduced number of samples (Fishman, 1996). These techniques aim at a high sampling density around the limit state and a relatively low sampling density in the remaining part of the domain.

2.4.2 First Order Reliability Method (FORM)

First order relates to the linearising of the limit state function, which is used by this method. The linearisation is applied in the point which is usually referred to as *design point*. The design point is the point in the limit state or failure surface ($Z = 0$) where the probability density is maximal. This point is not known beforehand and can be found by an iteration procedure. Hasofer and Lind (1974) defined the reliability index β as the shortest distance from the origin to the failure surface in the normalised u-coordinate system.

The same general limit state function as used for Monte Carlo (Equation 2.11) applies here as well. The FORM procedure uses a set of standard normal distributions for the iterations.

$$U = (u_1, u_2, \ldots, u_{n-1}, u_n) \tag{2.14}$$

The variables in U do by definition have a mean $\mu_{u_i} = 0$ and a standard deviation $\sigma_{u_i} = 1$. In addition, the variables are independent $\rho(u_i, u_j) = 0$. In the U-space the *design point* is the point where $Z = 0$ is located closest to the origin.

The physical variables X have to be found by transformation from U. For a normal distributed variable x_i, the transformation is straightforward:

$$x_i = \mu_{x_i} + u_i \sigma_{x_i} \tag{2.15}$$

For a variable x_j with an arbitrary other distribution $F_{x_j}(x_j)$, the transformation is based on equating the exceedance probabilities:

$$F_{x_j}(x_j) = \Phi(u_i) \tag{2.16}$$

More general it can be stated that an arbitrary transformation function is needed:

$$X = f(U) \tag{2.17}$$

The FORM procedure is based on a linearisation of the Z-function in the U-space, which can be written as:

$$Z_L(U) = B + a_1 u_1 + a_2 u_2 + \cdots + a_{n-1} u_{n-1} + a_n u_n \tag{2.18}$$

The vector U is the basis for each iteration step. Using U, Z needs to be derived. Assuming that Z is only explicitly available as function of X, transformation from U to X is the first step. Secondly, Z can be found by applying the limit state function to X. Thirdly, the core of the method, $A = dZ/dU$ needs to be derived as:

$$\begin{aligned} A &= (a_1, a_2, \ldots, a_{n-1}, a_n) \\ &= dZ/dU = (dZ/du_1, dZ/du_2, \ldots, dZ/du_{n-1}, dZ/du_n) \end{aligned} \tag{2.19}$$

Next, B can be found as:

$$B = Z - (a_1 u_1 + a_2 u_2 + \cdots + a_{n-1} u_{n-1} + a_n u_n) \tag{2.20}$$

Then, the vector of influence coefficients α and the reliability index β can be

found by:

$$\alpha = (\alpha_1, \alpha_2, \ldots, \alpha_{n-1}, \alpha_n) = \frac{A}{\sqrt{\sum_{i=1}^{n} a_i^2}} \tag{2.21}$$

$$\beta = \frac{B}{\sqrt{\sum_{i=1}^{n} a_i^2}} \tag{2.22}$$

Finally, a vector U_d in the *design point* can be estimated by:

$$U_d = -\alpha\beta \tag{2.23}$$

The quality of this estimation of U_d is dependent on the linearity of the system and the distance from the base point to the estimated U_d. As made clear by "first order" in the name FORM, the method basically assumes a linear system. In order to come up with a sufficiently accurate design point, an iteration procedure is applied, where in each step a new estimation of the design point is made, taking the previous estimation as a basis.

2.4.3 Bayesian Network

A Bayesian network is a compact representation of joint probability distributions via conditional independence. Bayesian networks are probabilistic graphical models. Qualitatively the network is described by nodes (random variables) and edges (direct influence). The quantitative part consists of a set of conditional probability distributions. Together they define a unique distribution in factorized form.

A clear, complete description of a Bayesian network can be found in Korb and Nicholson (2004) and reads:

> A Bayesian network is a graphical structure that allows us to represent and reason about an uncertain domain. The nodes in a Bayesian network represent a set of random variables from the domain. A set of directed arcs (or links) connects pairs of nodes, representing the direct dependencies between variables. Assuming

discrete variables, the strength of the relationship between variables is quantified by conditional probability distributions associated with each node. The only constraint on the arcs allowed in a Bayesian network is that there must not be any directed cycles: you cannot return to a node simply by following directed arcs. Such networks are called directed acyclic graphs, or simply *dag*s.

Besides this modelling ability, they also allow to study how changes in the uncertainty of one of those variables affect the others. When a change in uncertainty of variable X implies a change of uncertainty in variable Y, it is said that there is a dependence relation between X and Y. It is also said that X is the parent of Y. The origin of the Bayesian Network lies in an interpretation of Bayes Theorem:

$$P(B|A) = \frac{P(A|B) \cdot P(B)}{P(A)} \tag{2.24}$$

Under its Bayesian interpretation it asserts that the probability of a hypothesis B conditioned upon some evidence A is equal to its likelihood $P(A|B)$ times its probability prior to any evidence $P(B)$, normalized by dividing by $P(A)$ (so that the conditional probabilities of all hypotheses sum to 1).

In more formal, mathematical way a Bayesian network consists of (Zweig and Russell, 1998):

1. A set of random variables $X_1, X_2, \ldots, X_n$.
2. A directed acyclic graph in which each variable appears once. The joint probability distribution is factored as:

$$P(X_1 = x_1, \ldots, X_n = x_n) = \prod_{i=1}^{n} P(X_i = x_i | Parents(X_i)) \tag{2.25}$$

   The immediate predecessors of a variable in this graph are referred to as its parents, with the values $Parents(X_i)$.
3. A representation of the required conditional probabilities.

Bayesian networks are used in a wide variety of applications (e.g. weather forecast, speech recognition, search engines). They can roughly be subdivided in three categories: decision, diagnostic and prediction.

Chapter 3

Limitations of dune erosion models

The previous chapter introduced various dune erosion models. This chapter discusses the model sensitivity of the dune erosion rate for a number of potential influencing aspects in more complex situations. It mainly focusses on the influence of pre-storm cross-shore bathymetry and its variability, wave obliquity and coastline curvature. It is believed that these aspects are insufficiently taken into account in the current Dutch dune safety assessment. This chapter provides insight in the validity of the omissions and simplification and enhances the insight in the applicability of dune erosion models to complex situations. The next chapter will use these results, together with the stochastic nature of the related variables, to propose additions to the dune safety assessment method.

In the analysis, XBEACH[1] is considered as the state-of-the-art dune erosion model and the limitations of the other models are evaluated against the XBEACH results. Since XBEACH includes most processes that are relevant to storm-induced erosion events, it is used as a reference. The sensitivity results are closely related to models' assumptions and the implementation of specific processes.

[1] Information about the version used, can be found in Appendix A

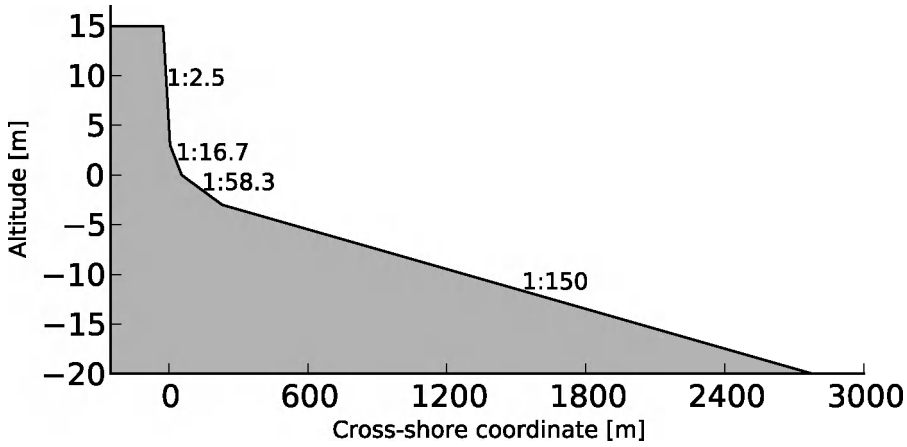

Figure 3.1: Reference cross-shore profile.

3.1 Primary variables

This section compares the model sensitivity of the rate of dune erosion to water level, wave height, wave period and grain size. These variables are considered to be of major importance for the dune erosion process. The water level, wave height and wave period describe the hydraulic loading, while the grain size is mainly related to the strength or feedback of the dune.

The comparison is based on simulations with stationary maximum storm surge conditions with a duration of 5 h. This simplification is related to the aim of getting a fair comparison (Section 2.3.1), since not all models are capable of dealing with time varying conditions. Starting point for the comparison is a set of representative extreme storm surge conditions, as specified in Table 3.1, and an initial cross-shore profile as depicted in Figure 3.1. This cross-shore profile is considered more or less representative for a large part of the Dutch coast and is referred to as the reference profile. Most of the dune erosion experiments that have been performed in The Netherlands are based on this profile (see e.g. Van Gent et al., 2008).

With respect to the reference situation, each of the four variables are separately perturbed within a range of 75 % to 125 %. The relative erosion volumes above the reference water level of NAP+5 m are shown on the vertical axes

variable	symbol	value	unit
water level	WL	NAP + 5	m
significant wave height	H_s	9	m
peak wave period	T_p	12	s
grain size	D_{50}	225	µm

Table 3.1: Representative storm surge conditions.

in Figure 3.2. The sign of the sensitivity is the same for all models, but the magnitude differs.

The top left panel shows the sensitivity to the water level. The sensitivity of DUROS+ and DUROSTA is nearly the same. XBEACH has a milder sensitivity.

The bottom left panel shows the sensitivity to the wave period. Here all models display a different sensitivity. XBEACH shows the strongest sensitivity, significantly larger than DUROS+, although both models were calibrated on a series of large scale experiments (Van Gent et al., 2008). Van Thiel de Vries (2009) shows for XBEACH a favourable agreement with the experiments. The different sensitivity might be explained by differences in up-scaling to full scale. DUROSTA is somewhere in between; Den Heijer (2005) concluded that the wave period effect in this model is in fact expressed as differences in the wave height towards the shore.

The top right panel gives an impression of the sensitivity of the different models for the wave height. DUROSTA has a mild approximately linear sensitivity over the whole range. XBEACH' sensitivity is close to that of DUROSTA for the lower range of wave heights, but has a slightly stronger sensitivity in the higher range. DUROS+ on the contrary has a stronger sensitivity in the lower range, but is approximately similar to DUROSTA in the higher range.

The bottom right panel indicates the sensitivity for the D_{50} grain size. DUROS+ results in the strongest sensitivity. The sensitivity of DUROSTA to the grain size has a bit smaller magnitude. XBEACH shows to be hardly sensitive to the grain size. The difference can be explained by the supply dominated offshore sediment transport in XBEACH as opposed to the demand driven transport in DUROSTA. The supply of sediment is controlled by the slumping of the dune face which does not involve the grain size.

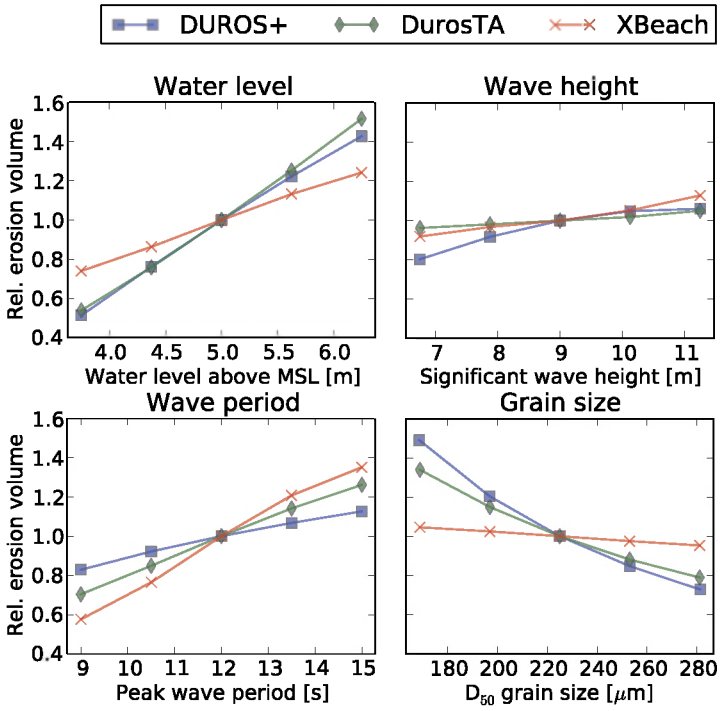

Figure 3.2: Overview of sensitivity of DUROS+, DUROSTA and XBEACH for water level, wave height, wave period and grain size.

3.2 Cross-shore bathymetry

The bathymetry describes the initial situation for any morphological investigation. In dune erosion simulations, the bathymetry is supposed to be the pre-storm bathymetry. However, when evaluating the safety of dunes as a sea defence, the bathymetry at an unknown moment in future, when a storm occurs, is desired. The model sensitivity to the bathymetry provides insight in the related uncertainty.

In contrast to the wave obliquity and coastal curvature, discussed in the next few sections, bathymetry is included in all models that are used for this comparison. However in DUROS+, the offshore part of the cross-shore profile is taken into account implicitly whereas the other two models include the whole bathymetry from the offshore boundary onwards. The omission of the offshore part of the bathymetry implies that this part of the profile has an only limited effect on dune erosion. This section aims at verifying the validity of this omission by investigating the importance of the landward as well as the seaward profile part based on XBEACH simulations.

3.2.1 JARKUS profiles[2]

In this section three cross-shore profiles (Figure 3.3) out of the JARKUS dataset are used as basis to investigate the influence of the upper and lower profile parts on dune erosion. The profiles are selected based on their slope below the NAP−4 m contour: steep sloped (7003775), mild sloped (4001740) and intermediate (7001503). The locations of the profiles are indicated on the map in Figure 3.4. A division has been made at the NAP−4 m contour between the upper (landward) part and the lower (seaward) part. This division is related to the maximum seaward extent of the erosion profile according to the DUROS+ model. The three divided profiles lead to a matrix of nine unique combinations of upper and lower profiles parts, of which three coincide with the original profiles and the remaining six are artificially combined.

For each of the nine profiles, the erosion rate has been estimated by XBEACH simulations. The hydraulic boundary conditions as well as the grain size are kept equal and time-invariant with a duration of 5 h for all simulations, in order to get a fair comparison with respect to DUROS+ (Section 2.3.1). The conditions

[2] This section has been published as Den Heijer (2012b).

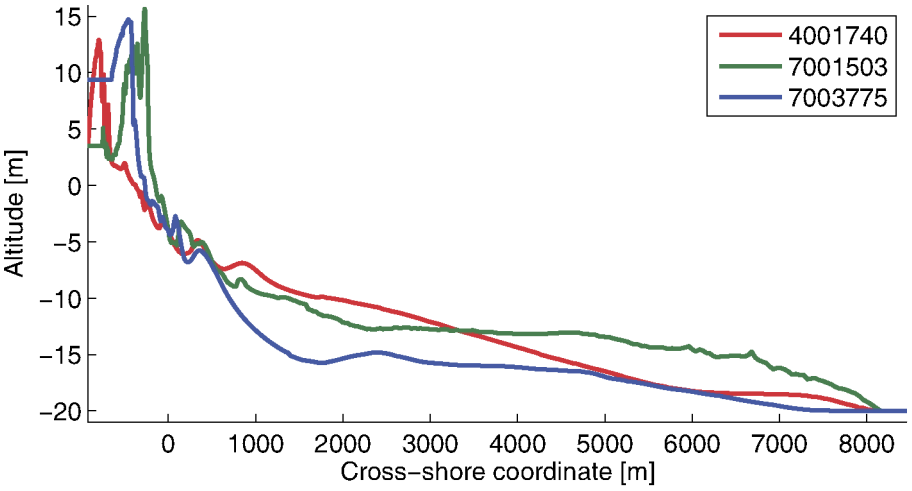

Figure 3.3: Three cross-shore profiles used as basis for the profile influence investigation.

as applied in the simulations are summarized in Table 3.1.

The nine simulations with bathymetries based on combinations of upper and lower profile parts allow for clear distinction between the influence of both cross-shore zones. The influence of the upper profile part can be isolated based on three distinct lower profile parts. And, the other way around, the influence of the lower profile part can be isolated for three distinct upper profile parts.

Figure 3.5 gives an overview of all combinations of landward and seaward parts of the cross-shore profiles together with an indication of the erosion volume, represented by the color of the tiles. The individual columns represent the sensitivity of the erosion volume for the seaward part of the cross-shore profile. Similarly, the individual rows represent the sensitivity for the landward part of the profile. The results show that the variation as function of the landward part of the profile (horizontal axis) is much larger than the variation as function of the seaward part of the profile (vertical axis). Figure 3.6a gives another representation of the influence of the seaward part on the simulated erosion volume. The erosion has been plotted as function of the seaward profile part and the markers indicate the landward part. The figure indicates that the erosion, given a particular landward profile part, only

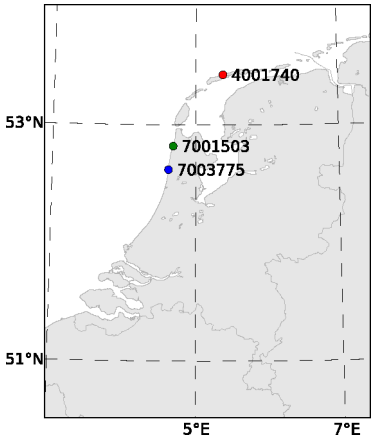

Figure 3.4: Map of The Netherlands with the locations mentioned in this section indicated.

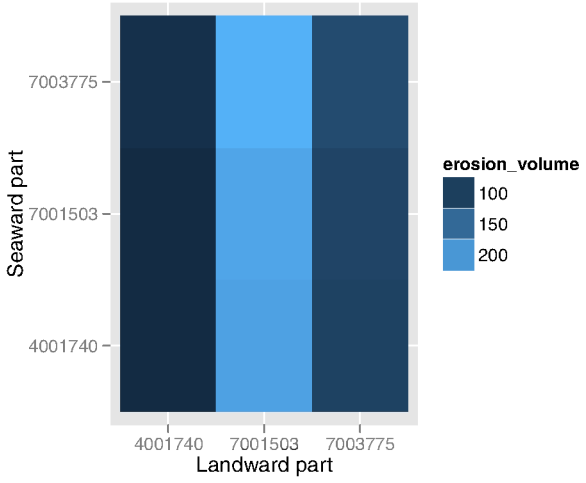

Figure 3.5: Matrix of combinations of landward and seaward profile parts with the color of the tiles indicating the resulting erosion volume as simulated by XBEACH.

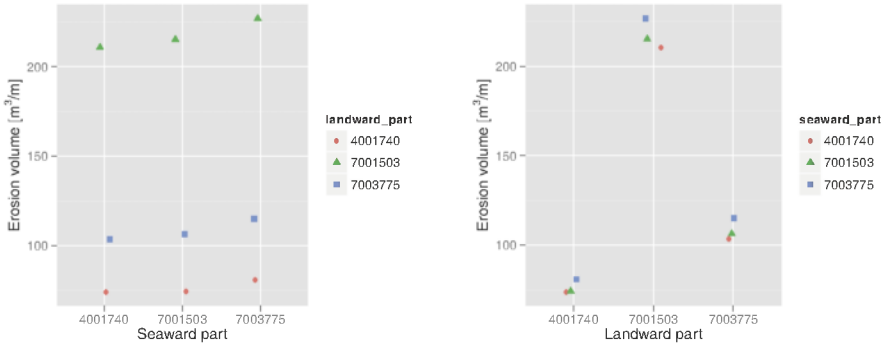

(a) The XBEACH erosion results as function of the seaward profile part.

(b) The XBEACH erosion results as function of the landward profile part.

Figure 3.6: Intercomparison of XBEACH results for different cross-shore profiles.

varies within a range of about 10 %. In contrast, the similar Figure 3.6b that visualizes the influence of the landward profile part shows that the erosion can vary up to almost 300 %.

Corresponding DUROS+ results calculations mainly vary as function of the landward part of the profile, since the seaward part (offshore of the toe of the sedimentation zone) is not explicitly taken into account in that model. Out of the three example profiles as presented here, only in case of (the landward part of) transect 7001503, the seaward part influences the erosion up to about 8 %. The reason is that the toe of the erosion profile in those cases reaches a bit below the NAP−4 m contour. So, a slightly different (lower) choice for the division contour between landward and seaward part would make DUROS+ to be fully dependent on the landward part of the profile and insensitive to the seaward part.

The sensitivity of the dune erosion rate for the bathymetry is most likely related to the wave propagation over the cross-shore profile. Figure 3.7 and 3.8 give an indication of the high and low frequency H_{rms} wave height. These figures relate to the simulations in the left column respectively the lower row of Figure 3.5. The wave heights in the figures are time averaged over the total simulation. The corresponding initial cross-shore profiles are included in top panels (a) of the figures as a reference, to be able to relate the wave height to

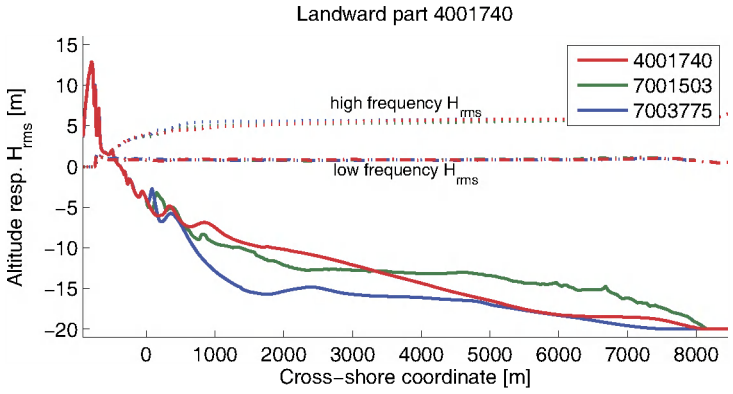

(a) Both high and low frequency H_{rms} wave height together with the corresponding initial cross-shore profiles.

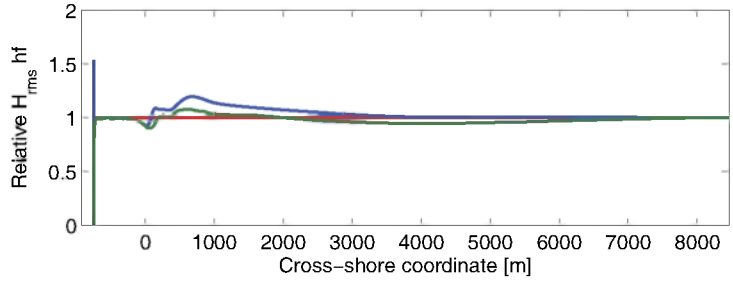

(b) Relative high frequency H_{rms}.

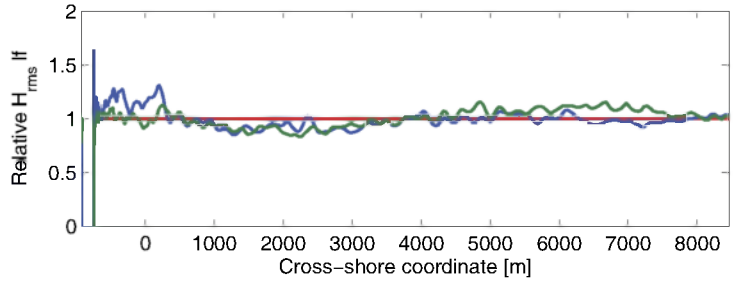

(c) Relative low frequency H_{rms}.

Figure 3.7: Example of the H_{rms} wave heights as simulated by XBEACH for three cases with different seaward profile part.

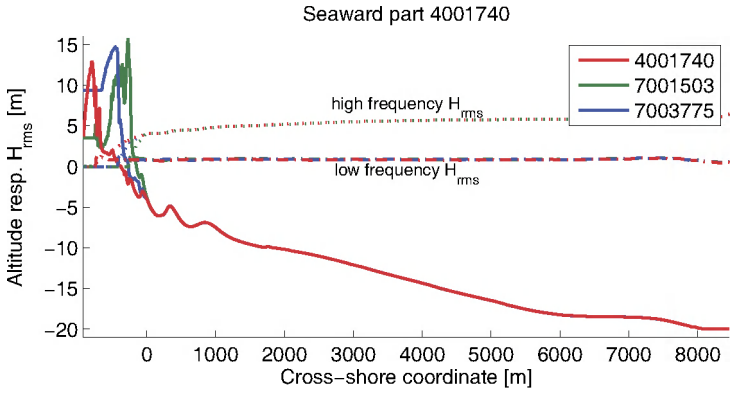

(a) Both high and low frequency H_{rms} wave height together with the corresponding initial cross-shore profiles.

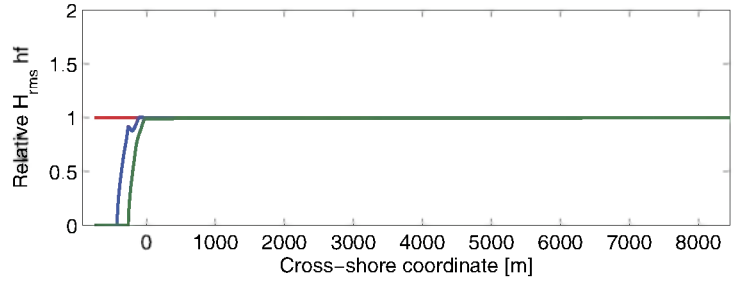

(b) Relative high frequency H_{rms}.

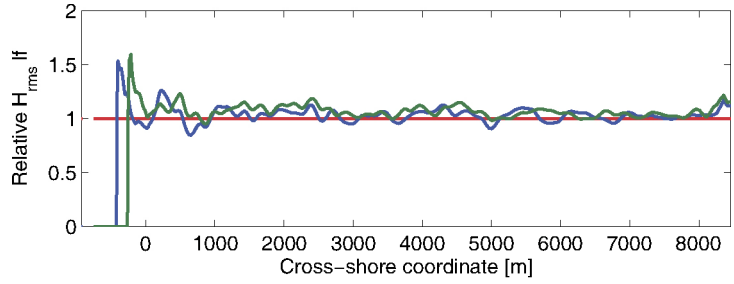

(c) Relative low frequency H_{rms}.

Figure 3.8: Example of the H_{rms} wave heights as simulated by XBEACH for three cases with different landward profile part.

the local depth. The panels b and c respectively show the high frequency and low frequency relative to those as simulated for transect 4001740 (in red).

In Figure 3.7a, the distinct seaward profile parts result in a slight diversion of the wave heights towards the common landward profile part. The relative H_{rms} wave height, depicted in Figure 3.7b and c show that this especially holds for the high frequency and to a lesser extent for the low frequency wave heights. Landward of the profile transition, at the NAP−4 m contour, the high frequency wave heights converge fast, whereas the low frequency ones express their different origins until the shoreline. So, the low frequency waves appear to dominate the influence of the offshore profile part on the erosion rate.

The common seaward part of the profile in Figure 3.8 causes approximately equal high frequency wave heights until the transition at the NAP−4 m contour. Landward of the transition, the high frequency wave heights diverge clearly (Figure 3.8b and c), since the three profiles have an obviously different shape and steepness in that area. The low frequency waves, on the other hand, show a slightly divergent behaviour over the entire cross-shore profile. This is likely to be related to the difference in profile shapes and in cross-shore distances to the waterline that lead to different long wave propagation and reflection.

3.2.2 Discussion

Three divergent cross-shore profiles have been used to investigate the influence of the bathymetry on dune erosion. The XBEACH results show that the upper part of the profile is of major importance for the dune erosion rate. Differences in the lower profile part do lead to divergent erosion rates, but these differences are much smaller compared to the upper profile part. This investigation with XBEACH does not provide evidence to falsify the assumption underlying DUROS+ that the seaward part of the cross-shore profile is of minor importance. It can be concluded that the inclusion of the lower profile part would potentially improve the safety assessment for dunes, but there is no urgent need to include it. Other influences, like wave obliquity and coastal curvature, are likely to have a larger influence on the dune erosion rate during extreme conditions.

3.3 Wave obliquity

A large part of the Dutch coast is subject to wave obliquity during extreme storm conditions. Although the majority of the dune erosion events involves oblique waves, most dune erosion experiments and numerical models only include the cross-shore dimension. The related assumption to allow for this simplification is that the wave angle has no significant influence on the dune erosion rate, as concluded by WL | Delft Hydraulics (1981). DUROS+ does not include wave obliquity, DUROSTA includes it in its 2DV approach and XBEACH in 2DH. This section investigates the effect of wave obliquity on dune erosion with the models DUROSTA and XBEACH. In this comparison, the reference cross-shore profile (Figure 3.1) is used and alongshore uniformity is assumed. In addition, the conditions given in Table 3.1 are used, with a duration of 5 h. The wave angles are defined at the offshore boundary of the model (25 m water depth) with respect to the shore normal.

3.3.1 DUROSTA

Since DUROSTA does not explicitly take the alongshore dimension into account, the wave angle effect is estimated using the cross-shore bathymetry only. The wave angle has been varied from 0° (shore normal) to 50°, with steps of 5°. Figure 3.9 shows a decrease of erosion volume for oblique waves up to over 20 % at 50°. A cosine shape is visible in the this figure, implying that the reduction of the cross-shore wave component is of major importance in the DUROSTA approach. Since no alongshore transport gradients are supposed to be present, no sink due to alongshore losses is contributed for in the model.

3.3.2 XBEACH

With XBEACH, the effect of the wave angle on dune erosion is modelled in a 2DH model, with an alongshore uniform bathymetry. The required alongshore extent of the model domain depends on the cross-shore distance from the offshore boundary to the water line and the incident wave angle (see Figure 3.10). Table 3.2 gives an overview of the simulated angles of wave incidence including the corresponding alongshore dimension of the model domain. XBEACH also allows modelling of oblique waves in a 1D (cross-shore) model, but for reasons of consistency with coastal curvature models

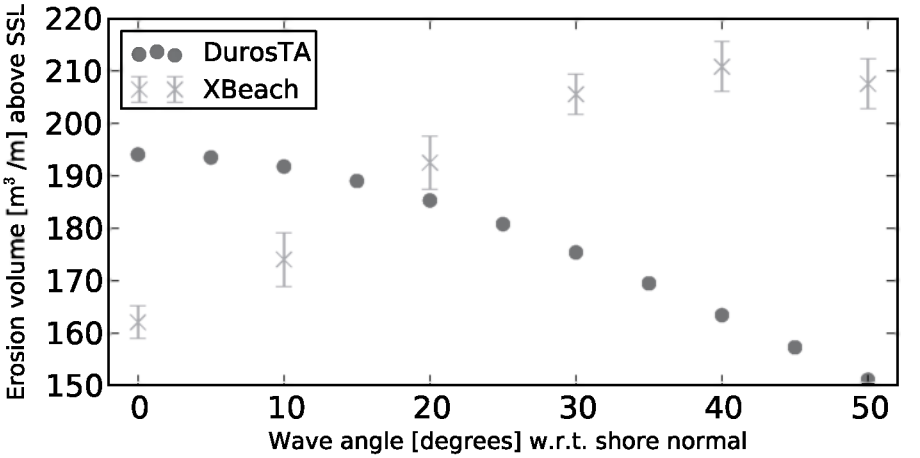

Figure 3.9: DUROSTA and XBEACH erosion volume above storm surge level (SSL) as function of the incident wave angle. The errorbars around the XBEACH results represent the 95 % confidence intervals.

in the next section also this case has been simulated in 2DH. The choice for a 2DH approach also provides information on the alongshore variation in dune erosion rates, leading to confidence intervals. The erosion results are considered in the alongshore central 40 % of the model domain.

Figure 3.9 shows the erosion volume per running meter coastline as function of the incident wave angle. In contrast to the DUROSTA results, XBEACH results in an increasing erosion volume for oblique incoming waves with a maximum at an angle of 40° with 30 % more erosion. The 95 % confidence intervals vary a bit in magnitude around 5 % of the mean values.

To understand the responsible mechanism for the XBEACH wave angle effect, which contradicts with DUROSTA, both cross-shore and alongshore sediment transport components need to be considered. In theory, no alongshore sediment transport gradients should be present, which are indeed not observed in the model on a global scale. When zooming in to the band near the waterline, alternating transport gradients are found with maxima of $\mathcal{O}(1 \times 10^{-4}\,\mathrm{m^3\,s^{-1}\,m^{-1}})$. For comparison, this is at least an order of magnitude smaller than the gradients as found along the curved coastline simulations in Section 3.4. Based on the relatively small magnitude and the alternating

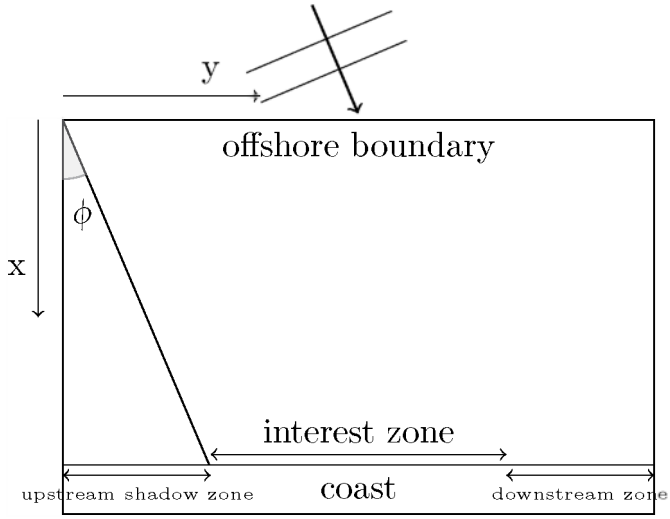

Figure 3.10: Illustration of XBEACH model domain for incident wave angle simulations.

Wave angle [degrees] w.r.t. shore normal	Alongshore length [m]
0	900
10	1800
20	3600
30	5800
40	8400
50	11900

Table 3.2: Overview angles of wave incidence (w.r.t. shore normal) and corresponding alongshore dimension of XBEACH model domain.

character of the gradients, they are considered as insignificant. Because of the absence of significant alongshore gradients, it is considered acceptable for analysis purposes to average most of the variables over the alongshore dimension, in the interest zone (central 40 %). Figure 3.11 shows the time averaged alongshore transport component in the middle panel and the cross-shore component in the bottom panel, where the cross-shore (initial and final) profiles in the top panel act as reference. The figures show that both alongshore and cross-shore transport rates increase with increasing wave obliquity. The magnitude of the cross-shore transport corresponds approximately to the pattern of the erosion rates as given in Figure 3.9. In contrast, the magnitude of the alongshore keeps growing up to the largest simulated wave angle of 50°.

The presented transport rates are based on the sediment concentrations and flow velocities as shown in Figure 3.12. The time averaged sediment concentrations in the top panel increase with increasing wave angle until a maximum at 40°. The maximum concentration slightly increases, but especially the cross-shore width of the zone with high concentration increases for larger wave angles. This is caused by a longer lasting wider range of higher concentrations with respect to the smaller angles. The middle panel of Figure 3.12 shows the alongshore flow velocity. Similar to the alongshore transport, the flow velocity keeps increasing towards the largest simulated wave angle. The offshore directed cross-shore velocity in the lower panel decreases for larger wave angles. The smaller cross-shore wave component leads to less wave set-up and therefore lower return current speeds for larger wave angles.

The effect of the wave angle on dune erosion as simulated by XBEACH can be explained by the offshore directed transport capacity due to the combined effect of alongshore and cross-shore processes. A wider cross-shore zone of higher concentrations as a result of higher alongshore velocities facilitates the erosion process for oblique waves. On the other hand, the cross-shore velocity (undertow) decreases for larger wave angles. The combination of these two aspects results in an increasing erosion rate up till an angle of 40° and decrease beyond.

3.3.3 Discussion

The two models show an opposite dependence for the dune erosion rate on the incident wave angle. DUROSTA only accounts for the cross-shore component, based on the assumption that the alongshore component does not play a

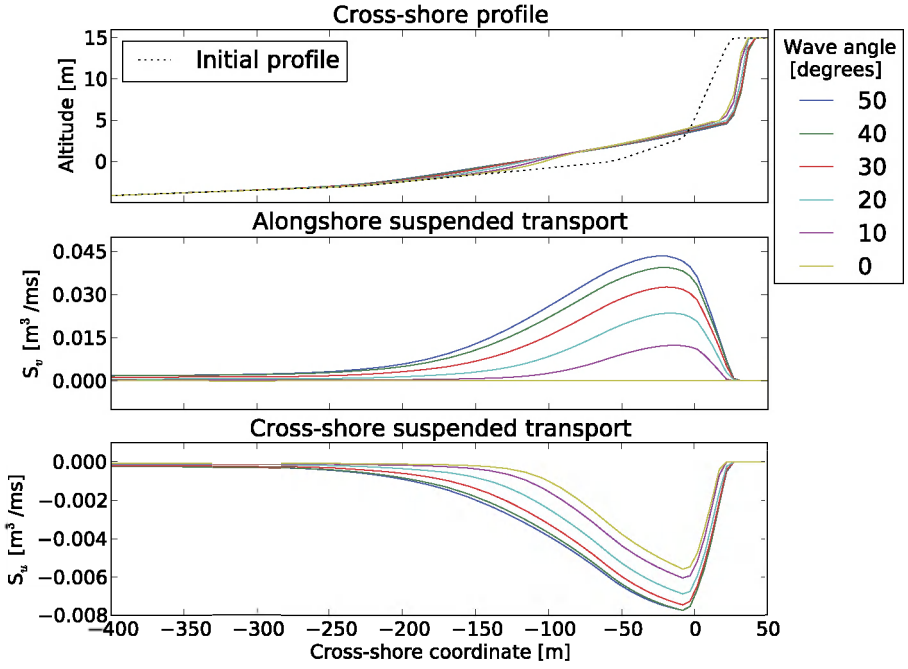

Figure 3.11: XBEACH cross-shore profiles and both alongshore and cross-shore sediment transport.

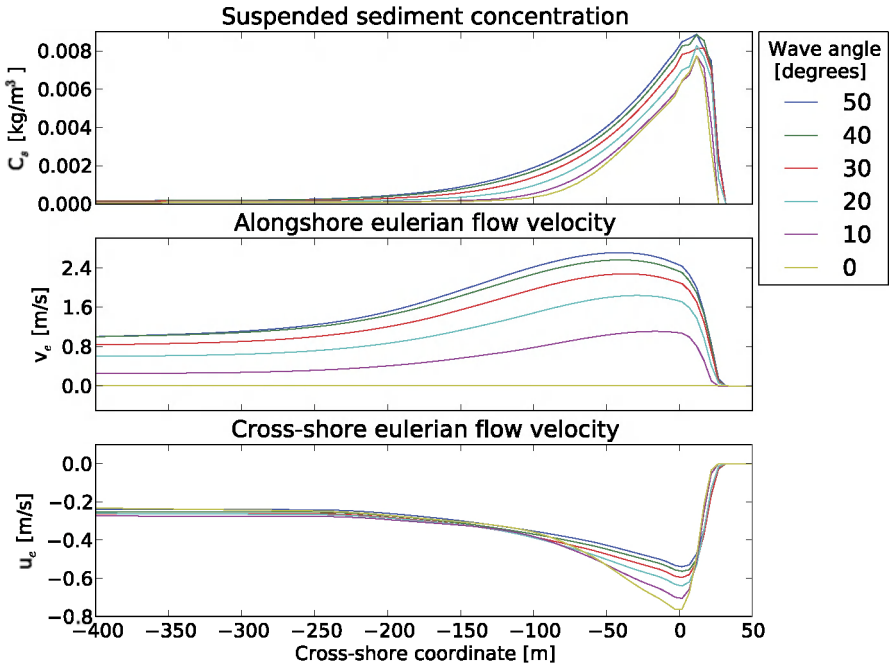

Figure 3.12: XBEACH sediment concentrations and flow velocities.

role due to the absence of an alongshore gradient. Therefore, the DUROSTA implementation leads by definition to maximum erosion for normal wave incidence and decreasing erosion rates for off normal angles showing a cosine like shape. In the 2DH XBEACH model, both the alongshore and cross-shore components, including their interactions, are taken into account, leading to an increased erosion for off normal angles up till 40° and decreasing erosion for larger angles.

The explicit inclusion of the alongshore dimension by the XBEACH model is considered crucial for a proper modelling of the effect of wave obliquity on dune erosion. Therefore, the XBEACH results are used for the probabilistic investigations in Chapter 4 and 5.

3.3.4 Conceptual wave obliquity model

The results in this section show that both the cross-shore and alongshore aspects are required to properly estimate the dune erosion rate when wave obliquity is involved. By capturing the relative erosion as function of the wave angle in a conceptual model, this section aims at the evaluation of the importance of the alongshore processes with respect to the cross-shore processes.

The erosion rates as found by DUROSTA (Figure 3.9) show a cosine shape ($cos\phi$). The peak cross-shore velocities, in the lower panel of Figure 3.12, show a similar shape by having its maximum for normally incident waves. On the contrary, the alongshore velocities and the related transports can be described by a $sin2\phi$ (Coastal Engineering Research Center, 1984).

If we assume that the relative erosion is proportional to the product of the cross-shore $cos\phi$ and the alongshore $sin2\phi$ component, a pattern as in Figure 3.13 (absolute value) would be found. This suggests a maximum of 38 % at an angle of 35°, qualitatively similar to the XBEACH results but quantitatively a bit exaggerated. The overestimation with respect to XBEACH suggests that the influence of the alongshore component is overestimated by the conceptual model.

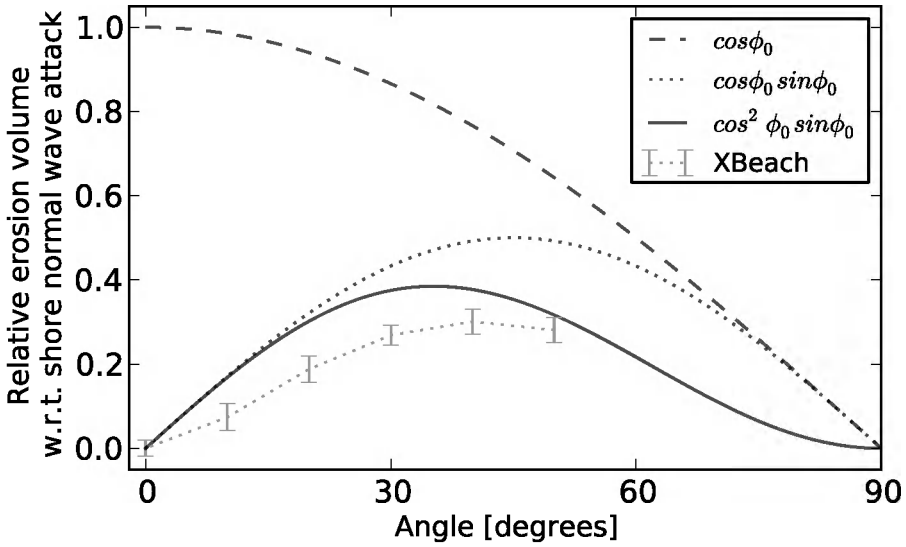

Figure 3.13: Illustration of the product of sine and cosine as contribution for the alongshore respectively cross-shore processes along a straight coastline with different wave angles.

Class	Curvature [$^\circ km^{-1}$]	Additional erosion [$m^3 m^{-1}$]
1	0 – 6	0
2	6 – 12	50
3	12 – 18	75
4	18 – 24	100
5	> 24	research needed

Table 3.3: Classification of coastal curvatures and additional erosion contributions according to Dillingh and Visser (1984).

3.4 Coastal curvature

This section investigates the effect of coastal curvature on the rate of dune erosion both for different radii as well as for different locations along the curved coastline. In the models under consideration, different approaches are used to account for the effect of coastal curvature on dune erosion. DUROS+ does not include curvature, but the Dutch safety assessment method provides guidelines to account for the curvature by introducing an additional erosion volume contribution. Dillingh and Visser (1984) classified the coastal curvature and derived corresponding additional erosion contributions, as shown in Table 3.3. DUROSTA estimates an alongshore transport gradient based on a double-ray approach as a mechanism for curvature related erosion. In XBEACH, the alongshore dimension is explicitly taken into account and a 2DH curvilinear model can be used to simulate a curved coastline. The influence of the cross-shore profile and its alongshore variation on the sensitivity of the dune erosion rate for coastal curvature is outside the scope of this investigation.

In this section DUROSTA and XBEACH are applied to estimate the erosion for a series of coastal curvatures. Constant hydraulic boundary conditions with a duration of 5 h are applied. The series of coastal curvatures that is simulated in this section, shown in Table 3.4, is inspired by the classification of Dillingh and Visser (1984). The comparison is executed with an alongshore uniform cross-shore reference profile (Figure 3.1). The radii are defined with respect to the NAP+5 m contour. The erosion rate as found with a similar model without curvature, is used as a reference.

Curvature [$^\circ km^{-1}$]	Radius [m]
0	∞
6	9500
12	4800
18	3200
24	2400
30	1900

Table 3.4: Overview of curvatures and corresponding radii in this study.

3.4.1 DUROSTA

The DUROSTA model is able to account for the effect of coastal curvature by including a contribution for the alongshore transport gradient. The alongshore transport gradient is estimated based on the difference in alongshore flow velocity with respect to a secondary ray (Figure 2.3). In this approach, the local coastline is assumed to be circular and the cross-shore profile alongshore uniform. This means that, apart from the regular input, the radius of the coastline curvature and the cross-shore coordinate of the coastline are sufficient to take the curvature effects into account. By default normal wave incidence at the main ray is assumed. By prescribing an oblique wave angle, other locations along the coastline can be modelled.

Figure 3.14 shows the erosion rates in terms of volumes in relation to the curvature radius and wave angle. The wave angle is here defined as the angle between the local shore normal and the wave direction at the offshore boundary (25 m water depth). For small wave angles, a progressive increasing erosion rate for smaller coastal radii is clearly visible. This behaviour can be explained by the fact that the model introduces the alongshore sediment transport gradient as a mechanism to account for the effect of the curved coastline. The sediment transport gradient is a sink for the cross-shore sediment balance. The smaller the radius, the larger the alongshore transport gradient. When this sink is larger, the sedimentation zone develops slower, enlarging the period of heavy wave attack on the dunes. As a result, the dune erosion process progresses faster, leading to more dune erosion at the end of the storm. For larger wave angles, the erosion volumes decrease (see Figure 3.9) and coastline curvature effect is diminished towards approximately zero at an angle of 60°. The interactions between cross-shore and alongshore processes are not implemented in the model.

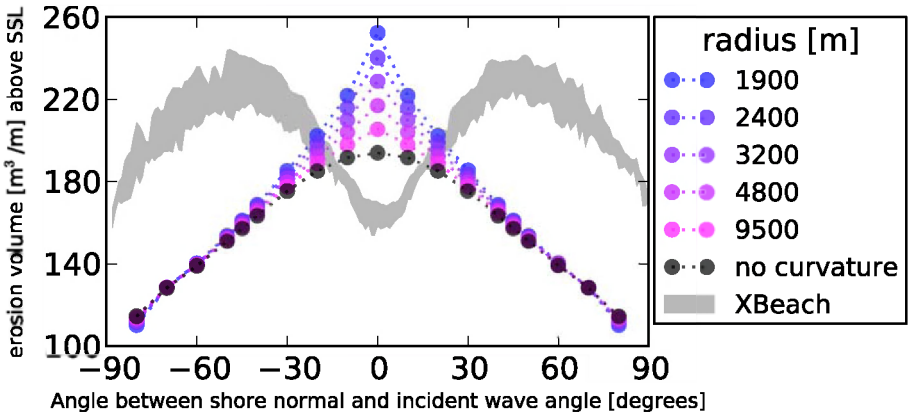

Figure 3.14: DUROSTA erosion volume above storm surge level (SSL) as function of incident wave angle for various coastal radii. The corresponding XBEACH results are included in gray.

3.4.2 XBEACH

In this section the 2DH capabilities of XBEACH are utilised by creating an idealised circular coastline model to simulate the phenomena that play a governing role in case of curved coastlines. A circular arc of 180° is modelled with a curvilinear grid, and the main incident wave direction is perpendicular at the middle of the arc. Figure 3.15 shows the layout of the model domain and Figure 3.16 gives an impression of the applied bathymetry and grid. The radius (Figure 3.15) is defined with respect to the waterline at storm surge level (NAP+5 m). For each of the investigated radii (Table 3.4), the curvilinear grid has been created in such a way that the alongshore grid size at the water line is equal for all radii. Since the cross-shore profile is alongshore uniform, the cross-shore grid is also kept alongshore uniform. The cross-shore grid is non-equidistant, with a grid size proportional to the depth. At the lateral boundaries the water level gradient is prescribed to be zero, so-called Neumann boundaries. To let the Neumann boundaries properly function, rectangular grid cells are required at the lateral boundaries. Therefore, the curvature is gradually diminished near both lateral boundaries. These extensions of the model area are outside the area of interest and omitted in the figures. The simulations are made with a morphological acceleration factor

(morfac) of 5. A sample of the model settings is presented in Appendix A.

In Figure 3.17, the post-storm erosion along the curved coastline is shown for different coastal radii as resulting from the XBEACH simulations. The XBEACH results for a straight coast with oblique waves have been added as a reference. For comparison, the range of DUROSTA erosion rates is shown in gray. The angle between the incident wave direction and the local shore normal is given on the horizontal axis, which is zero in the middle of the arc (see Figure 3.15), where the incident wave direction is shore normal. In contrast to the DUROSTA results, XBEACH shows zones of maximum erosion around (-)45° and minimal erosion at the location with approximately normal wave incidence.

Figure 3.18 gives an overview of the erosion development over time for the whole range of coastline orientations in the model. The darker colors indicate more erosion and the time axis is positive towards the center of the arc. The figure highlights zones of maximum erosion at about (-)45°. In addition, it is clearly visible that the erosion at 0° stays behind during the whole simulation.

Figure 3.19 shows the erosion, accretion and sediment balance as function of the coastline orientation (angle along the arc). The values are corrected for the wedge-shaped area between two adjacent cross-sections. The erosion is defined as the erosion above the NAP+5 m level per running meter coast; the accretion is the nett accretion below this level. The top panel contains the same XBEACH erosion results as Figure 3.17. The line indicating the 1900 m radius corresponds to the situation at 5 h in Figure 3.18. The erosion results in the top panel show a relatively large variation as function of the angle compared to the influence of the radius, being expressed in the different simulations. Moreover, the shape of the erosion plot is similar for all investigated radii, having minima at normal wave incidence and maxima around an oblique wave angle of 45° off normal. In contrast to the erosion, the accretion (middle panel) is dependent on the coastal radius and with that the sediment balance (bottom panel) as well. The stronger the curvature, the more sediment leaves the model via the lateral boundaries, leading to a negative sediment balance. From the lower panel of Figure 3.19 it can be observed that the rate of sediment conservation decreases with the radius. This means that less sediment is lost from the model for less curved coastlines, pointing towards full sediment conservation for a straight coast with normal incoming waves, which seems realistic. Note that the number of grid cells in alongshore direction is proportional to the radius. So, the model with the largest radius has five times more grid cells per degree compared to the smallest radius. As a result, the plots as function of the angle

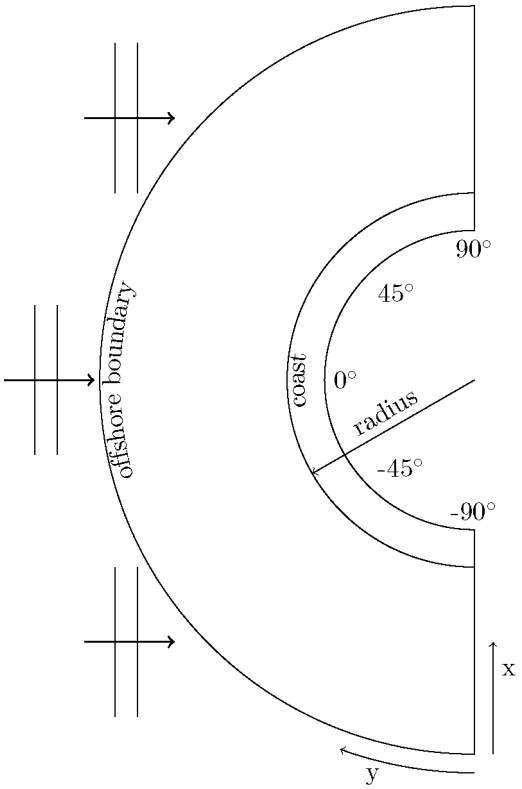

Figure 3.15: Illustration of XBEACH model domain for curved coastline simulations.

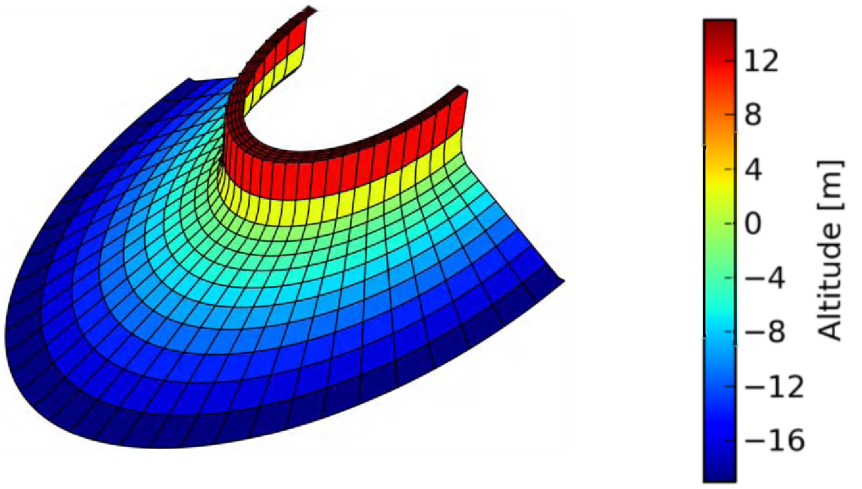

Figure 3.16: Impression of initial bathymetry and curvilinear grid for XBEACH model with curved coastline.

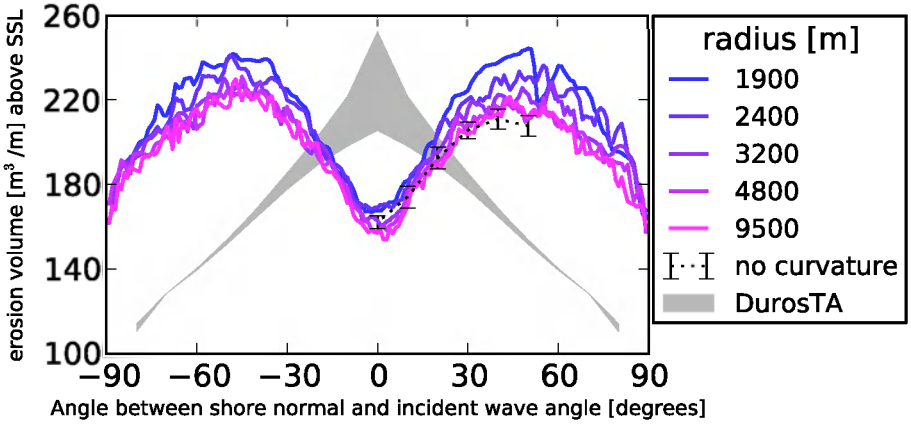

Figure 3.17: XBEACH erosion volume above storm surge level (SSL) as function incident wave angle for various coastal radii. The corresponding DUROSTA results are included in gray.

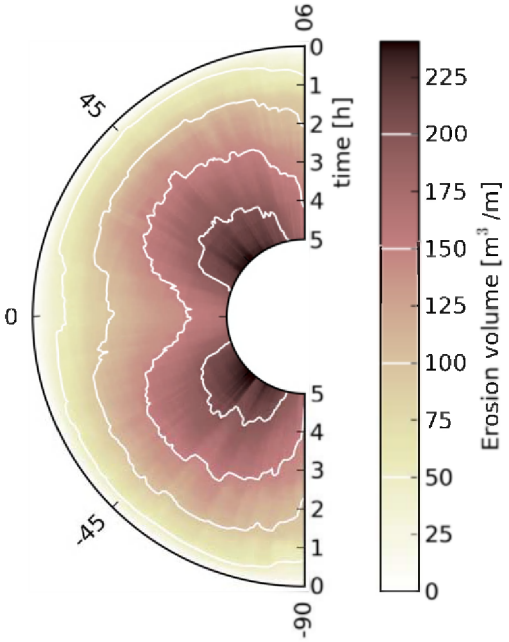

Figure 3.18: Erosion development in time for the whole range of angles.

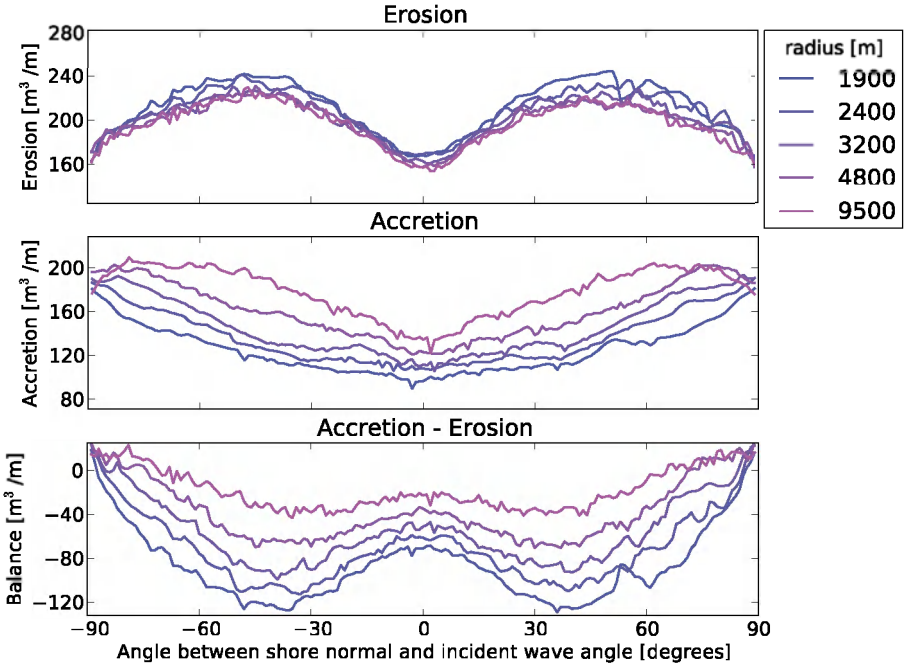

Figure 3.19: XBEACH erosion, accretion and sediment balance as function of the coastline orientation.

show finer wiggles for larger radii. Another reason for the wiggled character of the lines is the morphological acceleration factor (morfac). The results for comparable simulations without this factor (morfac = 1) are similar but much smoother.

The combination of the alongshore transport gradient and the cross-shore (offshore directed) transport should explain the observed erosion-sedimentation patterns. Figure 3.20 shows in the top panel the time averaged cross-shore integrated alongshore transport and in the middle panel the related alongshore transport gradient. The transport gradient is directly related to the sediment balance as depicted in the lower panel of Figure 3.19. The alongshore transport gradient shows a clear dependency on the radius, where the smallest radius results in the largest gradient. In addition, the transport gradient is dependent on the location along the coastal arc. A local minimum is found at 0° and maxima are found at about 30° to 40° off normal. The maxima are more pronounced for the smaller radii, partly because their transport gradients are larger anyway, which can be explained by a smaller adaptation length (a difference of 1° corresponds to a smaller alongshore distance when the radius of the coastline is smaller). The cross-shore transport, which contains the remaining part of the explanation, is presented in the top panel of Figure 3.21. This figure shows the maximum cross-shore transport which is offshore directed (negative). The variation as function of the angle is large compared to the differences between the different radii. The smallest (negative) values are found at normal wave incidence (0°). The differences between the radii are small, but the smaller radii show smaller magnitudes. The largest (negative) values occur between 50° and 70° off normal. The larger radii have their peaks at slightly smaller angles compared to the smaller radii, which is due to the adaptation length in a similar way as observed for the alongshore transport gradient.

The erosion pattern, as shown in the top panel of Figure 3.19, can be explained by the combination of the alongshore transport gradient and the cross-shore transport. The alongshore transport gradient is mainly dependent on the radius, larger gradient for smaller radii, and has its peak at about 30° to 40° off normal. The cross-shore transport is mainly dependent on the angle (location along the arc) and has its peak between 50° and 70° off normal. The slight dependency on the radius shows larger transport for larger radii. The resulting erosion combines these two and shows only minor dependency on the radius and a clear dependency on the location along the arc with maxima around 40° to 50° off normal.

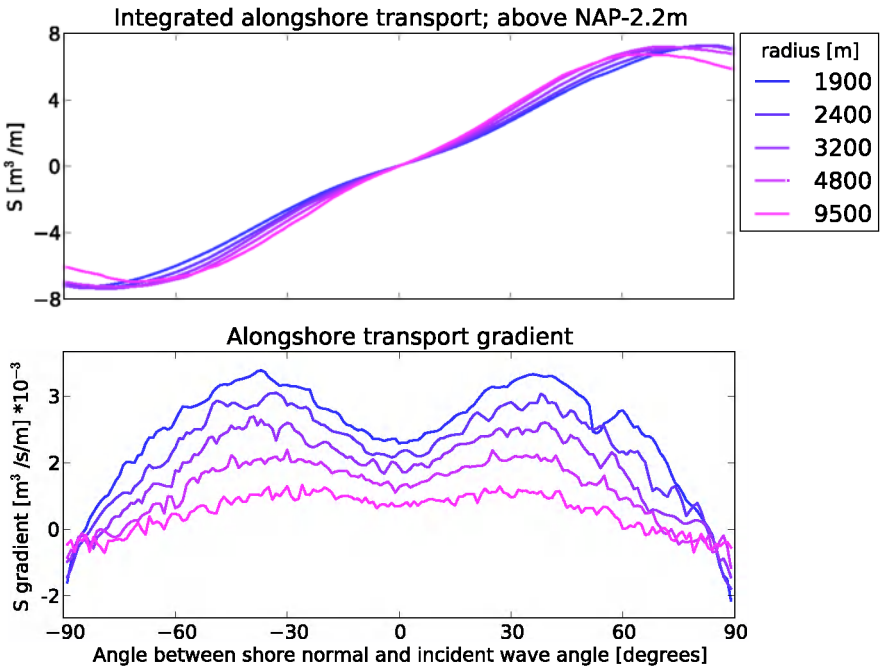

Figure 3.20: Integrated alongshore transport and alongshore transport gradient

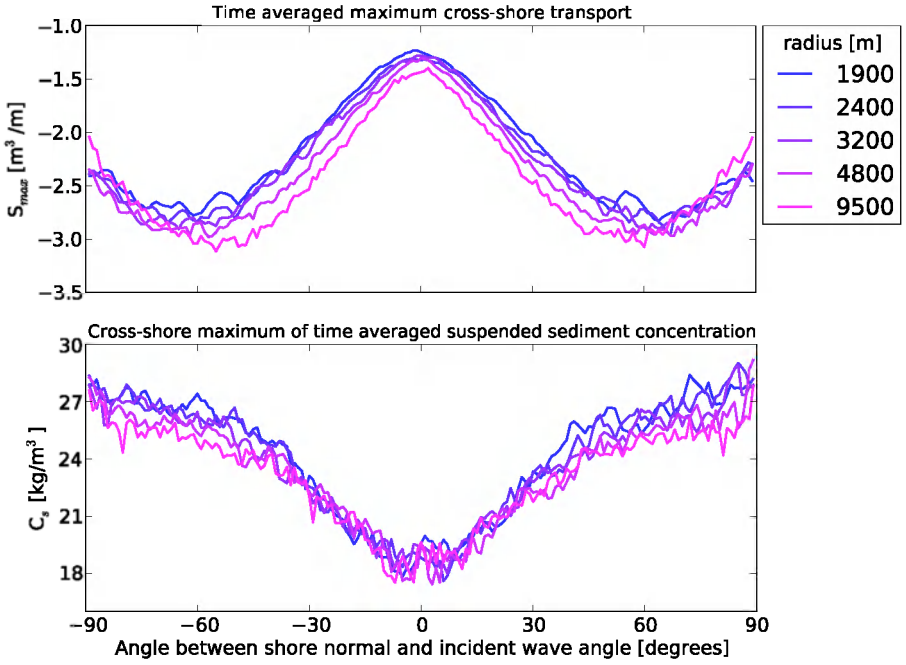

Figure 3.21: Time averaged maximum cross-shore transport and cross-shore maximum of time averaged suspended sediment concentration

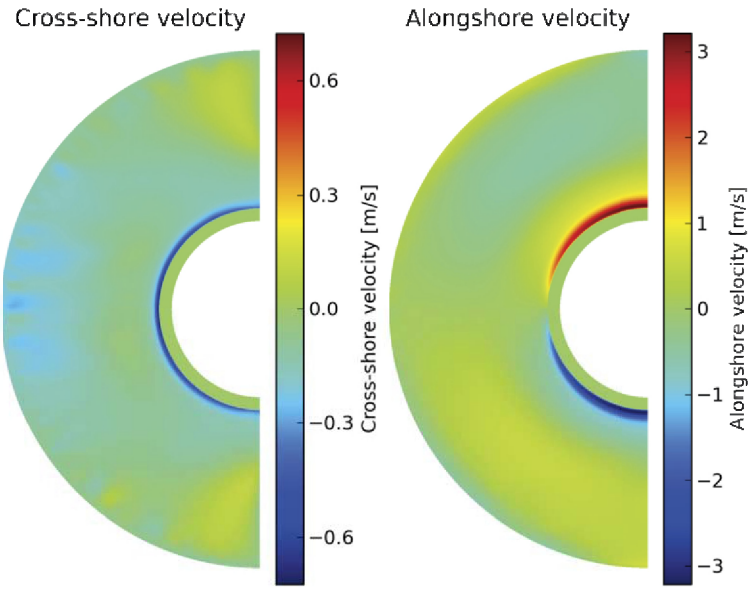

Figure 3.22: Cross-shore and alongshore (w.r.t. local coast orientation) Eulerian flow velocities

To further understand the erosion pattern as observed in the simulations, the flow velocities and suspended sediment concentration that cause the sediment transport (gradients) need to be considered. The peak sediment concentrations along the coast are given in the bottom panel of Figure 3.21. The minimum concentrations are found at normal wave incidence and no clear dependency on the radius is observed. The concentrations increase towards both lateral boundaries, with a steep gradient between 0° and (-)40° and a milder gradient for larger angles. Figure 3.22 shows the time averaged Eulerian flow velocities for one of the simulations. Apart from the scale, this picture looks similar for all investigated radii. The velocities are split in a cross-shore (left panel) and an alongshore (right panel) component. Note that these directions are defined relative to the local coastline. The left panel shows, in a strip along the waterline, offshore directed velocities. The magnitude is approximately constant in the region around normal wave incidence (between about -45° and 45°) and it fades out towards the lateral boundaries. The absence of a clear peak in cross-shore velocities at normal wave incidence can be explained by the 2D behaviour. The demand for water to flow in alongshore direction towards both lateral boundaries needs supply (onshore flow) at the location of normal wave incidence. This onshore flow obstructs the undertow and so prevents the clear peak in the cross-shore (offshore directed) flow velocities. This obstruction effect is also the reason for the relatively limited erosion rate at normal wave incidence. The alongshore velocities in the right panel are zero at the normal wave incidence location and grow both in magnitude and in cross-shore width towards the lateral boundaries. Intercomparison of simulations with different radii leads to the conclusion that generated alongshore currents are mainly dependent on the local angle of wave incidence and hardly on the radius. The maximum alongshore velocities at the lateral boundaries are approximately equal for all investigated radii.

The cross-shore and alongshore velocities, as considered above, are all wave driven since no tidal variation or ambient flow is included. The cross-shore velocities are related to the cross-shore radiation stress component and the wave-related mass flux, resulting in the offshore directed undertow. The alongshore velocities have two driving forces. The alongshore varying wave set-up results in alongshore varying water levels, with maxima around 0° (top panel Figure 3.23). The bottom panel of Figure 3.23 shows the gradients of the water level, that are larger for smaller radii. The larger gradients for smaller radii facilitate the runoff along the coastline leading to lower maximum water levels. The second driving force is the alongshore radiation stress component,

which becomes larger for more oblique incoming waves i.e. towards the lateral boundaries. The latter force is similar for all radii, albeit that the larger radii provide more adaptation length for the refraction process leading to smaller wave angles at the edge of the breaker zone with respect to the local coast normal. As a result the maximum alongshore velocities are slightly smaller for the larger radii.

In summary, the erosion pattern as function of the location along the coastal arc and for different radii, as simulated by XBEACH, can be explained by the combination of alongshore and cross-shore processes. The alongshore transport gradient is mainly sensitive to the coastal radius, with larger gradients for smaller radii. The cross-shore transport is mainly sensitive to the location along the coastal arc. The slight dependency of the cross-shore transport to the coastal radius shows larger transport for the larger radii, which is opposite to the alongshore gradient dependency. Both processes combined lead to an erosion pattern that is primarily dependent on the location along the coastal arc and only slightly on the coastal radius.

3.4.3 Discussion

Similar to the effect of wave obliquity, the two models show an opposite dependence of the dune erosion rate on the coastal curvature radius. DUROSTA accounts in the cross-shore component for the refraction process in the same way as discussed in the wave obliquity section, which gives a maximum at the area with normal wave incidence. From the alongshore component, the alongshore transport gradient is taken into account, leading to an increasing erosion for smaller radii. The latter effect especially holds around normal wave incidence. For larger angles, the nett result of the refraction effect combined with the alongshore transport gradient effect is dominated by the refraction leading to decreasing erosion. 2DH XBEACH simulations have been performed which include the cross-shore and alongshore processes and their interactions. From these simulations the erosion rate appears to be mainly dependent on the location along the curved coastline relative to the offshore wave direction. In addition to the alongshore transport gradient, additional stirring of the sediment due to the wave generated alongshore flow plays in important role. Taking these processes into account, the dependency on the coastal orientation relative to the offshore wave direction is of major importance. Maximum erosion is found at an angle of 45°.

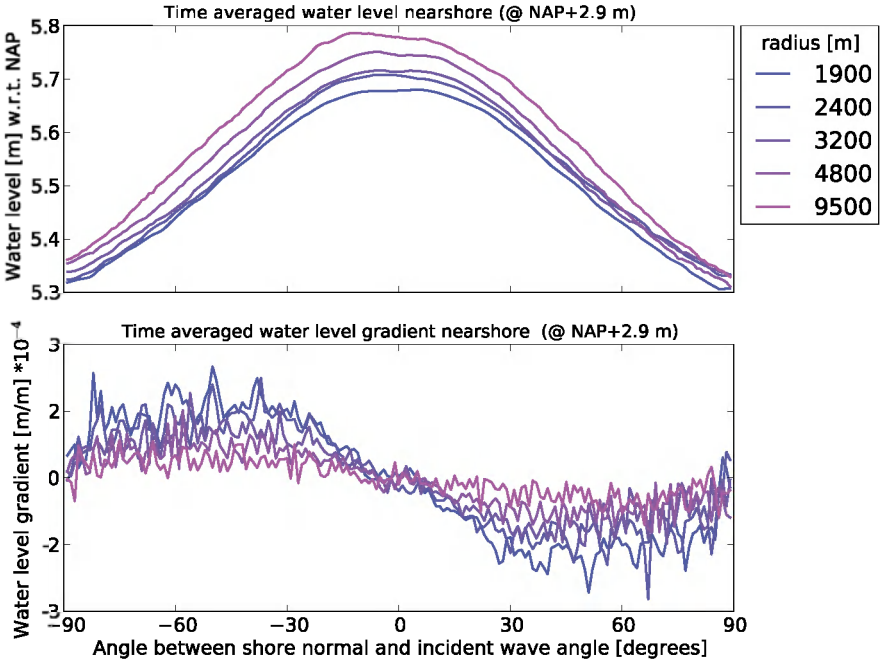

Figure 3.23: Nearshore time averaged water level along the coastline and its gradient

The dune erosion process along curved coastlines differs in a few aspects from the regular cross-shore processes. First of all, large alongshore flow velocities occur. Secondly, these velocities vary alongshore, leading to an alongshore gradient in alongshore transport. Thirdly, the wave set-up is alongshore varying, resulting in alongshore water level gradients near the coastline. This leads to alongshore varying loading and is an additional mechanism for generating alongshore flow.

All of the above mentioned additional processes are related to the alongshore dimension and include gradients along that dimension. The interactions between cross-shore and alongshore processes also play an important role. The 2DH XBEACH simulations do include these processes which are considered essential for proper modelling of dune erosion at curved coasts. The XBEACH results are selected for further use in the probabilistic investigations in Chapter 4 and 5.

3.4.4 Conceptual coastal curvature model

At curved coastlines, the alongshore processes and the interactions with the cross-shore processes are even more important than for straight coasts with oblique waves. In this section a conceptual model is introduced, similar to the wave obliquity model (Section 3.3.4), in order to provide insight in the relative influence of alongshore and cross-shore processes respectively.

Where at a straight coast the alongshore velocities can be described by $sin2\phi$, at a curved coastline $sin\phi$ appears to be a better representation. For the curved coastlines as considered here, the refraction process is 'lagging behind' because there is not only refraction but also the 'curving away' of the coastline. The alongshore velocities tend to keep growing towards an angle of 90°. The cross-shore velocities have their maximum at shore normal wave direction (0°) and fade away towards 90°, similar to a cosine shape ($cos\phi$). When assuming the influence of coastal curvature to be an interaction between cross-shore and alongshore processes, being expressed in the product of those two terms, a shape like illustrated in Figure 3.24 originates. This shape coincides approximately with the upper bound of the XBEACH results represented by the gray patch. The well-known CERC formula (Coastal Engineering Research Center, 1984), describing the alongshore component of the energy flux in the surf zone, includes a similar $sin2\phi$ term. The latter formula is, however, developed for non-curved coastlines. This suggests that the shape (not the

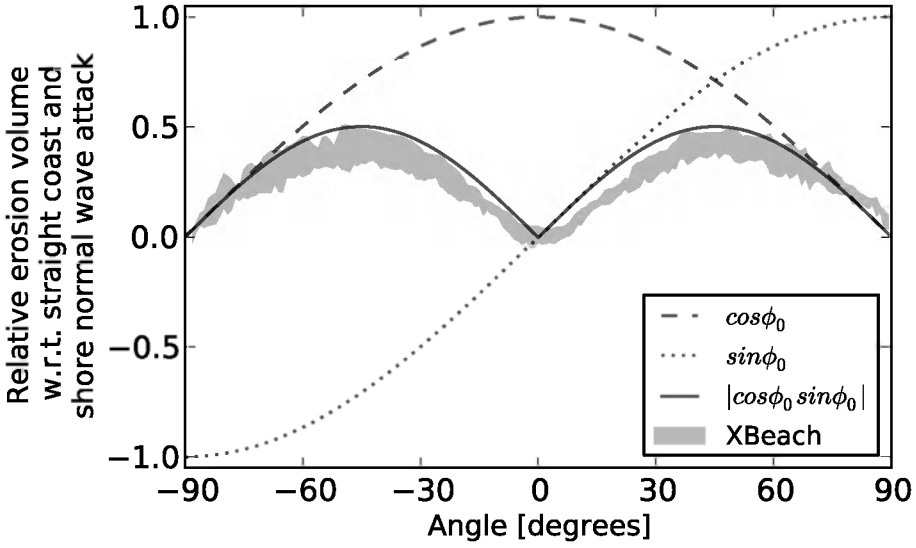

Figure 3.24: Illustration of the product of sine and cosine as contribution for the alongshore respectively cross-shore processes along a curved coastline. The XBEACH results relative to the reference have been included for comparison.

magnitude) of the erosion pattern along a curved coast is similar to the pattern of the energy flux alongshore component only, along a straight coast.

Compared to the similar approach for straight coasts with oblique waves (Figure 3.13) the angle at the peak increases to 45° and the maximum magnitude increases to 50 %. The two features, a higher peak at a larger wave angle, are in accordance with the XBEACH results for wave obliquity and coastline curvature respectively. This conceptual model approximately coincides with the XBEACH results for the smallest investigated curvature radius of 1900 m. This suggests that for this small radius, the importance of cross-shore and alongshore processes is about equivalent. The conceptual model is overestimating for the larger radii, which indicates that it overestimates the influence of the alongshore component in those cases.

Chapter 4

Probabilistic analysis

This chapter investigates, in probabilistic terms, the effect of the inclusion of wave obliquity and coastal curvature. The XBEACH results on these aspects, as obtained in the previous chapter, are utilised here in a probabilistic framework. A baseline is established for the 1×10^{-5} year^{-1} erosion rate using the FORM reliability method and the DUROS+ dune erosion model. The probabilistic sensitivity for the basic stochastic variables, such as storm surge level and wave conditions, is compared for DUROS+ and DUROSTA around the baseline conditions. As a preparation for the inclusion of more stochastic variables and processes at a later stage, FORM simulations with XBEACH as a dune erosion model are also presented. These simulations expose the threat of FORM convergence issues that are related to its combination with the process based XBEACH model. In addition, this approach needs a large number of simulations per cross-shore transect, being a practical drawback when using a computational-intensive model. Hence, to cope with computational-intensive models in practical applications, a Bayesian Network model is introduced, which is built and validated against DUROS+ results, in order to demonstrate its applicability. Here it is based on model data only, but the method is suitable to combine model, laboratory and field data. In the second part of this chapter, two approaches are followed to include the wave obliquity and coastal curvature. First, the change in the impacts of the 1×10^{-5} year^{-1} erosion rate is estimated with FORM when wave obliquity and different coastal radii are included. In the second step, the Bayesian Network model is used to estimate

the relative influences of wave obliquity and coastal curvature with respect to the reference case. The latter model will be applied in the next chapter for the estimation of the impact of wave obliquity and coastal curvature on the dune failure probability.

4.1 Present approach with FORM[1]

This section describes the application of the reliability method FORM in combination with DUROS+, DUROSTA and XBEACH to a reference case. The 1×10^{-5} year^{-1} erosion rate is estimated with the various models and the related design points are compared. First, the applications with DUROS+ and DUROSTA are extensively discussed, including a probabilistic sensitivity analysis. The parameters of the probability distributions in the model are varied in order to investigate the sensitivity of the dune erosion rate. Second, the XBEACH application is discussed, which initially led to convergence issues in FORM. The measures, needed to overcome the convergence issues, are described. Due to the persistence of the threat for FORM convergence issues and the computational cost of the XBEACH simulations, a comprehensive sensitivity analysis was not feasible. The encountered issues illustrated the limitations of FORM and the need for a different probabilistic approach when applying advanced dune erosion models.

4.1.1 Model setup

The probabilistic model, described in this section, uses the (deterministic) model setup from Section 3.1 as a starting point. The same reference cross-shore profile is used (see Figure 3.1). As opposed to the deterministic approach in Section 3.1, here the input for the dune erosion model is retrieved from probability distributions. These distributions are obtained from WL | Delft Hydraulics (2007) using the statistics for the Hoek van Holland area as summarised in Table 4.1.

[1] This section is mainly based on Den Heijer et al. (2008a,b).

Variable	Mean	Standard Deviation	Distribution type
Water level (h)	$f(P_e)$ Equation 4.2, 4.4	-	Conditional Weibull
Wave height (H_s)	$f(h)$ Figure 4.2	0.6 m	Normal
Wave period (T_p)	$f(H_s)$ Figure 4.2	1 s	Normal
Grain size (D_{50})	225 µm	$0.1 \times \mu_{D_{50}}$ (22.5 µm)	Normal
Surge duration	0	$0.1 \times A$	Normal
Model accuracy	0	$0.15 \times A$	Normal

Table 4.1: Probability distributions (WL | Delft Hydraulics, 2007) for the reference case.

Water level The frequency of exceedance of the water level is described by a conditional Weibull distribution:

$$F_e(H > h) = \rho \exp\left[-\left(\frac{h}{\sigma}\right)^{\alpha} + \left(\frac{\omega}{\sigma}\right)^{\alpha}\right] \tag{4.1}$$

where:

h	maximum water level during a storm surge [m] above NAP
F_e	frequency of exceedance of h [year^{-1}]
α	shape parameter that depends on the location along the coast
ω	threshold above which the function is valid [m] above NAP
σ	scale parameter that depends on the location along the coast
ρ	frequency of exceedance of the threshold level ω

Rewriting Equation 4.1 to make h explicit yields:

$$h = \sigma\left[\log(\rho) + \left(\frac{\omega}{\sigma}\right)^{\alpha} - \log(F_e(H > h))\right]^{\frac{1}{\alpha}} \tag{4.2}$$

The probabilistic framework uses a probability (P) instead of a frequency (F_e), requiring conversion of the expression. To convert the frequency of exceedence (F_e) to a probability (P) or probability of exceedance (P_e) the Poisson formula (Ross, 1987) is be used:

$$P[N(t) = n] = \frac{e^{-\lambda t}(\lambda t)^n}{n!} \tag{4.3}$$

where:

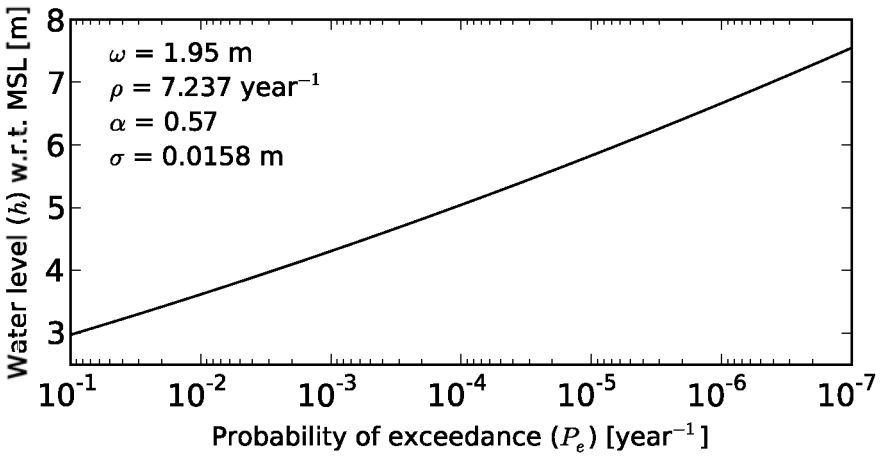

Figure 4.1: Water level as function of probability of exceedance (Equation 4.2 with parameters for Hoek van Holland).

$N(t)$	number of observations per unit of time [year^{-1}]
n	number of observations
λ	average number of occurrences per unit of time ($= F_e$) [year^{-1}]
t	time [year]
P	Probability of occurrence ($= 1 - P_e$) [year^{-1}]

The probability of exceedance ($P_e = 1 - P$) can be found using P from Equation 4.3 with $n = 0$, $\lambda = F_e$ (taken from Equation 4.2) and $t = 1$ as input. As a result, various terms disappear because they become one and the relation between probability of exceedance and frequency of exceedance yields:

$$P[N(t) = 0] = \frac{e^{-\lambda t}\cancel{(\lambda t)^0}}{\cancel{0!}} = e^{-F_e} = 1 - P_e \tag{4.4}$$

By applying the parameters α, ω, σ and ρ as derived for Hoek van Holland, Figure 4.1 is found. For water levels larger than MSL + 3 m ($P_e < 10^{-1}$ year^{-1}) the difference between F_e and P_e is considered negligible.

Wave height The wave height is correlated to the water level because during storms their common driving force is wind. The stochastic properties of the

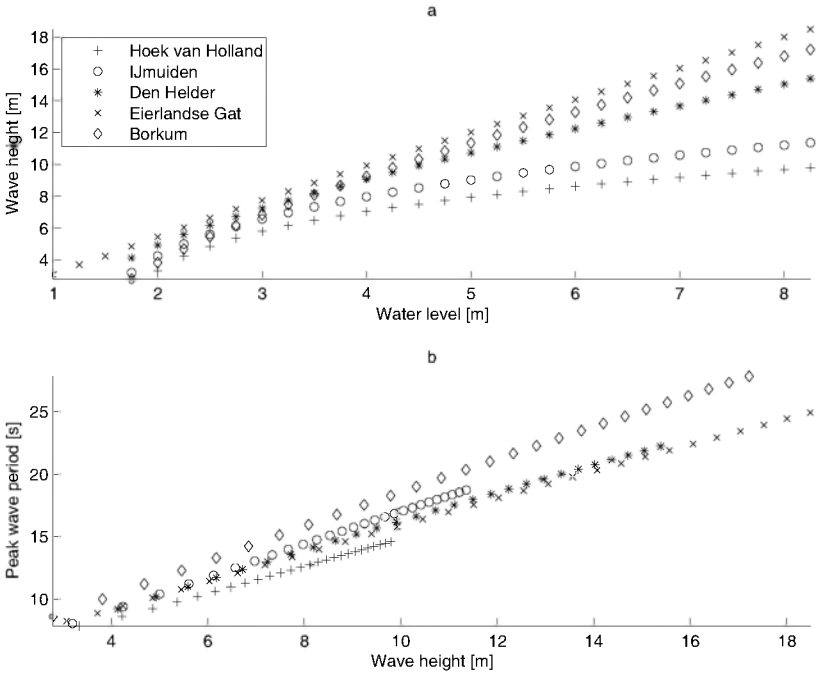

Figure 4.2: (a) Mean wave height as function of water level. (b) Mean peak wave period as function of wave height.

wave height are described by a normal distribution. The mean value is based on the work of Stijnen et al. (2005), that relates water level and wave height for five locations along the Dutch coast, including Hoek van Holland (see Figure 4.2 panel a). The standard deviation has a constant value set at 0.6 m, following Van de Graaff (1986).

Wave period The wave period is correlated to the wave height, and thus indirectly to the water level. Also the wave period's stochastic properties are described by a normal distribution. Again the mean value is obtained according to a relation from Stijnen et al. (2005), as shown in Figure 4.2 panel b. The standard deviation is set to one second.

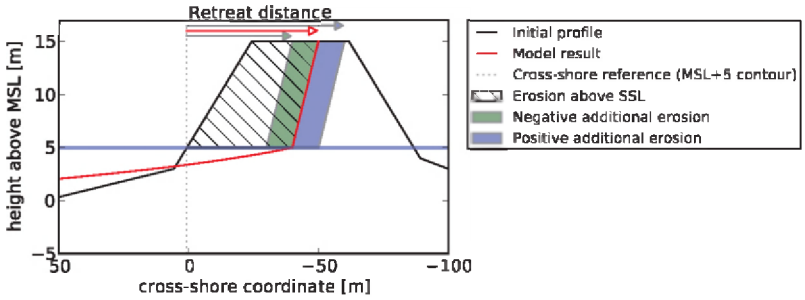

Figure 4.3: Illustration of additional erosion and definition sketch of retreat distance; the arrows indicate three examples of the retreat distance for respectively positive, zero and negative additional erosion.

Grain size Grain size distributions have been derived from sediment samples at 146 locations along the Dutch coast (TAW, 1984). Although it is unclear where in the cross-shore these samples have been taken, they are assumed to be representative for the entire cross-shore profile. Acquiring a higher level of spatial detail of the grain size could only be useful if the measurement density is sufficient and the model in use is capable of taking the spatial variation into account. The D_{50} grain sizes that can be derived from these samples are assumed to be normally distributed. The mean and standard deviation for Hoek van Holland are respectively 225 µm and 22.5 µm.

Surge duration The DUROS+ erosion is developed to represent an average representative storm duration, but does not include the storm duration explicitly. Hence, an additional erosion volume is introduced as a proxy for the influence of surge duration. The magnitude of the additional erosion is described by a normal distribution with a mean of zero and a standard deviation of 10 % of the erosion above storm surge level. In order to keep the inter-comparison between the models consistent, this approach is also followed for DUROSTA and XBEACH, although the latter models are capable of taking the storm duration explicitly into account. For the DUROSTA and XBEACH simulations, constant conditions with a duration of 5 h are applied.

The additional erosion volume is allocated by moving the dune front (above maximum storm surge level) horizontally with respect to its originally simulated position (see Figure 4.3). A positive additional erosion leads to landward

movement, implying more dune retreat, whereas a negative value reduces the dune retreat.

Model accuracy The model accuracy is, similar to the surge duration, implemented as a normally distributed additional erosion volume. Again the mean value is zero, but the standard deviation is in this case 15 % of the initially simulated erosion above maximum storm surge level.

The sensitivity analysis is performed on the 1×10^{-5} year^{-1} retreat distance (see Figure 4.3), being defined as the horizontal distance between the MSL + 5 m contour and the intersection of the simulated post-storm dune front and the pre-storm profile (Van de Graaff, 1986). The First Order Reliability Method (FORM), available within the probabilistic toolbox Prob2B (Courage and Steenbergen, 2005) as well as in OpenEarth (Den Heijer, 2012a), has been applied to derive the probability of exceedance for a predefined threshold value of the retreat distance. This threshold value can be considered as the (artificial) limit state, realizations resulting in larger retreat distances are identified as failure. The FORM procedure searches for the design conditions that approximately result in the threshold retreat distance and provides the probability the corresponds to these conditions. Iteratively, the 1×10^{-5} year^{-1} retreat distance can be derived.

The probability distributions as summarised in Table 4.1 are used as a reference situation. With respect to that reference, the characteristics of the probability distributions are altered, leading to a change in the 1×10^{-5} year^{-1} retreat distance. For the altering of the normal distributions, both the mean and the standard deviation have been increased and decreased. The standard deviations are varied between zero (i.e. deterministic) up to 133 % or 200 % of its reference value depending on the variable. The water level distribution has been altered in a way that the resulting water level for all probabilities is increased or decreased with a fixed value, varying between ± 0.5 m. For each set of altered probability distributions, the 1×10^{-5} year^{-1} retreat distance has been recalculated in order to represent the sensitivity.

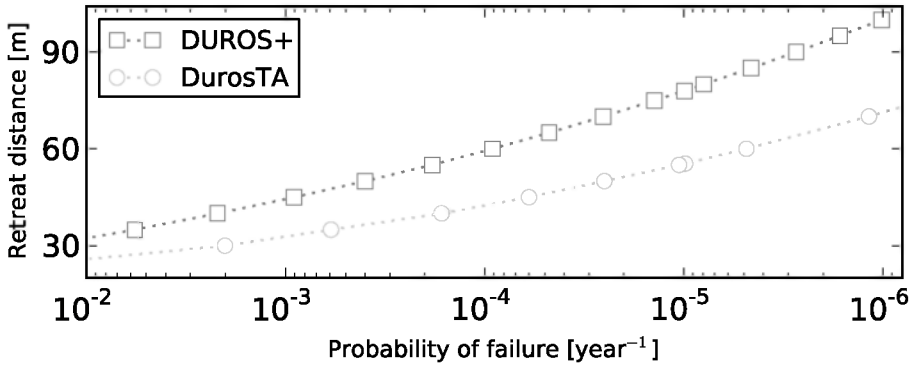

Figure 4.4: Probability of exceedance.

4.1.2 Resulting probability of exceedance

Figure 4.4 shows for both DUROS+ and DUROSTA the probability of exceedance for a series of retreat distances. The 1×10^{-5} year^{-1} retreat distance is 78 m for DUROS+ and 55 m for DUROSTA. These realisations serve as reference case in the sensitivity analysis presented in the next section.

The results for the 1×10^{-5} year^{-1} retreat distance are considered in more detail based on the design points and variable importances as presented in Table 4.2. As an indicator for the variable importance, the sensitivity coefficients α (see Section 2.4.2) are shown in the table. The design points and importances are similar for both models. The water level turns out to be by far the most important variable. A large importance for the water level can be expected based on its deterministic sensitivity (Figure 3.2), but the outstanding importance is closely related to the probabilistic model setup. The wave height distribution (mean) depends on the water level, and the wave period distribution (mean) in turn on the wave height. As a result, a high water level leads automatically to larger wave heights and longer wave periods. The distributions of wave height and wave period only have a marginal influence, compared to the water level. The advantage of this model choice is that these three distributions can be considered as independent by the probabilistic method. The disadvantage is the overestimation of the importance of the water level. In reality, the wind induces both surge and waves (height and length).

model retreat distance	DUROS+ 78 m		DUROSTA 55 m	
	value	$\alpha^2 \times 100\ \%$	value	$\alpha^2 \times 100\ \%$
Water level	5.52 m	90.5	5.49 m	89.6
Grain size	208 µm	3.3	208 µm	3.3
Accuracy	$0.12 \times A$	3.3	$0.12 \times A$	3.8
Duration	$0.05 \times A$	1.5	$0.06 \times A$	1.7
Significant wave height	7.94 m	1.3	7.85 m	0.7
Peak wave period	12.7 s	0.2	12.9 s	1.0

Table 4.2: Variable values in the design points, for the 1×10^{-5} year^{-1} retreat distance, and importance of variables.

4.1.3 Resulting sensitivity

To get more insight in the sensitivity of the 1×10^{-5} year^{-1} retreat distance for the individual distributions and its parameters, the results of a probabilistic sensitivity analysis are presented in the Figure 4.5. The markers represent the calculated 1×10^{-5} year^{-1} retreat distances; the solid markers represent the reference cases. Figure 4.5 (a) through (c) are the most sensitive variables, whereas Figure 4.5 (d) is an arbitrary example of the other characteristics to which the retreat distance is hardly sensitive.

Figure 4.5 (a) shows the sensitivity of the 1×10^{-5} year^{-1} retreat distance for the water level distribution. The probability distribution has not been changed, but the resulting water level has been altered with an offset for all probabilities. The wave height (and wave period) are related to the original (reference) water level distribution, to make sure that the resulting differences are caused by the water level only. As clearly appears from this figure, the water level has significant influence on the 1×10^{-5} year^{-1} retreat distance for both DUROS+ and DUROSTA. In fact, this investigation could be seen as some kind of fictitious sea level change. However, in case of real sea level change, it will change gradually, allowing the profile to adapt itself (Bruun, 1962). This adaptation has, depending on the rate of sea level change, a reducing effect on the presented sensitivity.

Figure 4.5 (b) shows a decreasing 1×10^{-5} year^{-1} retreat distance for larger values of the mean grain size. For a correct interpretation of this figure, it should be realised that the standard deviation of the grain size is relative

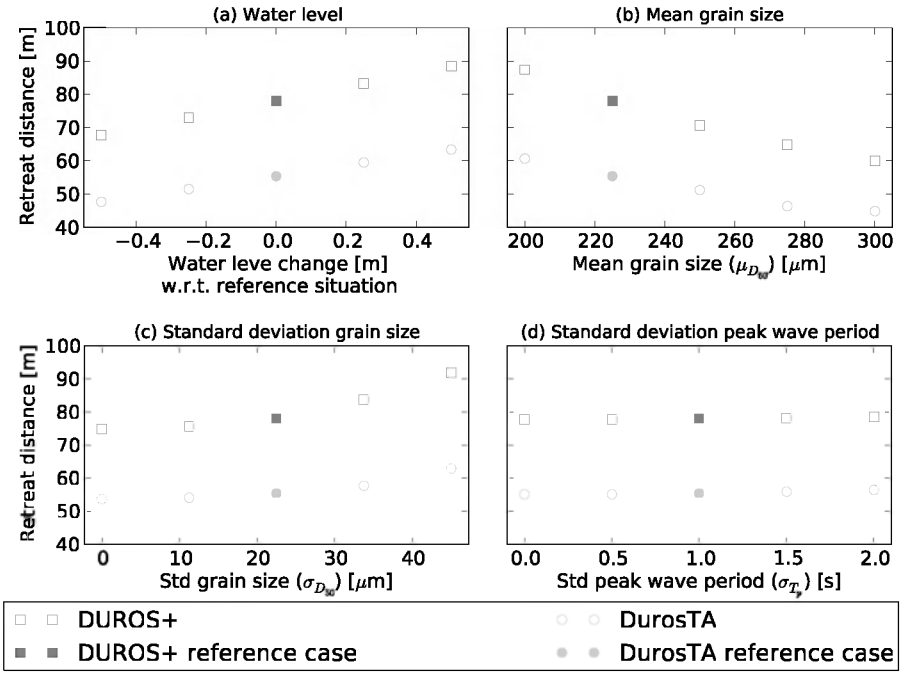

Figure 4.5: Probabilistic sensitivity results (solid markers represent reference case).

to the mean grain size ($\sigma_{D_{50}} = 0.1 \times \mu_{D_{50}}$). A larger mean grain size will therefore implicate in this investigation a larger standard deviation, in absolute terms. Increasing the standard deviation separately, will result in larger retreat distances, as follows from panel (c) of Figure 4.5. Despite this counteracting effect of the standard deviation, the mean grain size still shows a clear dependency. In practice, the mean grain size will be related to the cross-shore profile slope. Courser grains will allow steeper slopes, which in turn will lead to more erosion, being another counteracting effect which is not accounted for. The rather strong dependency on the grain size seems to conflict with the the relatively low sensitivity coefficients in Table 4.2. Due to the relation between water level, wave height and wave period, the water level gets an artificially high sensitivity coefficient (around 90 %). Since the α^2 of all variables by definition sum up to one ($\sum_{i=1}^{n} \alpha^2 = 1$), such a high value for the water level coefficient implies low values for the coefficient of the other variables. It is remarkable that despite the α^2 of the grain size being way lower than the one of the water level, still the retreat distance shows a strong dependency to the grain size. This illustrates that in cases with artificial independent variables (which are physically dependent), the sensitivity coefficients are not always reliable.

Increasing standard deviation of the grain size leads to larger $1 \times 10^{-5}\,\text{year}^{-1}$ retreat distances as expressed in Figure 4.5. This dependency is especially present for standard deviations larger than the reference value of 22.5 µm.

Finally, Figure 4.5 (d) shows the sensitivity of the standard deviation of the $1 \times 10^{-5}\,\text{year}^{-1}$ retreat distance to the peak wave period, being an arbitrary example of one of the stochastic properties that hardly influence the $1 \times 10^{-5}\,\text{year}^{-1}$ retreat distance. This does not mean that this variable is unimportant. However, within this range and in the context of the other stochastic variables, no significant sensitivity is observed.

4.1.4 XBEACH

This section describes a series of FORM calculations using XBEACH as dune erosion model. As opposed to the previous section, where also the sensitivity of the models for various distribution properties is described, here the main focus is on the design point comparison. Initial convergence problems of the FORM algorithm, when combined with XBEACH, are discussed. A similar probabilistic sensitivity analysis as presented in the previous section with

DUROS+ and DUROSTA was not feasible.

A relative computationally expensive dune erosion model like XBEACH requires an efficient reliability method in order to keep the overall computational cost of the probabilistic approach acceptable. The FORM method is potentially applicable but has the drawback that it cannot cope with discontinuities (Grooteman, 2011). The erosion rate as function of the (stochastic) forcing variables, included in the model, should be continuous. This requirement can potentially be violated when using XBEACH. Since the model includes the process of episodic slumping, the erosion in time shows a staircase shape on a short time scale. In addition, the wave time series is a random realisation based on the wave spectrum which can vary between simulations. All together, the resulting gradient of the erosion rate to the forcing variables, based on sets of two simulations with slightly different input, can easily behave irregularly. As a result, the FORM algorithm potentially runs into convergence issues.

The starting point for the FORM simulations with XBEACH as dune erosion model are similar to those described in Section 4.1.1. The only difference is that the contributions for the surge duration and model accuracy are not taken into account as stochastic variables. These contributions are set to deterministic values of zero. The XBEACH simulations are performed with constant conditions for a duration of 5 h, similar to those presented in Section 3.1.

Initially, there were a few issues that prevented FORM to converge, when using the default settings. The convergence of FORM could be improved by choosing a fixed random seed which leads to a similar wave time series for each simulation. A second issue that prevented convergence was found in the weak but irregular sensitivity of the erosion rate to the grain size, in XBEACH. As a result, the grain size gradient could be alternately positive and negative, preventing FORM to converge. Because of the weak sensitivity (according to XBEACH), it is considered acceptable to assume the grain size to be deterministic in order to prevent this problem. Finally, convergence plots showed converging and stable tendency, but just insufficient to meet FORM's default convergence criteria. With the threshold ϵ_Z set to 0.5 m, convergence could be reached in most of the simulations. The ϵ_Z prescribes the maximum deviation of the resulting retreat distance from the predefined one. The resulting probability of failure for a number of retreat distances is shown in Figure 4.6. The cases where FORM did not converge, are indicated. Although the convergence criteria were not met in some of the cases, all points

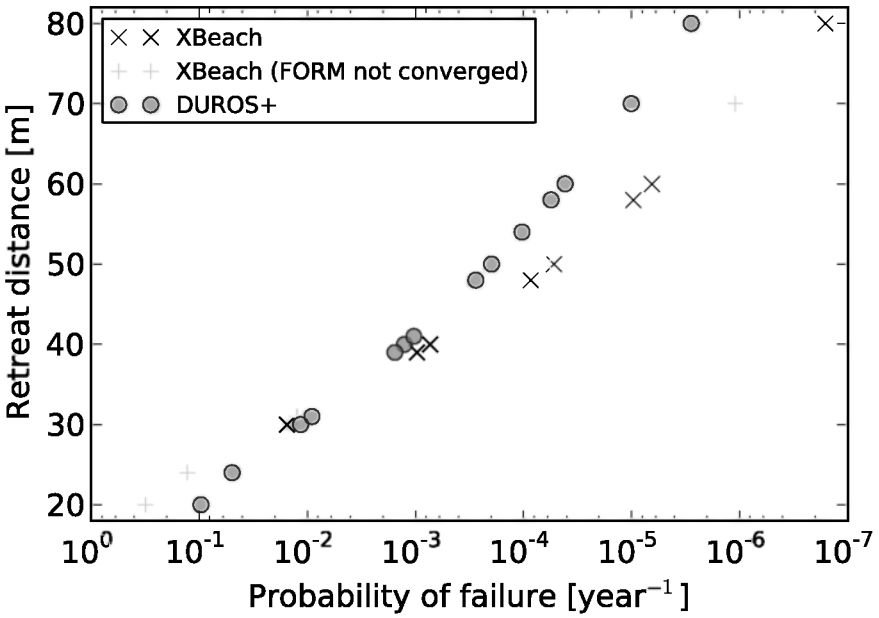

Figure 4.6: Retreat distance as function of the Probability of failure for respectively XBEACH and DUROS+.

are still reasonable in line with the others. The XBEACH and DUROS+ curves have a significantly different slope compared to the DUROS+ with DUROSTA comparison (see Figure 4.4) and intersect around $1 \times 10^{-2}\,\text{year}^{-1}$.

The design point results of the $1 \times 10^{-5}\,\text{year}^{-1}$ simulation, that corresponds to a retreat distance of 58 m, are presented in Table 4.3. The corresponding DUROS+ retreat distance[2] is 70 m. It can be concluded that the erosion rates differ between both models, but the related variable values in the design points are nearly the same.

[2]This result differs from those in Table 4.2 in the sense that only three stochastic variables are included.

Model	XBEACH		DUROS+	
Retreat distance	58 m		70 m	
	value	$\alpha^2 \times 100$ %	value	$\alpha^2 \times 100$ %
Water level	5.78 m	98.0	5.78 m	98.6
Significant wave height	8.1 m	1.2	8.1 m	1.2
Peak wave period	13.1 s	0.8	12.9 s	0.2

Table 4.3: Variable values in the design points, for the 1×10^{-5} year^{-1} retreat distance, and importance of variables for the XBEACH case as well as for the corresponding DUROS+ case.

4.1.5 Conclusion

In the preceding sections, probabilistic investigations with the FORM reliability method have been described. The method is powerful in the sense that that a design point can be found with a relatively limited number of samples. For a successful application of FORM, the probabilities and the limit state functions must be continuous. The application with XBEACH illustrated the limitations of FORM when using an advanced dune erosion model. To be able to assess the dune safety at complex dune areas, where advanced dune erosion models are required, another probabilistic method is needed.

4.2 Present approach with Bayesian Network[3]

This section describes an investigation on the usefulness of Bayesian Networks in the safety assessment of dune coasts, as an alternative to the FORM approach discussed in the previous section. A network is described that successfully predicts the erosion volume based on hydraulic boundary conditions and a number of cross-shore profile indicators. Field measurement data along a large part of the Dutch coast, together with simulated dune response under extreme conditions, is used to train the network. The storm impact on the dunes was calculated with the DUROS+ model.

Four steps need to be taken to create a Bayesian Network model: data gathering, network construction, training and validity checking. The steps are interlinked with each other, because the required data depends on the nodes

[3]This section is mainly based on Den Heijer et al. (2012) and Knipping (2012).

in the network. In addition, depending on the results of the validity check, the steps may be repeated in order to reach satisfactory results. This section provides more detailed information about the steps and the related model choices.

4.2.1 Model setup

For this research, Dutch cross-shore transects of bed levels together with corresponding offshore wavebuoy data and grain size, serve as input to the Bayesian Network model. The model is developed to predict dune erosion volumes due to an extreme storm event described by its hydraulic boundary conditions and given the local cross-shore profile.

The data needed for the training of the Bayesian Network can be divided in three categories, specified in Table 4.4. Cross-shore profiles along the Dutch coast are available in the JARKUS dataset. For generation of the data, cross-shore profiles at the same coastal areas as selected by Den Heijer et al. (2011) have been used (see Figure 5.3). The hydraulic boundary conditions have been sampled from probability distributions as obtained from WL | Delft Hydraulics (2007) (see Table 4.1). The dune response data has been gathered based on simulations with DUROS+ (Van Gent et al., 2008).

Figure 4.7 gives an overview of the Bayesian Network with the nodes (variables) and their relations (edges). The main variable of interest is the erosion volume. The erosion volume is used here as indicator because of its generalisability, which is useful in the Bayesian Network application where a large number of transects are included. The retreat distance, which was used in the FORM applications in the previous section, is much more cross-shore profile (thus location) specific.

The erosion volume is dependent on several loading and strength variables. The loading variables are described by probability distributions. The strength variables are related to the coastal area and need to be derived from individual cross-shore profiles. In addition to the grain size (Table 4.1), four profile indicators are defined to characterise the cross-shore profile, illustrated in Figure 4.8:

1. Profile volume, V_{prof}
   Profile volume enclosed by horizontal reference levels MSL+3m (dune foot) and MSL-4m, together with the vertical boundaries landward and

Type	Data	Source
measured	profile information	JARKUS
extrapolated	hydraulic boundary conditions	WL | Delft Hydraulics (2007)
modelled	coastal response to a storm	DUROS+ (Van Gent et al., 2008)

Table 4.4: Types of data that serve as input for the Bayesian Network.

seaward of the intersection of the horizontal reference levels with the initial bottom profile. (Green box in Figure 4.8) This area indicates the potential accretion volume and is independent of dune height.

2. Slope of V_{prof}, s_{vol}
   Slope of the volume as indicated in profile indicator 1 (dotted line). This slope is comparable to the foreshore slope and is added to give more information of the shape of the profile volume.
3. Beach width, W_b
   Beach width is the cross-shore distance between the crest of the first dune row and the shoreline. So, in fact here the beach width represents the regular beach width extended with half of the first dune row width.
4. Maximum crest level of first dune row, z_c
   Maximum crest level of the first dune row. The dune height is an important indicator of the strength of a dune, since it gives information about the dry volume of sand.

The network needs to be trained, after the data gathering and the construction of the network. Training is performed by feeding cases to the network in order to establish the conditional probabilities. A case is a set of (node) variable values that correspond to each other. It is important to realise that the predictions cannot go beyond the data ranges of the nodes and also cannot cover combinations that are not in the training dataset. In that respect, the difference between the Holland coast and the Wadden area is relevant. The Holland coast is a mainly closed and approximately straight without deep channels and with only limited variation in foreshore slope. The Wadden coast, on the contrary, consists of a series of barrier islands with very mild sloped areas but also deep channels at some locations.

After the training of the network, a validity check has to be done. The term validity, in the present application, defines the degree to which the Bayesian Network can represent the dune response to a storm event as modelled by DUROS+. If the sensitivity of the Bayesian Network reproduces the anticipated

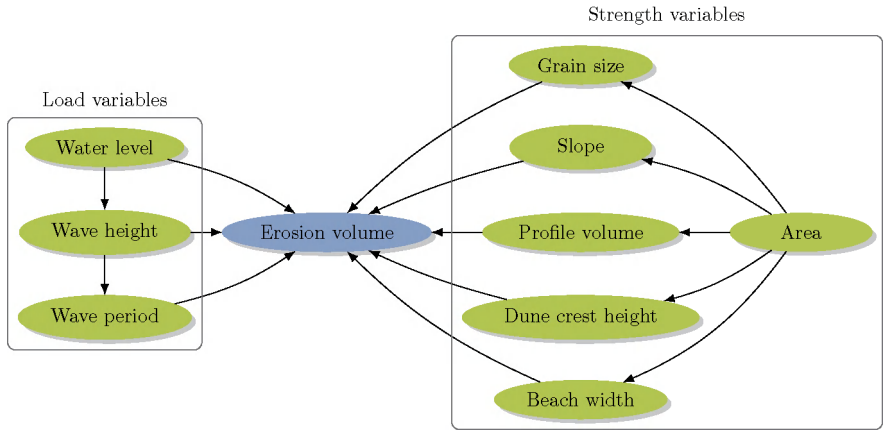

Figure 4.7: Overview of the Bayesian Network.

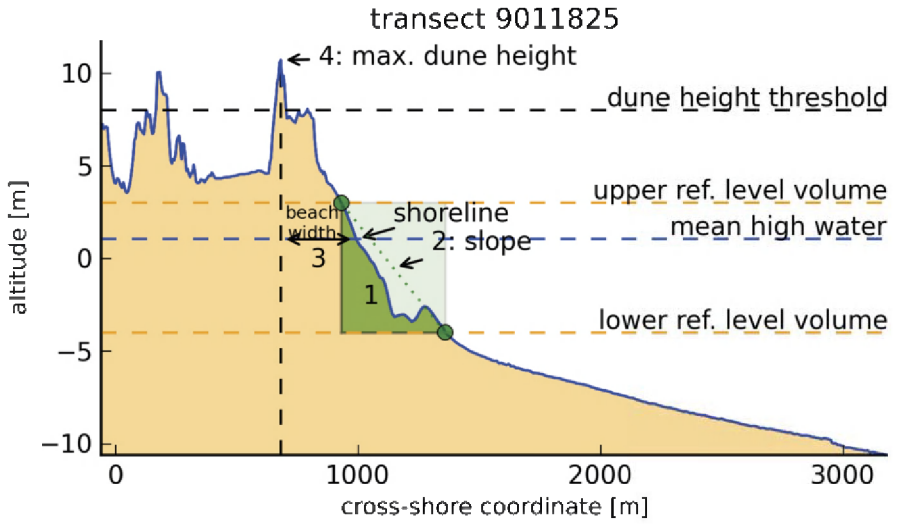

Figure 4.8: Profile indicators for an arbitrary pre-storm cross-shore profile. The numbers correspond to the numbers in the list of profile indicators.

behaviour, then the model has *face validity*. For instance, one would expect a generally smaller grain size at the *Wadden area* with respect to the *Holland* coast, based on the underlying data (TAW, 1984). In addition, a high erosion volume should generally correspond to a high water level.

In addition to the face validity, that can be considered as a first check, the prediction skill of the network needs to assessed in a hind cast. To that end, the predicted erosion volumes by the Bayesian Network are compared to the erosion volumes as calculated by DUROS+, considered as observations in this section. To determine the degree to which the Bayesian Network can recover the simulated erosion volume (morphological change) and whether its uncertainty estimates are consistent with the actual prediction errors, two evaluation methods will be used. First, the prediction skill will be quantified using a simple linear regression model relating predictions to the actual observations (in our case DUROS+ calculations). Second, the prediction skill is quantified by evaluating the likelihood of each observation, as predicted by the Bayesian Network, and comparing this likelihood to the prior likelihood. Both methods will be explained in detail below. The methods will be applied to hind cast predictions using the training dataset to update some of the variables (e.g. water levels, wave height, profile volume and dune crest).

4.2.2 Prediction skill

A simple linear regression model is used to quantify the prediction skill, relating predictions to actual observations. Therefore we wish to find the equation of the straight line

$$\hat{y} = \alpha + \beta\bar{x} \tag{4.5}$$

Here, $\hat{y}$ is the regression estimate based on $\bar{x}$, the Bayesian-mean predicted value, and includes corrections for bias α and slope β. The Bayesian-mean value is

$$\bar{x}_i = \sum_{j=1}^{J} p\left[D_j|inputs_i\right] D_j \tag{4.6}$$

where the summation is over the $j = 1, 2, ..., J$ discrete bins from the prediction obtained for each case i and D_j the value of the bin. $p\left[D_j|inputs_i\right]$ is the probability density of bin j, given the evidence $inputs_i$.

The regression skill for this prediction is

$$s = 1 - \frac{\sum_{i=1}^{I} \sigma_{x,i}^2 \left[y_i - \hat{y}_i\right]^2}{\sum_{i=1}^{I} \sigma_{x,i}^2 \left[y_i\right]^2} \tag{4.7}$$

where the summation is over all considered cases, $i = 1, 2, ..., I$. The skill describes a weighted percentage of observed variance that is explained by the Bayesian-mean prediction. The weighting factors are the prediction variance around the Bayesian-mean value and do not depend on the observations. The variances are computed as

$$\sigma_{x,i}^2 = \sum_{j=1}^{J} p\left[D_j | inputs_i\right] \left[D_j - \bar{x}_i\right]^2. \tag{4.8}$$

The Bayesian-mean value represents a robust predicted value (Plant and Stockdon, 2012) and the variance of the prediction provides a measure of prediction uncertainty used as weighting term in the regression and skill estimates. However, the Bayesian-mean value is only appropriate if the result is more-or-less normally distributed. When a result is bi-modal for instance the Bayesian-mean value will fall between the two most likely outcomes and is a bad prediction in that case. The prediction skill based on linear regression will be an inappropriate measure for the validity in these type of cases. As an alternative to the regression approach, the next section describes the log-likelihood ratio as another validity evaluation.

4.2.3 Log-likelihood ratio

The log-likelihood ratio makes it possible to describe the skill of the updated probability distributions by evaluating the likelihood of each observation, and comparing this likelihood to the prior likelihood. Likelihood is a measure of how likely an event is. For instance for a forecast F with given observables O, $p(F|O)$, the likelihood function is the probability of the observations if the forecast is known: $p(O|F)$. The likelihood term can include both model and observation errors. Thus, if the model and measurements were error free, an observation would be likely only if it is equal to the forecast value. In reality, there are numerous errors causing spread in the likelihood function.

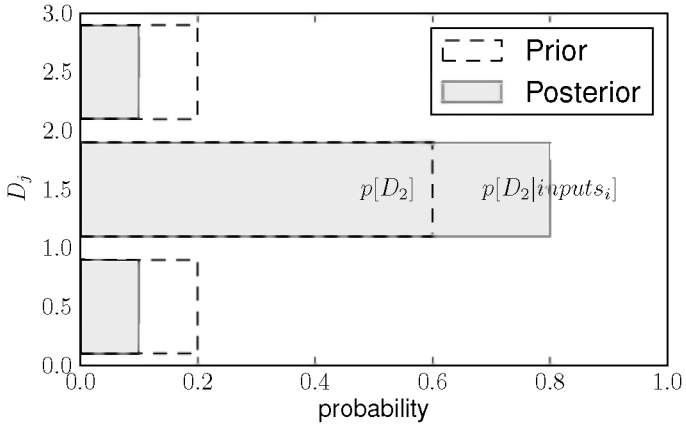

Figure 4.9: Given $D_2 = D_i$ this figure shows the prior probability of a value in bin D_2 together with the posterior probability (after update with evidence $inputs_i$) of the same bin. The posterior probability is higher than the prior probability, the log-likelihood formulated in Equation 4.9 is positive, so one is more certain about the outcome.

Here, we use the maximum which describes the likelihood of a set of parameter values, given some observed outcomes, that is equal to the probability of those observed outcomes given those parameter values. Since, one is interested in the *most* likely parameters the likelihood is labelled as *maximum* likelihood. In this case the log-likelihood ratio will be used (Equation 4.9) to describe the maximum likelihood. A logarithmic function will be used to make the process of differentiating (to find the *maximum* likelihood) easier. Moreover, because the logarithm is an increasing function, the likelihood function and the log-likelihood function attain their extreme values for the same values.

$$L = log\left\{p\left[D_j|inputs_i\right]_{D_j=D_i}\right\} - log\left\{p\left[D_j\right]_{D_j=D_i}\right\} \tag{4.9}$$

The first term on the right is the updated probability evaluated at the discrete bin j that matches the observed erosion volume for the i^{th} case. If the updated probability is higher than the prior probability for the observed value, then the prediction is improved compared to the prior and the log-likelihood ratio is greater than zero. This indicates that the updated probability distribution is both different compared to the prior distribution and more accurate. On

the other hand, if the updated probability of the observed value is lower than the prior probability, it indicates that the updated probability is either more uncertain than the prior or it is more confident but actually wrong.

Thus, the likelihood ratio scores give the ability of the Bayesian Network to make skillful estimates of both mean value and uncertainty. A summation of the log-likelihood ratio over all observed cases provides a measure of how much better (or worse) the Bayesian Network prediction performed over the entire data set.

4.2.4 Results

Once the Bayesian network is constructed and trained, it can be used for prediction by updating the prior probabilities (black dashed lines in Figure 4.10) of the input variables with data. Some face validity checks as well as the prediction skill and log-likelihood ratio of the network are dealt with in this section.

In the first face validity check, shown in Figure 4.10, the area has been selected, as the island Schiermonnikoog in the Wadden area. In general, the Wadden area is characterised by small grain sizes, mildly sloping profiles, wide beaches and low dunes. All four features are visible in the posterior distributions. In addition, the posterior distributions show that the profile volumes are relatively high and the erosion volumes are in the lower regions. In the network, the hydraulic conditions are not directly connected to the area. This means that no influence of the area choice is expected on the hydraulic conditions nodes, which is confirmed by Figure 4.10. The second validity check concerns the selection of a relatively high water level, shown in Figure 4.11. Again, because of the absence of a direct link between the area and profile information, now only the hydraulic variables and the erosion volume are influenced. Since a high water level (WL_t) is likely to coincide with high waves and long wave periods, we see a tendency to the higher bins of both wave height ($Hsig_t$) and wave period (Tp_t). In addition, we see a larger probability for higher erosion volumes, w.r.t. the prior distribution, which is in line with the expectations.

In order to derive the prediction skill, erosion volumes at several locations along the Dutch coast were hindcasted with testcases obtained from the distributions underlying the dataset described in previous section. A testcase thus is a set of variables representing a scenario and serves as input for

the Bayesian network in order to make a prediction for the erosion volume. Since DUROS+ results are considered as observations, a comparison between observed and predicted erosion volume is possible.

Figure 4.12 shows a comparison between predicted and observed erosion volumes for the network which was trained on the Holland coast area and applied for prediction of other transects in the same area. Although the spread is considerable (not precise), the average agreement is fairly good (accurate), being represented by a skill of 0.88 and a log-likelihood ratio of LR=19. This means that the network is capable of predicting on average the erosion volumes fairly well, if the cases to predict are covered by the training dataset. The spread can be reduced by increasing the number of bins (categories) per variable. Disadvantage of increasing the number of bins is that more data is needed to properly train the model.

In Figure 4.13 a similar predicted-observed comparison is made, for the same network that in this case was trained on the Wadden area data and used for prediction of the Holland coast. In this example, there is a deviation between both the profile indicators as well as the boundary conditions for both areas. In this case, typical features of the prediction area are not captured by the training data, leading to a worse skill and log-likelihood ratio (0.52 respectively LR=-12). The low skill indicates that the best estimate from the Bayesian Network did not match the DUROS+ predictions as well as they did in the Wadden test and that the predicted uncertainty from the Bayesian Network did not correspond to the actual prediction errors. Adding more training data to both improve the best prediction and include the actual uncertainty is required.

4.2.5 Conclusions

The applications of the Bayesian approach have demonstrated that a Bayesian Network is useful for quantifying the erosion rate and reflecting sensitivities of predictions to input uncertainties. Especially for the aggregation of model results from advanced dune erosion models, it is considered as a valuable alternative to FORM. We demonstrate that the Bayesian approach can (1) capture the DUROS+ model accurately, and return 88 % of the simulated variability of this model; (2) give fast predictions of dune erosion including the confidence interval; (3) deal with heterogeneous and missing data.

At the same time, it should be noted that these favourable conclusions are only possible if the cases to be predicted are well represented within the training

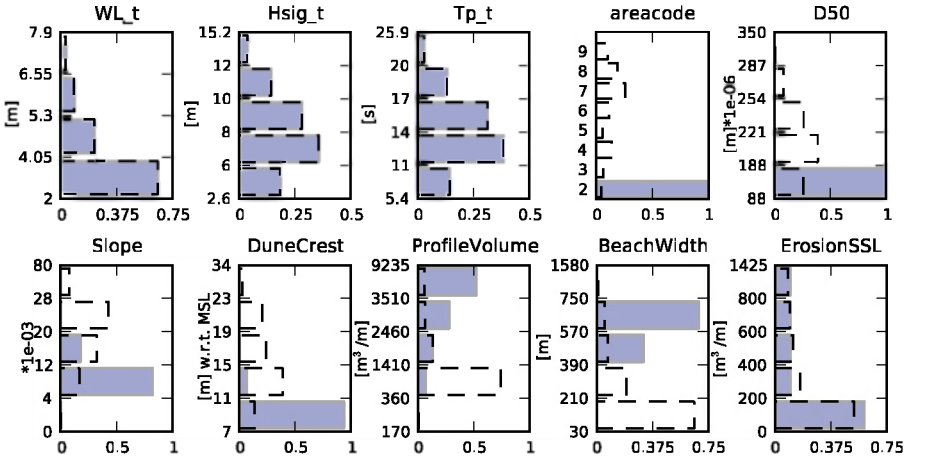

Figure 4.10: Prior (black dashed lines) and posterior probability distributions of Bayesian Network's variables. The island Schiermonnikoog (areacode: 2), being part of the Wadden area, has been selected.

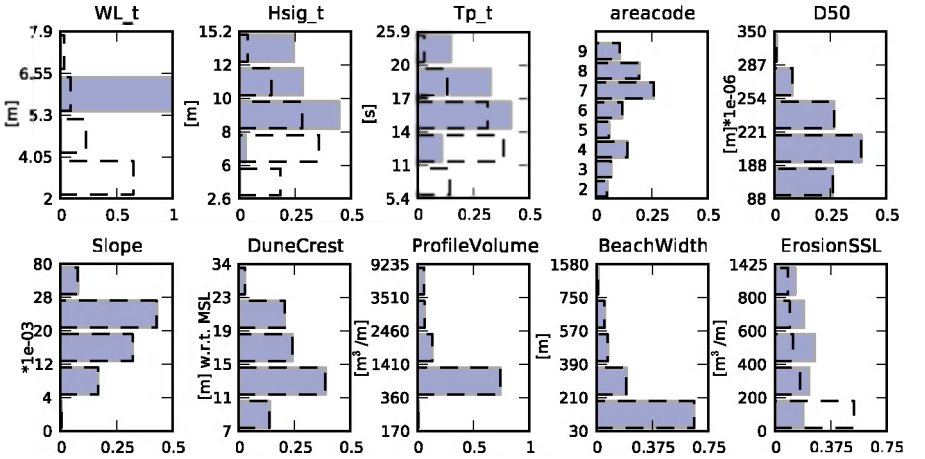

Figure 4.11: Prior (black dashed lines) and posterior probability distributions of Bayesian Network's variables. The water level bin around MSL+6 m has been selected.

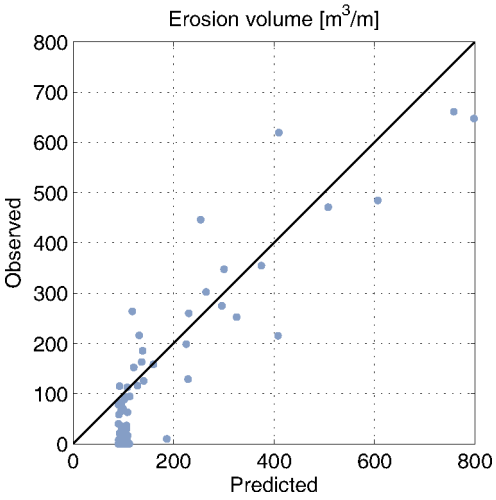

Figure 4.12: Observed vs. predicted for the Bayesian Network when trained on the Holland coast and applied on other transects in the same area.

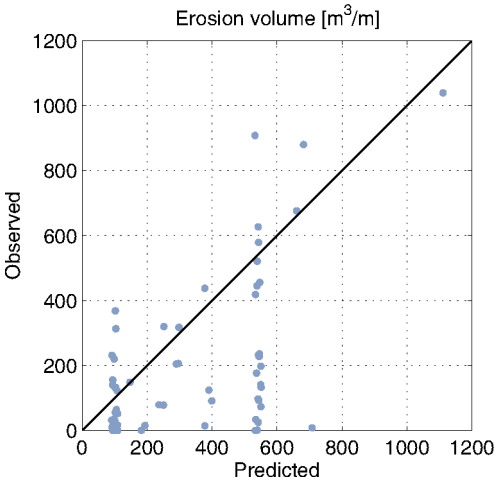

Figure 4.13: Observed vs. predicted for the Bayesian Network when trained on the Wadden coast and applied on the Holland coast transects.

data ranges. A Bayesian Network is only capable of interpolating and not extrapolating its training data. In addition, the precision of the results in this section is limited (considerable spreading). This can be improved by increasing the number of bins per variable, implying that more training data is required.

4.3 Extended approach with wave obliquity and coastal curvature

This section discusses two approaches to introduce the effects of wave obliquity and coastline curvature into the probabilistic safety evaluation. The influence of bathymetry is not considered separately here, since it is already included in the present approach and it appeared from Chapter 3 to have little influence compared to wave obliquity and coastline curvature effects. The coastline curvature is not considered as a stochastic variable. However, the response to the wave angle is different depending on the curvature. To account for wave obliquity and coastline curvature, in this section the probabilistic model is extended with the stochastic variable wave angle, where the coastal curvature is accounted for in the response to wave obliquity.

With FORM, the influence of wave obliquity and coastline curvature on the $1 \times 10^{-5}\,\text{year}^{-1}$ erosion rate is investigated for the reference cross-shore profile (Figure 3.1) with Hoek van Holland boundary conditions. For this investigation, the DUROS+ is used with an additional erosion contribution based on the XBEACH simulations presented in Chapter 3. In addition, a Bayesian Network dedicated to the relative effects of wave obliquity and coastline curvature is presented as an exploration of the potential impacts of those additional variables to the normative erosion along the Dutch coast. The Bayesian Network is trained with data from Chapter 3.

4.3.1 FORM

To account for wave obliquity and coastline curvature, this section adds the wave angle as additional stochastic variable in the probabilistic model presented in Section 4.1.3. For reasons of simplicity, the DUROS+ model is used as a dune erosion model and the contributions for the additional effects are accounted for by an 'additional erosion volume'. The additional erosion volume represents the relative erosion, w.r.t. the reference case with a straight

coast and shore normal wave attack, which is based on the XBEACH results from Chapter 3. FORM is used here as a reliability method because it is efficient and it provides information about the design point.

Wave angle distribution

The stochastic variables of the reference case are based on the Hoek van Holland situation, similar to the investigation of Van de Graaff (1986). When including the wave direction into the probabilistic calculation, also the orientation of the coastline as well as the wave direction become of interest. To illustrate the effect of the wave angle, we stick to the Hoek van Holland situation and use the cross-shore transect orientation (311°) and the wave direction distribution from that area. Due to the funnel shape of the North Sea, the wave direction is highly correlated with the water level, especially for extreme events. Solely north-north-westerly wind directions can, due to their long fetch, create extreme waves and surge (Figure 4.14). Data analysis of two wave stations at the North Sea shows wave angles converging towards a narrow range around 335° for increasing water level threshold. In this section, the wave direction is simplified to a uniform distribution between 321 to 351° relative to north. This corresponds to 10 to 40° relative to the cross-shore transect of consideration (311°), indicated in Figure 4.14.

Calculation procedure

Although the procedure is similar to the one in Section 4.1, some more explanation is needed about the inclusion of the additional erosion due to wave obliquity and coastal curvature. In each individual dune erosion calculation, within the FORM simulation, a wave angle is selected from its distribution as is done for the other stochastic variables (water level, wave height, wave period, grain size, surge duration and model accuracy). Based on this wave angle, a relative additional erosion value can be found in Figure 4.15 based on the results from Chapter 3. The relation between additional erosion and wave angle is dependent on the coastal curvature. In this way, the curvature effect is included in the calculation although it is not a stochastic variable. With inclusion of the additional erosion, the retreat distance is derived like it is done in Section 4.1.

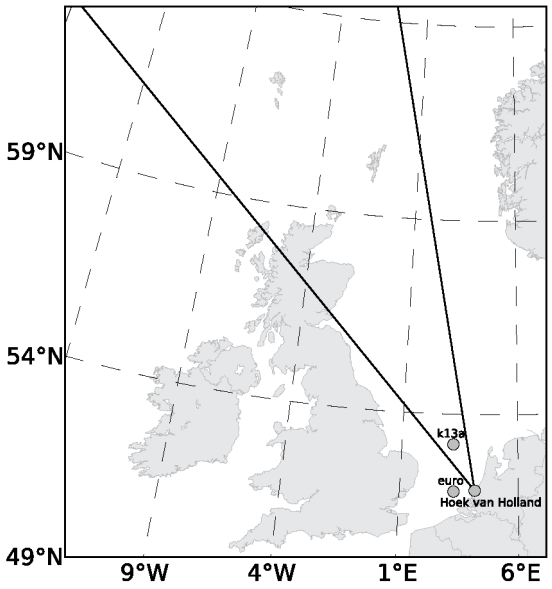

Figure 4.14: A relatively small range of wave angles, during extreme storm conditions, is relevant for a transect near Hoek van Holland. The wave stations k13a and euro platform are used for the training of the wave direction node in the Bayesian Network.

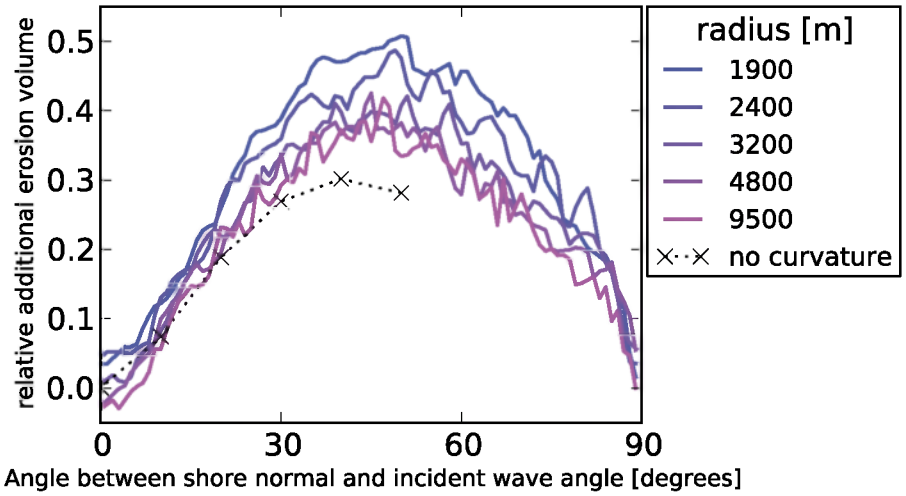

Figure 4.15: Additional erosion as function of the wave angle, for various curvature radii as well as for a straight coastline.

Results

In the reference case, presented in Section 4.1.3, the $1 \times 10^{-5}\,\text{year}^{-1}$ retreat distance is 78 m. When introducing the wave angle as additional stochastic variable, given a straight coast, the $1 \times 10^{-5}\,\text{year}^{-1}$ retreat distance increases towards 91 m. The corresponding design points for the reference case as well as the case which includes the wave angle are listed in Table 4.5. Generally, the water level is by far the most important variable. This is for a large part due to the physical importance of the water level for the dune erosion process. In terms of the α value, this importance is even higher due to the model setup where the wave height and wave period are correlated to the water level (as discussed in Section 4.1.3). In addition, the additional erosion volume contributions are implicitly also related to the water level. The reason is that the water level is of major importance for the erosion volume calculated by DUROS+. Since the additional erosion contributions for the accuracy, the duration and the wave angle are defined as a volume portion of the initial erosion, the absolute value of the additional erosion (or retreat distance) becomes larger when the initial erosion is larger. In that way, the

Model	DUROS+		DUROS+ wave angle straight coast	
Retreat distance	78 m		91 m	
	value	$\alpha^2 \times 100$ %	value	$\alpha^2 \times 100$ %
Water level	5.52 m	90.5	5.56 m	91.4
Grain size	208 µm	3.3	207 µm	3.3
Accuracy	$0.12 \times A$	3.3	$0.10 \times A$	2.4
Duration	$0.05 \times A$	1.5	$0.04 \times A$	1.0
Significant wave height	7.94 m	1.3	7.97 m	1.3
Peak wave period	12.7 s	0.2	12.8 s	0.2
Wave angle	0°	0.0	28°	0.4

Table 4.5: Variable values in the design points, for the 1×10^{-5} year^{-1} retreat distance, and importance of variables for the reference case as well as for a straight coast with the wave angle included.

FORM algorithm might tend to find a design point for a slightly higher water level, and hence a slightly higher wave height and wave period, by introducing the additional stochastic variable for the wave angle (Table 4.5 right hand side), with respect to the reference case (left hand side). If all stochastic variables would be completely independent, the introduction of an additional stochastic variable would reduce the α^2 of all original variables a bit.

Similar to Table 4.5, Table 4.6 shows the variable values in the design points for two cases including coastline curvature. All the other conditions are kept the same as in the previous example with a straight coast. These two cases represent the hypothetical situation that the coast at Hoek van Holland would be curved at two different rates. In the calculation, for each case simply another line from Figure 4.15 has been taken into account. The resulting 1×10^{-5} year^{-1} retreat distance, for curvature radii of 9500 m and 1900 m is 92 m and 97 m respectively. So, a mildly curved coast (radius 9500 m) gives a slight increase of the erosion rate with respect to a non-curved coast when the waves come in obliquely. For a strongly curved coast (radius 1900 m) the erosion rate increases still more. Due to the inclusion of the coastal curvature, the wave angle becomes more important. As a result, the α^2 of the wave angle increases whereas the α^2 of all other variables slightly decreases. This is the normal behaviour when a stochastic variable becomes more important.

Model Retreat distance	DUROS+ wave angle radius 9500 m 92 m		DUROS+ wave angle radius 1900 m 97 m	
	value	$\alpha^2 \times 100$ %	value	$\alpha^2 \times 100$ %
Water level	5.55 m	91.2	5.53 m	91.0
Grain size	207 µm	3.3	207 µm	3.3
Accuracy	$0.10 \times A$	2.3	$0.09 \times A$	2.0
Duration	$0.04 \times A$	1.0	$0.04 \times A$	0.9
Significant wave height	7.96 m	1.3	7.95 m	1.3
Peak wave period	12.8 s	0.2	12.7 s	0.2
Wave angle	29.4°	0.8	30.6°	1.3

Table 4.6: Variable values in the design points, for the 1×10^{-5} year^{-1} retreat distance, and importance of variables including the wave angle for two cases with different curvature.

4.3.2 Bayesian Network

This section presents a Bayesian Network that approximates the relative erosion due to the influence of wave obliquity and coastline curvature. Whereas the previously presented approach with FORM gives detailed information on a specific situation, the Bayesian Network is more useful for an exploration of the influence of specific variables along the whole coast. It can be used as a quick safety assessment tool to find locations that need detailed consideration. In addition, a Bayesian Network provides a way to apply computational expensive models in a probabilistic framework. The network presented in this section uses the XBEACH results from Section 3.3 and 3.4, the orientation and curvature information from JARKUS data and wave direction information from a few wave measurement stations at the North Sea.

Network setup

Figure 4.17 gives an overview of the network. The network is designed to estimate the *erosionfactor*, indicating the relative erosion with respect to the reference situation where no influences of wave obliquity and coastline curvature are included. Based on the simulations from Chapter 3, the curvature radius and the wave angle relative to the local shore normal (*phi*)

are considered as the influencing factors (parents in Bayesian Network terms). The relative wave angle is derived from the local orientation of the coast (*theta*) and the wave direction (*wavedir*). Both the coast orientation and curvature radius are derived from the spatial bathymetry information (JARKUS). The coastal radius is found by fitting circles through the NAP+5 m contours at each transect and its 10 adjacent ones at both sides. The coastal areas that are distinguished in the JARKUS data, are covered by the *areacode*. Only the convex coastal curves are considered, concave parts of the coastline are treated as straight. The reason is that the effect of concave coastal stretches is outside the scope of this thesis and it is not expected to lead to more erosion compared to a straight coast.

The wave direction has been derived from two wave stations in the North Sea (Figure 4.14). The measurement interval ranges from 1989 to 2010. Since only the wave directions that coincide with relatively high water levels are relevant for dune erosion, the wave direction data has been filtered. The wave angles that coincide with the $\frac{1}{500}$ highest water levels have been selected. These water levels are larger than NAP+1.39 m and NAP+1.55 m at the K13a respectively the Euro platform. The filtering considerably narrows the band of wave directions to mainly north westerly ones (Figure 4.16).

The Bayesian Network is trained by the three datasets mentioned above. The JARKUS data is used to train the relations between the areacode, theta and radius nodes. The XBEACH simulation results from Chapter 3 are used to train the relation between combinations of radius and relative wave angle (phi) and the erosionfactor. Wave station data is put into the wavedir node.

Results

The prior probabilities are shown in Figure 4.18. All nodes contain bar plots, where all bins together sum up to one. In the nodes that represent angles, the bars are plotted in polar coordinates in order to make their directions more intuitive. From Figure 4.18, a number of observations can be made. The *areacode* node gives an impression of the number of transects in the areas, showing that area 7 (Noord-Holland) contains the most transects. The nodes *radius* and *theta* (transect orientation) are derived from the individual transect properties within the areas. Obviously, the radius node has the majority of its observations in the bin with the largest radius, which can be considered as straight coast. The majority of the transects is oriented (theta) between westerly

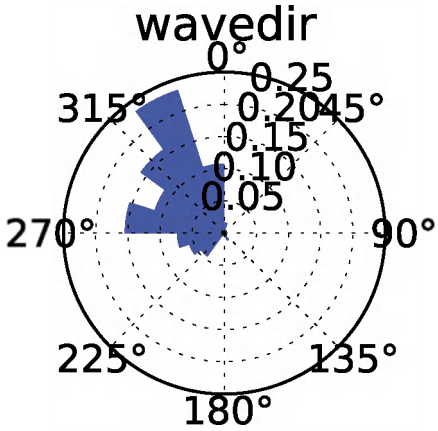

Figure 4.16: Distribution of wave directions as used in the Bayesian Network.

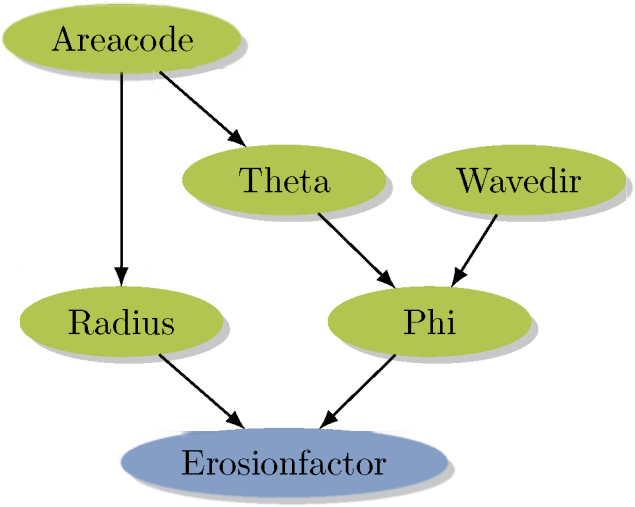

Figure 4.17: Overview of Bayesian Network for wave obliquity and coastline curvature.

and northerly directions. The two large bins between 270° and 310° cover the complete Holland coast. The prior wave direction distribution is the same as shown in Figure 4.16, showing mainly north north westerly directions. The wave angle (*phi*), relative to the local shore normal, is the absolute value of the difference between *theta* and *wavedir*. Therefore, it ranges from 0° to 180°. The angle larger than 90° are included for completeness, but the network does not contain any valuable information about erosion 'around the corner'. Finally, the *erosionfactor* results in a distribution tending towards values significantly larger than one, with a peak at the bin around 1.3. The reason is that large parts of the Dutch coast are attacked by oblique waves, during extreme conditions, and some parts are also curved. The prediction skill is not derived, since the underlying data set is currently too small to divide in separate subsets for training and testing of the Bayesian Network.

To illustrate the application of the network, and show its face validity, a few cases are discussed:

Case 1: a strongly curved coastline When considering a strongly curved coastline with a radius smaller than 2300 m, Figure 4.19 shows a modified erosionfactor distribution with respect to the prior probabilities. In this situation the erosionfactor is skewed towards the higher values, larger than 1.35. The areacode is also influenced, since the straight parts of the coast do not meet the selection criteria. Most of these omitted straight coastal sections are located along the Holland coast, resulting in a theta distribution that includes mainly northerly oriented transects. Finally, the relative wave angle (phi) distribution is slightly modified due to the change in theta. There is no change in the wave direction distribution. This example shows that strongly curved parts of the coast are potentially threatened by more erosion if coastal curvature and wave obliquity is taken into account.

Case 2: a strongly curved coastline and nearly shore normal wave direction Figure 4.20 shows the posterior probability distribution for the situation where in addition to the strongly curved coastline as discussed in the previous case, it is assumed that the waves approach the coast nearly shore normal. This additional evidence totally changes the erosionfactor distribution. Now the peak is around 1.1 and the bins larger than 1.25 are approximately zero. As a result of the restriction to the relative wave angle (phi), also the wave direction and transect orientation are influenced. This example shows that additional

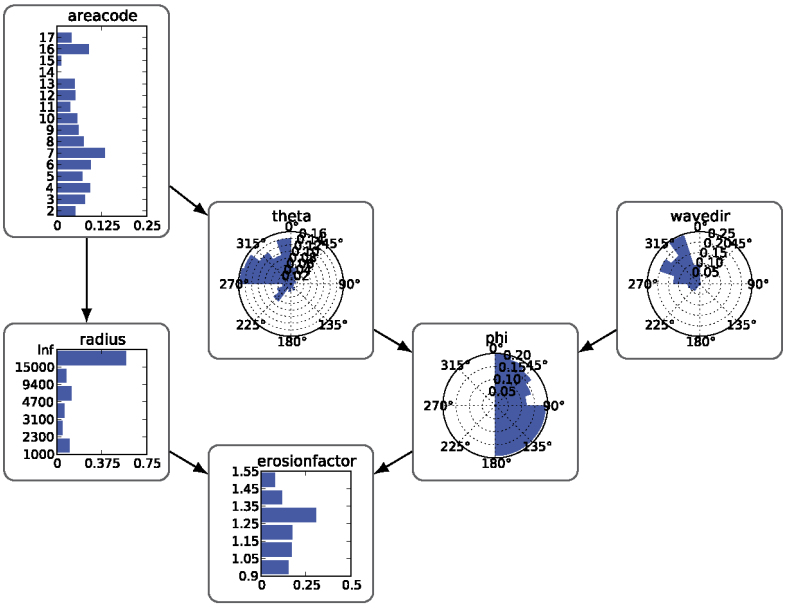

Figure 4.18: Bayesian Network with prior probabilities.

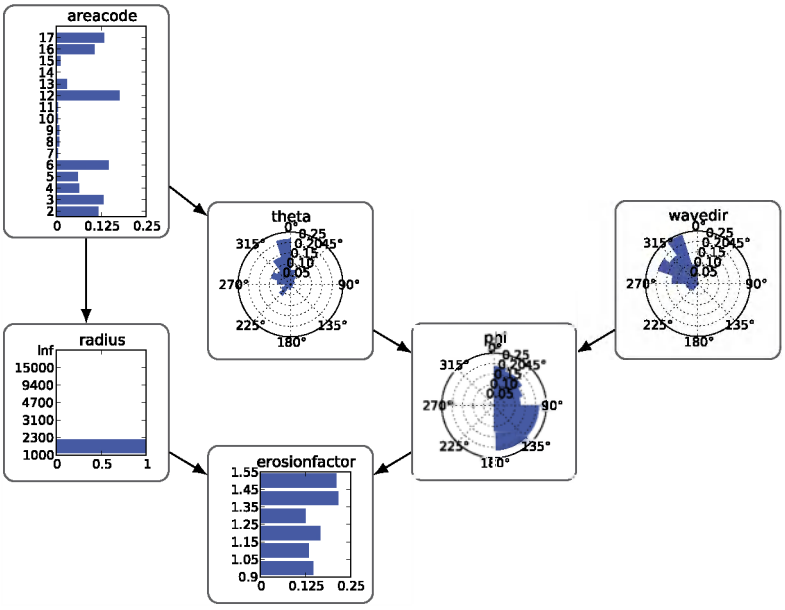

Figure 4.19: Bayesian Network with evidence for a strongly curved coastline.

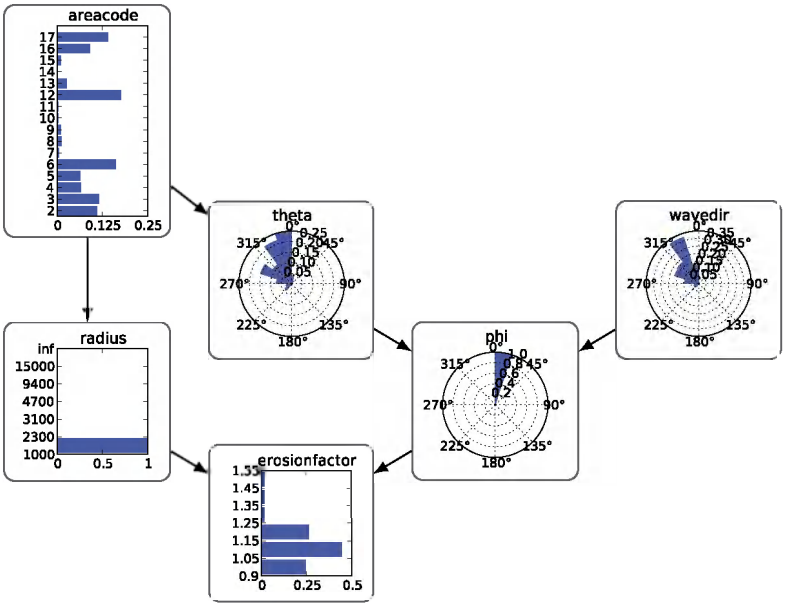

Figure 4.20: Bayesian Network with evidence for a strongly curved coastline and nearly shore normal wave direction.

evidence can totally change the expected erosionfactor.

Case 3: a specific coastal area (Noord-Holland) When selecting the Noord-Holland coastal area (area 7), as presented in Figure 4.21, both the radius and the transect orientation (theta) are strongly confined. The main part of this area is approximately straight coast, or locally mildly curved. The transect orientation is solely a bit larger than 270° (westerly). As a result of the narrow theta distribution, the relative wave angle phi is also confined. The wave direction is considered independent from the area and hence not influenced by the selection of an area. The resulting erosionfactor has a major peak around 1.3. The upper tail is related to the limited curved locations. The lower tail, which is larger, is related to the cases with small relative wave angles (phi). This example illustrates how individual areas can be explored in order to

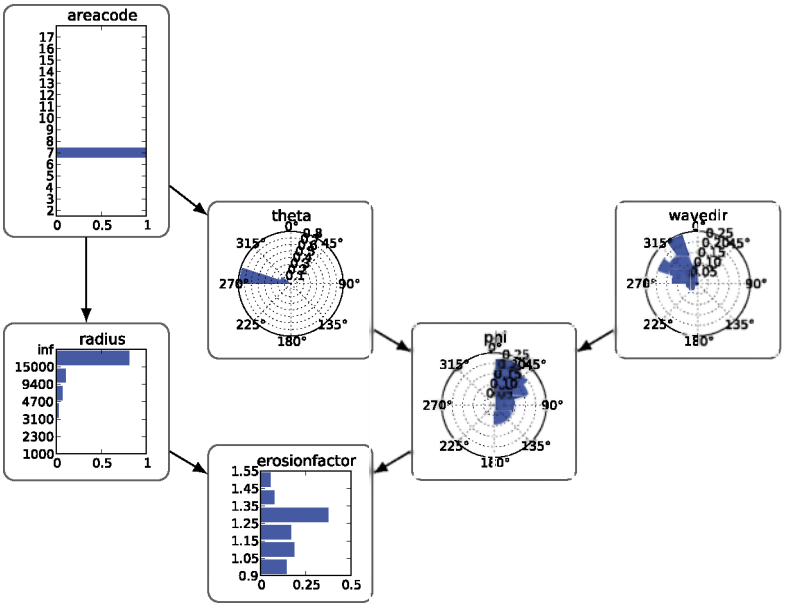

Figure 4.21: Bayesian Network with the Noord-Holland area selected.

identify their susceptibility for additional erosion due the inclusion of wave obliquity and coastal curvature.

4.4 Discussion

4.4.1 FORM vs. Bayesian Network approach

In this chapter, various probabilistic approaches have been discussed. With FORM, it is possible to efficiently estimate a failure probability based on a limit state. However, a proper functioning of FORM requires continuous probability distributions and continuous behaviour of the response model. The application of XBEACH with FORM in Section 4.1.4 illustrated that even a 1D case with a simple cross-shore profile can violate these requirements

and have difficulties to converge. The Bayesian Network, put forward as an alternative, can efficiently produce an erosion volume distribution. This distribution is divided in rather course bins, leading to results that are not precise. Consequently, the probability of failure will be discrete and also course. Especially, the distinctiveness for small probabilities, being of interest for dune failure, will be insufficient.

To make a fair comparison between the FORM and Bayesian Network approach, similar results should be compared. This could either concern a measure for erosion rate, or a probability of failure. Both comparison approaches are not straightforward. A complicating factor is the fact that the distinction between dune erosion model and probabilistic method differs between the two approaches. In the FORM approach, the dune erosion model and the reliability method are clearly distinct. The Bayesian Network more or less combines the dune erosion model and the reliability method. The dune erosion model is represented by the underlying training data, but cannot be retrieved separately since the network will always result in a probability distribution. A comparison in terms of erosion rate, does not involve FORM but compares a dune erosion model with a Bayesian Network. Such a comparison has been made in terms of erosion volume resulting from DUROS+ in Section 4.2.

The discrete character of the Bayesian Network complicates the comparison of failure probabilities. The number of bins in the nodes, especially the resulting erosion volume, is insufficient to distinguish probability of failure in the order of magnitude being of interest for dune safety ($\mathcal{O}(1 \times 10^{-5}\,\text{year}^{-1})$). A distribution function can be fitted to smooth the remaining discreteness as a practical solution to this issue. A three parameter log-normal distribution is considered suitable for this. Van Gelder (2000) shows that the product of n stochastic variables converges to a log-normal distribution. The three parameter log-normal distribution is flexible and easy to fit through distributions with long tails.

4.4.2 Generic value of the results

The relation between wave obliquity respectively coastline curvature and dune erosion has been derived based on a limited series of XBEACH simulations. In addition, these simulations are based on a simplified situation, in terms of cross-shore profile, alongshore uniformity and hydraulic boundary conditions. The used profile is considered representative for the major part of the Dutch

coast and the hydraulic loading is supposed to result in a morphological response that is comparable to an $\mathcal{O}(1 \times 10^{-5}\,\text{year}^{-1})$ storm event at this type of cross-shore profile. Both in the FORM and in the Bayesian Network approach, the simulated wave obliquity and coastline curvature effects are used as the "true" effects. In the Bayesian Network, additional uncertainty is added by the binning. This is however not directly related to the variance in the obliquity and coastline curvature effects. The true variance should be based on the sensitivity of the dune erosion rate to changes in bathymetry and hydraulic conditions for a range of wave obliquity and coastline curvature combinations. This sensitivity has not been derived in this thesis. It is recommended to derive these sensitivities in future studies. The results from that can be used as additional training data for the Bayesian Network, allowing the network to capture more variance.

Chapter 5

Case study of Dutch dune coast

The previous chapter explored different probabilistic methods to incorporate the effects of wave obliquity and coastline curvature on dune erosion. This chapter estimates the impact of the wave obliquity and coastal curvature effects in terms of failure probability of the dunes as a sea defence. The failure probability of the first dune row will be used as an indicator in this chapter. A modelling approach that is closely related to the current safety assessment method is described in the first part of this chapter, to establish a reference. In the reference calculation, the failure probability of the first dune row is estimated using the DUROS+ dune erosion model combined with the Monte Carlo reliability method. The second part of this chapter additionally includes the effects of wave obliquity and coastline curvature. Here the model setup is similar, also using DUROS+ and Monte Carlo, while the additional effects are included by means of a Bayesian Network. The difference of the two failure probabilities provides information about the local impact of wave obliquity and coastal curvature in terms of failure probability.

5.1 Reference approach[1]

This section makes an estimation of the failure probability of the first dune row of the major part of the Dutch dune coast. It uses the present approach in the sense that the same dune erosion model (DUROS+) and the same stochastic variables and probability distributions are used. The focus is on the first dune row because it allows for a fair comparison of the failure probabilities alongshore. In addition, it is not envisaged to derive the safety level of the hinterland, which makes it different from the regular safety assessment method. Furthermore, in this section a fully probabilistic approach is used, resulting in a probability of failure, while the regular safety assessment uses a semi probabilistic approach, resulting in sufficiently safe or not (binary).

This section presents a resilience map of the first dune row of the Dutch Holland and Wadden coast based on a fully probabilistic approach. To test the applicability of the DUROS+ dune erosion model a selection is made of areas that meet the model assumptions. Areas where the first dune row does not meet the normative resilience level, indicate a need for detailed inspection. Some of these areas show a need for a more detailed 2DH dune erosion modelling approach. Although the method is demonstrated on a Dutch case, the probabilistic approach and the steps to determine where to use a 1D empirical (Van Gent et al., 2008) or a 2DH process based model (such as Roelvink et al., 2009) are generic in nature and can be applied elsewhere in a similar manner, provided of course the necessary data are available.

5.1.1 Methods

This section describes the probabilistic approach and discusses the selection method to find the part of the coast that can be modelled with the DUROS+ model given the model's assumptions, and the probability distributions to be used in the Monte Carlo analysis. For the description of the DUROS+ model is referred to Section 2.3.1. The rather strict limitations of the model, as applied in this study, hold especially for the DUROS+ model. In the formal safety assessment method prescribed by the Dutch government, several model additions and assumptions enable the assessment of the majority of the coastal transects. Please note that the investigation as presented in this section is a proof of concept and cannot be considered as a full safety assessment.

[1] This section is mainly based on Den Heijer et al. (2011).

Required model input

Crucial input for the DUROS+ model is the pre-storm cross-shore bathymetry. The details of the bathymetry determine the outcome of the erosion-sedimentation balance and hence the landward extent of the erosion profile. Detailed profile information, including foreshore, beach and first dune rows is therefore critical. As a result a well established monitoring programme is crucial to actually enable safety assessment. In the Dutch case the cross-shore profiles are obtained from the JARKUS dataset (Rijkswaterstaat, 2008). The JARKUS data contain in total 2178 cross-shore transects which are measured yearly since 1965. For this study, the transects of 2008 have been used. The transects have an alongshore spacing between 150 m and 250 m. The orientation of the transects is approximately shore normal. The JARKUS data as well as the analysis scripts used in this investigation have been provided by OpenEarth (Van Koningsveld et al., 2010).

Besides profile information, the DUROS+ model requires as input: the maximum storm surge level, the significant wave height, the peak wave period and the sediment grain size (needed to determine the sediment fall velocity). The first three inputs are commonly derived from time series of (directional) offshore wave buoys. The better the information on the (statistics of the) hydrodynamic boundary conditions, the better the safety assessment. In the Dutch case a number of offshore wave buoys is available with decades of high resolution time series. The final input, grain size, requires sediment sampling. Such a sediment sampling campaign has been executed in The Netherlands and grain size distributions are available at 146 locations along the entire Dutch coast (TAW, 1984). The cross-shore location of these samples is not reported and hence the resulting grain size is considered as representative for the entire cross-shore profile.

Definition of failure

As a starting point, the DUROS+ model is applied in each individual calculation within the probabilistic framework. The erosion above storm surge level is used as erosion indicator. Based on the storm surge level, the first dune row's available volume in the cross-section can be derived. If, for given loading conditions, the total dune volume above storm surge level has eroded, potential failure is detected for the transect. Hence, both examples in Figure 5.1 show potential failure. Whether potential failure is also considered as actual

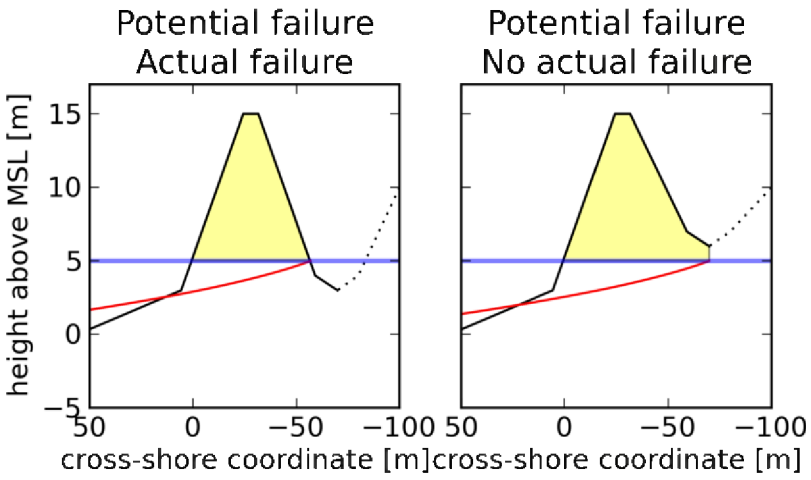

Figure 5.1: Illustration of distinction between potential and actual failure of the first dune row.

failure, depends on the storm surge level relative to the dune valley level. Only if the storm surge level exceeds this valley level, actual failure[2] is recorded (see Figure 5.1). For the calculations as presented in this section both potential and actual failure is derived, but only the results of actual failure are discussed and depicted in the figures. The results for potential failure will be used for comparison purposes in Section 5.2.

Probabilistic framework

The probability of failure of the dunes is based on the probability distributions of the relevant loading and strength variables. Here the water level, wave height, wave period, D_{50} grain size and (a contribution for) storm duration are considered as stochastic variables. The initial (pre-storm) cross-shore bathymetry and wave direction (shore normal) are taken into account as deterministic, meaning that variations are omitted.

Monte Carlo (Fishman, 1996) is used as a reliability method. For each selected

[2]Further discussion on failure definition will follow in Section 5.2.

transect, random samples are taken from the probability distributions of the boundary and initial conditions. For each of these sampled combinations of conditions the response of the dune is calculated with the dune erosion model (Section 2.3.1). Based on the definition of failure, as discussed above, it is decided whether failure is occurring under these conditions. The probability of failure for a transect can be found by dividing the number of failures by the total number of samples.

An advantage of the Monte Carlo method is that it is easy to apply. A disadvantage is that for small probabilities of failure many calculations have to be carried out to get an accurate result, leading to computationally expensiveness. To cope with this, the more efficient Monte Carlo Importance sampling technique (Fishman, 1996) is applied. With this technique, the most important stochastic variable (which is the water level in the present application) is scaled to get more extreme samples, leading to more failures. To prevent an overestimation of the failure probability, the result is corrected for the scaling of the stochastic variable. In this way, a relatively accurate result can be found with a limited number of samples. The calculations as presented here have been carried out with 100 samples per transect.

The current method to safety assessment is to perform probabilistic calculations on a limited number of selected locations along the coast. The resulting design conditions are interpolated along the coast and as such used as input for deterministic calculations for each transect, leading to a binary result: safe or not safe. The reference approach distinguishes itself from the safety assessment method by following a fully probabilistic approach for each transect along the whole coast, to examine the probability of failure of the first dune row. This gives insight in the resilience of the first dune row along the Dutch coast. To properly estimate the safety level of the hinterland, locations where the failure probability of the first dune row is higher than the local normative safety level have to be considered in more detail with a more advanced dune erosion model (Steetzel, 1993; Roelvink et al., 2009).

Selection of transects

One of the most important assumptions in DUROS+ is the sediment balance in the cross-shore, implying the assumption of alongshore uniformity. The model is therefore only applicable to reasonably straight coasts. Furthermore DUROS+ is validated for fully sandy transects only. Therefore locations with hard layers

or structures are omitted in this investigation. Another assumption is that the pre-storm cross-shore profile is known at least in the vertical range where the profile is likely to change during the storm. Finally, information about the wave conditions has to be available. These assumptions lead to the following inclusion criteria for JARKUS transects where the model is deemed applicable:

- the angle between the extended transect and the connection line between the two relevant boundary condition locations must be between 70° and 110°. This requirement implies in practice that the strongly curved Wadden island heads are left out of consideration.
- sections of the coastline containing hard structures (*Hondsbossche and Pettemer Zeewering*) and harbour entrances are left out.
- the transect must at least reach from NAP−5 m to NAP+5 m (NAP is the Dutch vertical datum, approximately mean sea level). With this requirement, transects that only contain the underwater profile up to the beach, or only contain part of the beach and the dune are excluded.
- Wave measurement data of sufficient quality, from which useful probability distributions may be derived, are only readily available near Hoek van Holland and northwards. Therefore, the southern part of The Netherlands, the Delta region, is left out of consideration.

The remaining transects, covering 50 % of the Wadden coast and 75 % of the Holland coast, are cropped at the landward side if more than one dune row is present in the data. This means that the failure probability of only the most seaward dune row is calculated. Two main reasons have led to this choice. Firstly, this gives the best comparable (unambiguous) results. Comparison between the failure probability of one big dune row at an arbitrary location with two small dune rows at another location is only possible if the model's capabilities for one and two dune rows is comparable. Secondly, after failure of the first dune row, any further erosion or overwash processes should be considered in 2DH since the dune area behind the first dune row is usually much less uniform alongshore.

Probability distributions

The probability distributions that were used for the development of the safety assessment method for the Dutch dune coast (WL | Delft Hydraulics, 2007)

Location (station)	ω [m]	ρ [year^{-1}]	α [-]	σ [m]
Hoek van Holland	1.95	7.237	0.57	0.0158
IJmuiden	1.85	5.341	0.63	0.0358
Den Helder	1.60	3.254	1.60	0.9001
Eierlandse Gat	2.25	0.5	1.86	1.0995
Borkum	1.85	5.781	1.27	0.535

Table 5.1: Parameter values in Weibull distribution for maximum surge level for Dutch Coast (source: WL | Delft Hydraulics, 2007).

have been reused in this investigation (see Table 4.1 for a summary of the distributions used).

Water level The stochastic properties of the water level are described by a conditional Weibull distribution (Equation 4.2). The parameters in the distribution depend on the station of concern (Table 5.1). The resulting water levels as function of the probability of exceedance are given in Figure 5.2. In Figure 5.3 the measurement locations for the boundary conditions along the Dutch coast are depicted. One of those stations, *Steunpunt Waddenzee*, is virtual in the sense that the data at this location is obtained by interpolating between the two neighbouring locations.

Wave height The wave height is correlated to the water level because during storms their common cause is wind. The stochastic properties of the wave height are described by a normal distribution. The mean value is related to the water level by a relation obtained from Stijnen et al. (2005). In this way, the deviation of the wave height w.r.t. the mean value can be considered independent of the water level. Stijnen et al. (2005) describe the relation between water level and wave height for 5 locations along the Dutch coast, as presented in Figure 4.2 panel a. The standard deviation is a constant value of 0.6 m. Since the sensitivity to the standard deviation of the wave height appeared to be small (Section 4.1.3), this value is not varied along the coast.

Wave period The wave period is correlated to the wave height, and thus indirectly to the water level. Also the wave period's stochastic properties are described by a normal distribution. Again the mean value is obtained

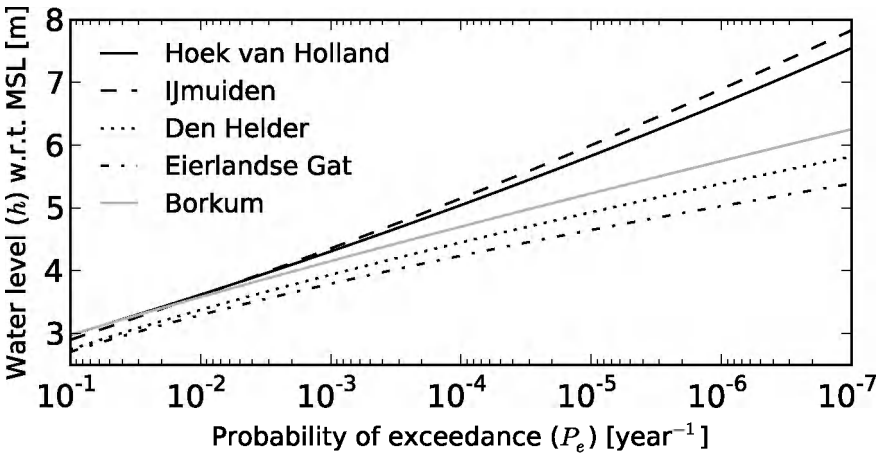

Figure 5.2: Water level as function of probability of exceedance for 5 stations along the Dutch coast.

according to a relation from Stijnen et al. (2005), as shown in Figure 4.2 panel b. The standard deviation is set to 1 s. Because of the minor sensitivity for this standard deviation (Section 4.1.3), this is a fixed value along the whole coast.

Grain size Grain size distributions have been derived from sediment samples at 146 locations along the Dutch coast (TAW, 1984). 105 out of these are located in the area of the selected transects. Although the cross-shore location of these samples is not reported, they are assumed to be representative for the entire cross-shore profile. The D_{50} grain sizes that can be derived from these samples are assumed to be normally distributed. Mean D_{50} grain sizes vary between 159 µm and 277 µm. Standard deviations of the D_{50} grain sizes vary between 8 µm and 37 µm. The finer sediment mainly occurs in the Wadden area in the northern part of The Netherlands. This is also related to the fact that the profile slope is relatively mild there.

Storm duration The DUROS+ model (see Section 2.3.1) is based on a representative storm duration and does not include the storm duration as a separate variable. To account for variation in the storm duration, a normally distributed additional erosion contribution is added to the erosion volume (with respect to

the original erosion A as computed with DUROS+, indicated as "DUROS-plus Erosion above SSL" in Figure 2.1). The mean value is zero and the standard deviation is 10 % of the original erosion above the water level. The use of a normal distribution implies that the additional volume also can be negative, effectively leading to a reduction of the erosion with respect to the original DUROS+ result (Figure 4.3).

Other influences In the method described by WL | Delft Hydraulics (2007) contributions for the uncertainty of the model and for the temporal variation in cross-shore profile volume are also proposed. In this investigation these variables are left out of consideration. The contribution of the profile variation could be taken into account but appears to have only a minor influence. The contribution of the uncertainty of the model is mainly relevant for design or assessment purposes and therefore considered to be outside the scope of this investigation.

5.1.2 Results

In this section the DUROS+ model is applied in a fully probabilistic manner using the information available at the Dutch coast: JARKUS transects, offshore wavebuoys, grain size and storm duration estimates.

Transects included in the probabilistic analysis

The Dutch coast is commonly divided in three areas (see Table 5.2):

1. the **Wadden area** in the north with a series of islands and inlets in between (848 transects),
2. the central **Holland coast** (593 transects) and
3. the **Delta area** in the south with several inlets most of which have been closed with dams and barriers as part of the Delta plan (737 transects).

In the Wadden area only 429 transects, out of the 848, are selected (51 %). The main reason for excluding transects in this area is the occurrence of coastal curvature at the island heads. In these areas the DUROS+ model, in its basic form, is not applicable for two main reasons. Firstly, the model is not developed for the strongly curved coastlines as occur here. Secondly, in these

Area	available transects	selected transects	normative safety level [year^{-1}]	transects not meeting safety level
Wadden area	848	429	5×10^{-5}	45
Holland coast	593	448	1×10^{-5}	23
Delta area	737	0	4×10^{-5}	-
total	2178	877	-	68

Table 5.2: Overview of total available and selected transects as well as transects where the first dune row does not meet the requirements.

areas near the inlets high (tidal) current velocities can occur, which are also not included in the current model setup. A 2DH modelling approach, or at least an incorporation of the 2DH phenomena, is needed here.

At the Holland coast 448 out of the 593 transects have been selected (76 %). Exclusions in this area are mainly due to some dikes and hard structures. In addition, in the south of the Holland coast area, some transects have been excluded because they only cover the shallow water part and the beach. A process based model which includes hard layers, such as XBEACH (Roelvink et al., 2009; Van Dongeren et al., 2009) or DUROSTA (Steetzel, 1993), is needed for this kind of areas.

The Delta area is excluded as a whole because of the lack of readily available wave boundary conditions. In this area with its dams, storm surge barriers and inlets a more advanced model like XBEACH (Roelvink et al., 2009) is needed, provided that the right data is available. Figure 5.3 shows the distribution of the selected transects for the year 2008. Table 5.2 gives an overview of the numbers of available and selected transects per area.

Applying the selection criteria, described in Section 5.1.1, 877 transects out of 2178 transects (40 %) are considered suitable to include in the fully probabilistic approach. Without the Delta area the percentage of included transects is 61 %. For 753 out of these 877 profiles a failure probability could be determined using the probabilistic approach. For the other 124 profiles, no failures where recorded in the Monte Carlo simulations. Considering the sampling range, the failure probabilities for these transects can be considered as lower than 1×10^{-17} year^{-1}. As an estimate for these we use 1×10^{-17} year^{-1}.

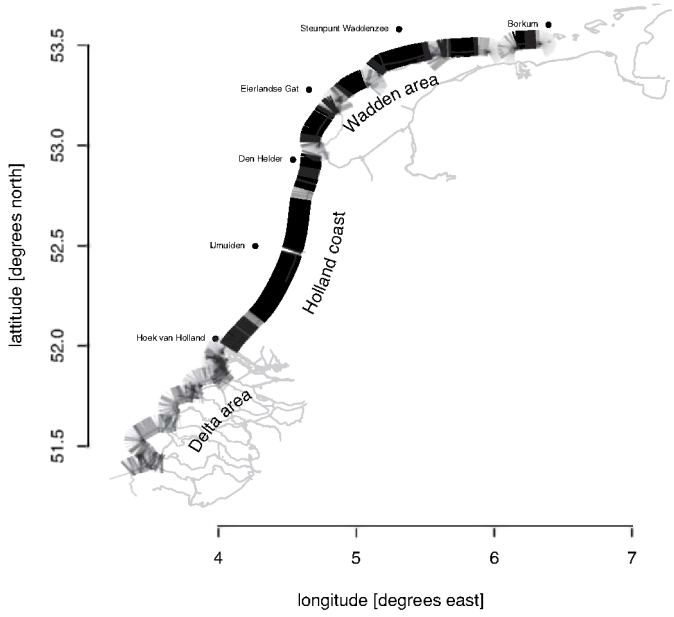

Figure 5.3: Overview of transects that were selected as suitable for DUROS+ (black). The remaining, not selected, transects are shown in gray.

Alongshore distribution of failure probability

The expected maximal failure probability along the Holland coast is 1×10^{-5} year^{-1} as this is the normative safety level for dunes as primary sea defences. The calculated failure probabilities are summarised in Figure 5.4, that shows that about 10 % of the selected transects have a higher failure probability than 1×10^{-5} year^{-1} for the first dune row.

As can be seen in Figure 5.5, most of the locations with the highest failure probability can be found in the Wadden area. The Wadden islands have a required safety level of 5×10^{-5} year^{-1} per year (with the exception of Texel, where it is 2.5×10^{-5} year^{-1}) and part of the islands are outside the primary sea defences.

Four example locations are considered in detail. From north to south, a transect with the largest failure probability (p=1/26 year^{-1}) at the tail of the Wadden island Terschelling (Figure 5.6 panel a), a transect just North of the *Pettemer Zeewering* (Pettemer Sea defence) (Figure 5.6 panel b), a transect near Bergen with a probability of failure of about the normative value of 1×10^{-5} year^{-1} (Figure 5.6 panel c) and finally a transect just North of the harbour entrance of IJmuiden (Figure 5.6 panel d).

An example of a dune with a high failure probability is the tail of the Wadden island Terschelling (Figure 5.6 panel a). The crest of the first dune row of this profile is only 8 m above mean sea level and the dune is narrow. Behind a dune valley of about 400 m, there is a second low dune row. The high failure probability of the first dune row of this transect is not expected to lead to any safety problems because this transect is outside the protected area, i.e. there is a large buffer area in front of the populated area.

Just North of the Pettemer Sea defence are nine transects where the first dune row does not meet the normative safety level. One of these is depicted in panel b of Figure 5.6. Figure 5.7 shows the surrounding area in Google Earth, including the nine transects and an elevation map based on LIDAR data. The LIDAR data show that there are some relatively low areas in the second dune row. A proper assessment of the failure probability of this dune area is only possible with a 2DH process-based model, due to the non-uniform topography behind the first dune row. The Pettemer Sea defence is one of the known weak spots of the Dutch coast (Ministeries VROM et al., 2006). The last severe storm that affected the area was in November 2007, when the dunes were severely eroded. There are plans to increase the safety level by nourishments across the

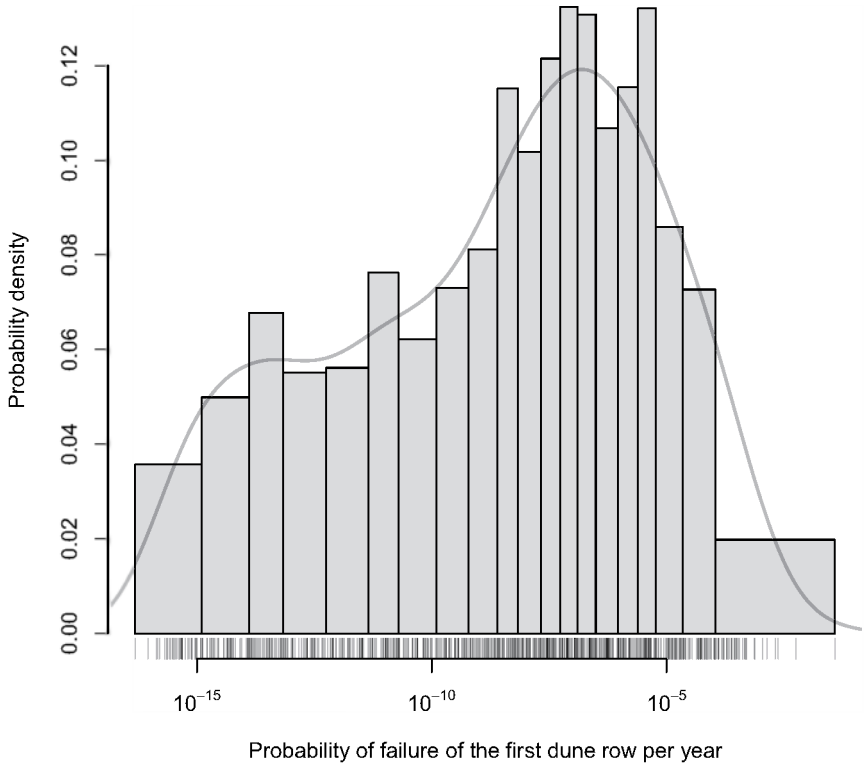

Figure 5.4: Histogram of the probabilities ($p > 1 \times 10^{-17}$ year^{-1}) of failure of the first dune row (all calculated transects). The bin-width is variable and each bin contains an equal number of observations. The graded line is the Kernel density function. In the rug plot along the horizontal axis the individual data points are indicated.

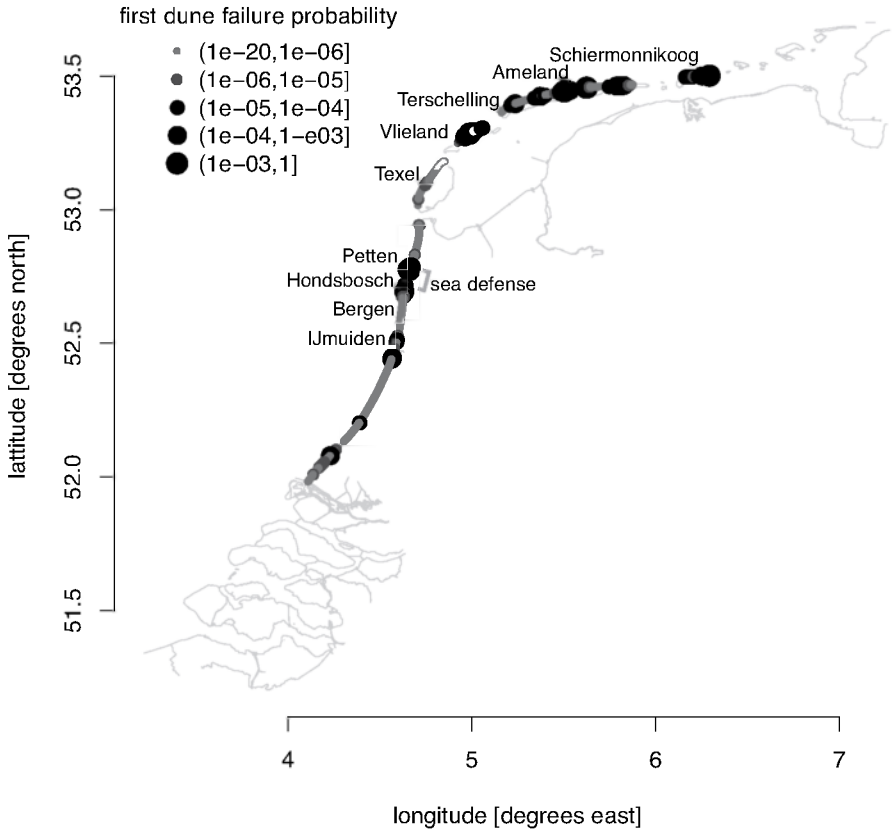

Figure 5.5: Map of the locations with the probability of failure of the first dune row.

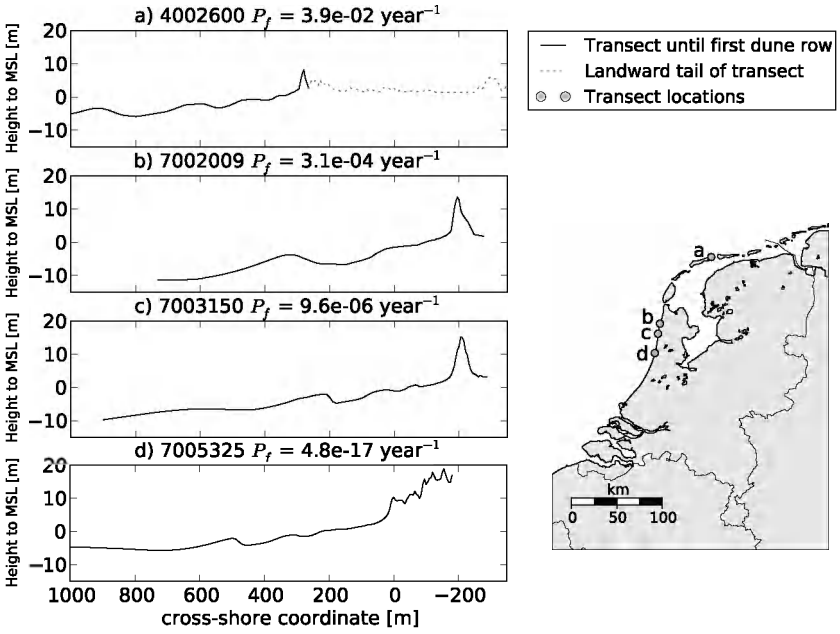

Figure 5.6: Four examples of profiles with the calculated probability of failure (P_f) of the first dune row.

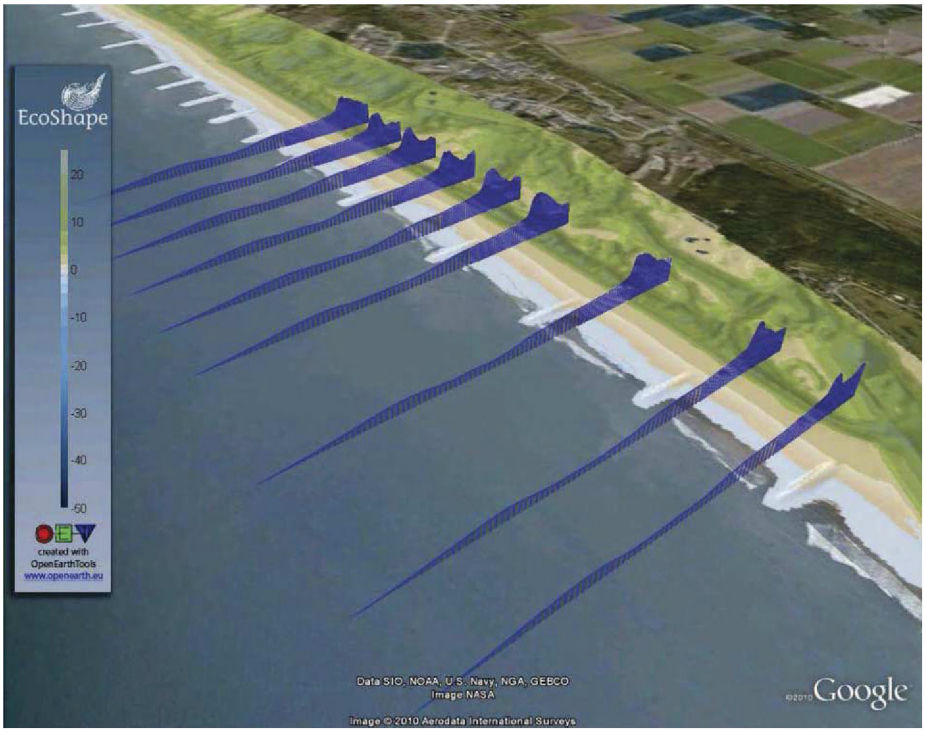

Figure 5.7: A Google Earth view of the area just North of Petten. The transects (measured in 2008) where the first dune row does not meet the requirements are indicated.

whole sea defence ranging from Petten to 6 km southwards.

A transect with a probability of failure of the first dune row around the normative safety level is located near Bergen. This dune reaches about 15 m above sea level but is relatively narrow. A relatively wide dune area is present at this location. For more insight in the situation after failure of this first dune row, detailed 2DH process-based modelling is required.

The last example is a transect just North of the harbour entrance of IJmuiden where the first dune row is very wide and high (almost 20 m above MSL) and therefore it results in the smallest probability of failure.

5.1.3 Discussion

Some of the choices and results of the research presented in this section could be considered as having a subjective nature, providing room for discussion. The basic form of the DUROS+ model and the assumptions on probabilities of boundary conditions were used, omitting the additional features of the safety assessment method, as presently used in The Netherlands, to cope with non-standard cases. Due to the limitations of the model, selection criteria have been used for exclusion of a part of the available transects. In addition, the failing transects and the validation of the failure probability results is discussed.

Limitations of the method

Extreme boundary conditions The dune erosion calculation of a transect only leads to failure when extreme conditions are imposed. Assuming that most transects have a safety margin, the boundary conditions for this study have been further extrapolated than for the regular safety assessment, in order to be able to find failure occurrences. More extreme extrapolation decreases the precision of the boundary conditions and could result in conditions that are physically not realistic. However, along this line the transects with the highest failure probabilities, being the most critical, can be considered as most precise.

DUROS+ for extremer conditions As mentioned in Section 2.3.1, the applied model is developed for dune erosion only. As long as the height and the width of the remaining dune body are sufficient with respect to the hydraulic loading, dune erosion is the most likely mechanism. However, in this study

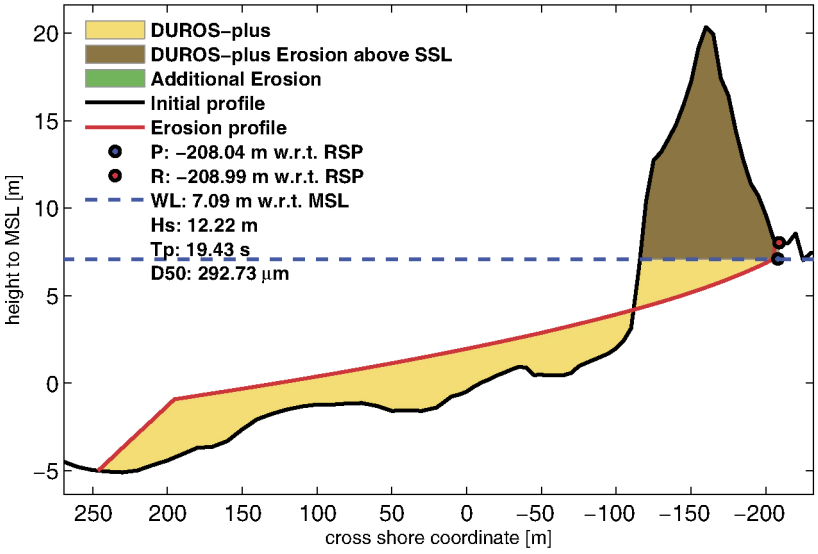

Figure 5.8: Example of a calculation that results in just non-failure.

a considerable part of the calculations are around the transition between non-failure and failure where the impact of a storm (Sallenger, 2000) shifts from dune erosion (collision) to overwash and inundation. Since the latter regimes are not captured by the DUROS+ model, the model is not capable to accurately simulate the failure of a dune. In cases where according to the model, just no failure occurs, in practice at some stage of the event also overwash would start to play a role (Figure 5.8). Additional erosion due to this type of situations is omitted in this study.

The model has been applied beyond its validated range, being about a 1×10^{-5} year^{-1} frequency, leading to decreasing reliability of the model results for smaller frequencies. This is, however, considered as acceptable since the most critical transects are based on the more reliable calculations. It is assumed that the ratio between failure and non-failure cases at these locations is not significantly influenced by those individual calculations that are just around the edge of failure.

DUROS+ for non-standard dunes The DUROS+ model has been developed for the so-called reference profile. This is a cross-shore profile that is considered as more or less representative for the Dutch coast. The reference profile corresponds best with the transects at the Holland coast. It is not clear whether application of DUROS+ in the Wadden area, where the grain size is smaller and the profile slopes are milder, leads to realistic results (Deltares, 2008). Experimental research by Deltares (Hoonhout et al., 2011) led to the conclusion that DUROS+ gives conservative results for the tested cross-shore profiles. The series of experiments was not sufficient to draw conclusions about the performance of DUROS+ at mild sloped profiles in general. As a result, the failure probabilities as found for the non-standard dune profiles should be interpreted with care.

The dune erosion model does not account for some aspects like vegetation or hard structures. The safety calculations are carried out with a 1D model, using measured cross-shore transects with an alongshore spacing between 150 m and 250 m. In areas which are non-uniform alongshore, the alongshore position of the transect could influence the failure probability. If the weakest location in a coastal section is in between two transects, the failure probability will be underestimated.

Limitations of the first dune row approach The calculations presented in this section are based on the JARKUS transect data. A transect is considered as failed when no dune body above the storm surge level is left in the first dune row. Only when this first dune row is the sole line of defence, the safety of the hinterland is directly at stake when failure of the dune occurs. Otherwise, when more dune rows or other lines of defence are available, the probability of failure as presented here is to be considered as a conservative upper limit of the failure of the total defence system at that particular location. However, after the first dune row has failed, other processes have to be taken into account. The problem becomes two dimensional behind the failed dune and should be modelled by a combined morphological and inundation model in at least 2 dimensions. So, the current safety assessment with the 1D DUROS+ model can only be applied to the first dune row dune row due to 2D effects after the first dune row has failed.

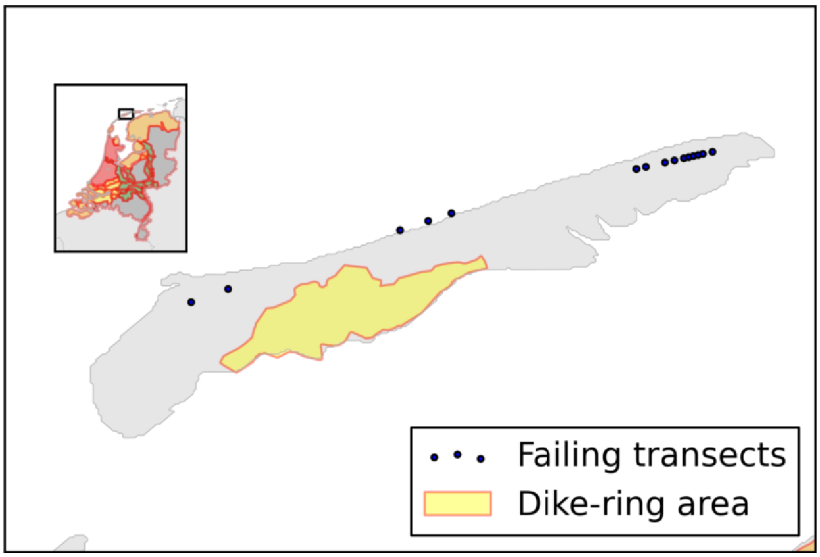

Figure 5.9: The transects at the Wadden area where the first dune row does not meet the normative safety level are well outside the dike-ring area (example of island Terschelling).

Failing transects

Most of the transects, 45 out of 68 (Table 5.2), where the first dune row does not meet the normative safety level are located in the Wadden area. The Wadden islands differ from the rest of the Dutch coast in the sense that the urban and formally protected area covers only a small part of the islands' area (Figure 5.9). That means that a part of the dune area, especially at the island heads, do in fact not have a sea defence function. Out of the 45 transects, 25 are clearly beyond the protected area and the remaining 20 either inside or very close to the primary defence area at the islands Schiermonnikoog, Ameland and Terschelling. At these 20 transects, as well as at 23 along the Holland coast, it is found that the first dune row does not fulfil the safety requirements, meaning that more detailed consideration in at least 2D is needed to confirm a sufficient safety level.

Validation

Since the majority of the failure probabilities is extremely low, compared to the period with reported observations, validation with field data is difficult. The dune erosion model is calibrated and validated for a large number of laboratory experiments at different scales (Vellinga, 1986; Van Gent et al., 2008). Only the the order of magnitude of the largest probabilities of failure can be related to observations in recent history. The largest probability of failure is $1/26$ year^{-1} and is found at the eastern island head of Terschelling. In recent decades, overwash has been observed at some of the Wadden island heads, so in this respect the order of magnitude of this probability of failure can be considered as realistic. The largest calculated failure probability along the Holland coast is of $\mathcal{O}(1 \times 10^{-3}\,\text{year}^{-1})$. The fact that no failure of dunes has been observed on the Holland coast in the last century gives from this viewpoint confidence in the order of magnitude.

5.1.4 Conclusions

The aim of this section is to present a reference resilience map of the first dune row of the Dutch Holland and Wadden coast using a fully probabilistic approach and to test the applicability of the DUROS+ model (Van Gent et al., 2008). Since the Dutch dune coast has a relatively alongshore uniform first dune row, the 1D approach is generally suitable as a simple but effective assessment of this first line of defence. If the resilience of the first dune row is not sufficient, 2D phenomena start to play a role due to non-uniformity of the dune area behind and more advanced dune erosion and inundation modelling is required for a proper assessment.

The DUROS+ model in its most basic form was used to quantitatively assess dune resilience. The Monte Carlo method was used for the probabilistic investigation. Important research questions were (1) where can the DUROS+ model in combination with the fully probabilistic approach be applied along the Dutch coast? and (2) what is the alongshore variability of failure probability using this probabilistic approach?

Regarding the applicability of the method it can be concluded that the assumptions that underly the DUROS+ model in its most basic form result in the exclusion of a significant amount of transects from a fully probabilistic analysis. The Delta area was not considered because of insufficient information

on boundary conditions for that area. About 50 % of the transects in the Wadden area and 75 % of the transects along the Holland coast passed the inclusion criteria for analysis. The excluded transects are found in areas with highly curved coastlines and coastlines containing hard layers or structures. Further assessment of the transects that were excluded requires modification of the basic DUROS+ concept or more generic model concepts. To enable broader coverage of failure probability assessment the use of a more generic model for the remaining 40 % of the coast is recommended.

Regarding the alongshore variability of dune resilience it can be concluded that at 45 transects in the Wadden area, the first dune row does not meet the normative safety level of 5×10^{-5} year^{-1}. Twenty of these are not part of the primary sea defence and reflect the natural process of new dune rows building up. At 23 transects of the Holland coast the first dune row does not meet the normative safety level of 1×10^{-5} year^{-1}. In all of these cases, more dune bodies are present landward of the first dune row. A further safety assessment of these areas is only possible by applying a 2DH process-based model due to the often alongshore non-uniform character of the dune area behind.

Regarding the usefulness of the fully probabilistic approach, firstly, it can be concluded that this is the first time that actual spatial varying failure probabilities along the Dutch coast have been calculated. The results provide important additional information by a resilience map as opposed to the binary result (fail or safe) as obtained from the presently applied approaches. In addition, the resilience can be steering in the decision about the need for more advanced dune erosion modelling. Secondly, it was demonstrated that developments in computing power and also the development of more sophisticated analysis routines and approaches indeed have made a fully probabilistic approach a feasible alternative to current deterministic and semi-probabilistic approaches. It is noted that the current dune erosion model in its most basic form is not able to cover all of the Dutch coast without making additional assumptions. To extend the coverage of the analysis of failure probabilities along the Dutch coast it is recommended to (1) involve more process-based model concepts that can cope with the situations DUROS+ can not, and (2) to expand the currently available data on boundary conditions.

5.2 Extended approach with wave obliquity and coastal curvature

This section aims at the estimation of the failure probability of the first dune row along the major part of the Dutch coast with inclusion of the effects for wave obliquity and coastline curvature. Comparison with the results of the reference calculation as presented in the previous section give insight in the change in failure probability due to these additional effects. The failure estimation is applied to the same areas as considered in the previous section. In addition, the probability distributions for the variables that they have in common are kept the same. The relative erosion volume due to the effect of wave obliquity and coastline curvature is obtained from the Bayesian Network presented in Section 4.3.2.

5.2.1 Methods

Since this investigation is meant to compare the probabilities of failure to those of the reference situation, the same approach is used with some additions. This section describes the dune erosion model, probabilistic method and probability distributions as far as they differ from the reference case which is described in Section 5.1. It should be mentioned here that the selection procedure for the transects, as described in Section 5.1.1, excludes the majority of the strongly curved areas. Although the method as introduced in this section is capable of assessing the more curved areas as well, we still use here the same selected transects. This means that the majority of the transects covers approximately straight coastal sections but also some curved parts are taken into account (see Figure 5.10a).

Dune erosion model and failure definition

As a starting point, similar to the method of the previous section, the DUROS+ model is applied in each individual calculation within the probabilistic framework. The erosion above storm surge level is used as erosion indicator. The relative erosion due to wave obliquity and coastline curvature is sampled as multiplication factor. The product of the DUROS+ erosion volume above storm surge level and the multiplication factor gives the estimation of the total erosion volume.

Based on the storm surge level, the first dune row's available volume in the cross-section can be derived. If the total erosion volume is equal or larger[3] than the available volume, potential failure is detected for the transect with corresponding loading conditions. Actual failure requires, like in the previous section, the water level to exceed the dune valley level.

For the generation of a resilience map, as presented in the previous section, the actual failure is the most suitable indicator to use. When focussing on the difference between failure probabilities with and without the influence of wave obliquity and coastal curvature, the potential failure ratio is more informative. This can be explained by the fact that the difference in failure probability is dependent on the individually sampled cases that just do or do not fail in the reference situation. The used model generally predicts more erosion for the combined effects of wave obliquity and coastline curvature. Hence, the relevant cases are practically limited to the ones that just do not fail in the reference situation. Cases which result in failure for the reference approach, will most probably also fail in the extended approach. In addition, cases which result in relatively little erosion in the reference approach, are likely to still not fail when the erosion volume corrected for the influence of wave obliquity and coastline curvature. Especially for the cases that are at the edge of the non-failure domain, the additional requirement for the water level relative to the dune valley level can be decisive. We can consider an example of an individual case where in the reference approach just non-failure (potential) is found. Inclusion of the wave obliquity and coastal curvature effects will result in potential failure. However, if the water level is below the valley level, no actual failure is recorded. Assuming that this situation occurs in all relevant samples, the ratio of the actual failure probabilities will be one, whereas the potential failure probability ratio will be not equal to one. The latter ratio gives insight in the effect of wave obliquity and coastal curvature on dune erosion, whereas the first incorrectly suggests no effect.

Probabilistic approach

Similar to the reference case in the previous section, the Monte Carlo method is used. However, for the present application a Bayesian Network is coupled to it to estimate the effect of wave obliquity and coastline curvature. Per individual

[3] Due to the multiplication factor, it is theoretically possible that the erosion volume exceeds the available volume.

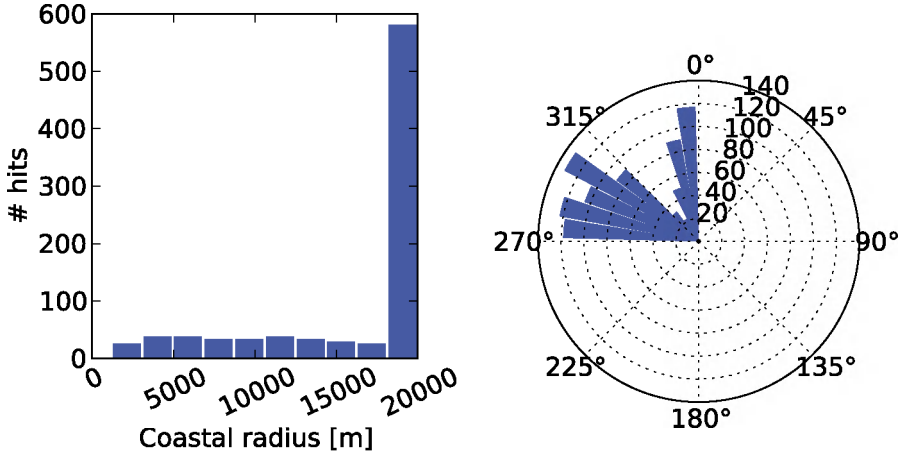

(a) Histogram of coastal radii.

(b) Histogram of transect orientation.

Figure 5.10: Coastal radii and transect orientation distributions as represented in the selected areas.

transect, a posterior distribution of the erosion factor can be obtained from the Bayesian Network by providing evidence for the local transect orientation and coastal radius. Histograms of these features for all selected transects are shown in Figure 5.10. An example of the Bayesian Network output for a transect at the Holland coast is given in Figure 5.11. The erosion factor distribution as provided by the Bayesian Network, is sampled with Monte Carlo.

Similar to the calculations in the previous section, Monte Carlo with importance sampling is applied in order to sample the more extreme water level events. The sampling technique as applied here is slightly different, due to an update of the tools used. The sampling in the current investigation leads to slightly less extreme water level samples. Comparison with the method from the previous section does not show significant differences in the resulting failure probabilities. Only in case of failure probabilities smaller than about $1 \times 10^{-15}\,\mathrm{year}^{-1}$, the current method tends to result in a zero probability, whereas the old method might result in a finite value smaller than $1 \times 10^{-15}\,\mathrm{year}^{-1}$. To make sure that the slight change in the method does not influence the anticipated failure probability ratios, the current run does include results with and without the wave obliquity and coastal curvature influence.

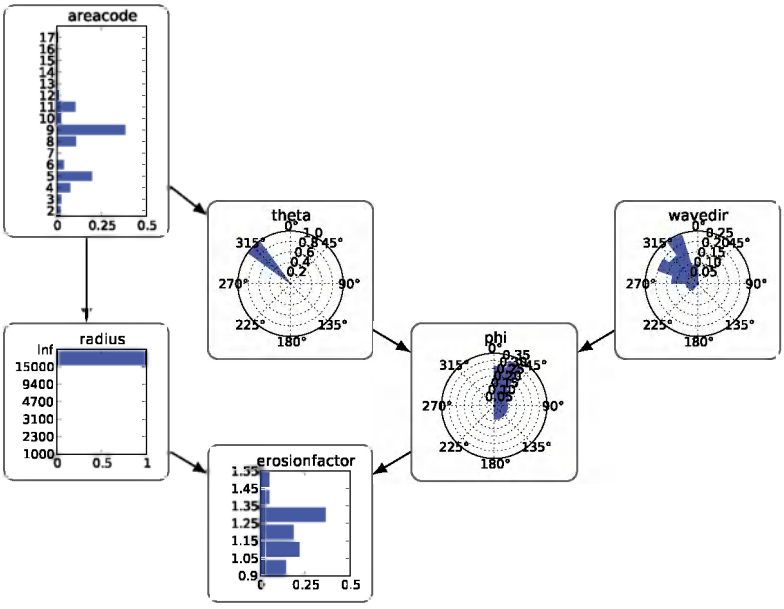

Figure 5.11: Bayesian Network for a transect at the Holland coast.

The ratios are based on these results.

Probability distributions

All probability distributions are kept the same to those described in the previous section, only a distribution for the erosion factor has been added. The erosion factor distribution is based on the local radius and transect orientation as well as the wave direction. Both the radius and the transect orientation are considered as fixed for a particular location at the coast. Therefore, these variables are provided as evidence to the Bayesian Network. The wave direction distribution is assumed to be the same along all considered areas. The distribution is based on two wave measurement stations as described in Section 4.3.2 and shown in Figure 4.16. By sampling the erosion factor with Monte Carlo, the wave direction distribution is sampled implicitly via the Bayesian Network. Figure 5.11 gives an example for the posterior probabilities in the Bayesian Network given a particular transect at the Holland coast. The combination of the transect orientation (theta) and coastal radius, that are provided as evidence to the network, together with wave direction distribution lead to a posterior erosion factor distribution. Given a location, additional evidence could be added to the areacode node, but that would not influence the erosion factor at all since the radius and theta evidence are already provided.

5.2.2 Results

The result of this investigation focusses on the probability of (actual) failure and the ratio of the potential failure probability. The failure probabilities, with inclusion of the effect of wave obliquity and coastline curvature, are generally larger compared to the reference calculations. Figure 5.12 shows the change (factor) in the (potential) failure probability due to wave obliquity and coastline curvature as function of the failure probability without these additional effects. In Figure 5.13 the (potential) failure probabilities including wave obliquity and curvature effects are plotted versus their reference values. The results for the Holland coast and the Wadden area are plotted separately since the areas are typically different. At the Holland coast, where mainly wave obliquity plays a role, the majority of the ratios is smaller than 10 (64%). 93% has a ratio smaller than 100. The even larger ratios mainly correspond to reference failure probabilities that are smaller than 1×10^{-7} year^{-1}. At the Wadden area, the

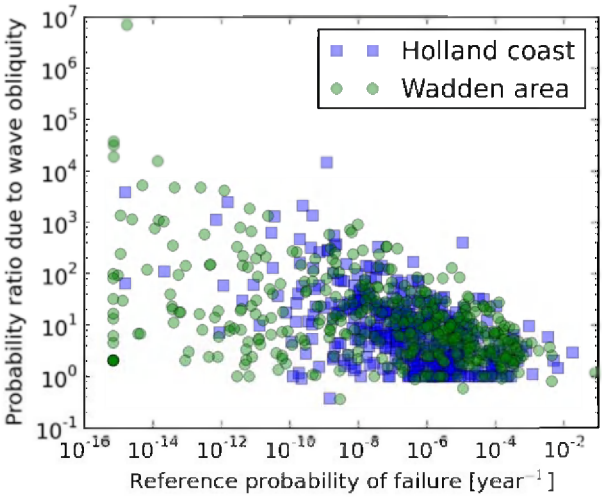

Figure 5.12: Relative failure probability due to wave obliquity and coastal curvature.

ratios are generally larger. 82% of the Wadden transects have a ratio smaller than 100, and 92% smaller than 1000. Also here, the ratios larger than 100 correspond to failure probabilities that are smaller than 1×10^{-7} year^{-1}.

Various groups of change in probability of failure due to the inclusion of wave obliquity and coastline curvature can be distinguished and need to be discussed in more detail. First of all, a part of the failure probabilities that include the wave obliquity and coastline curvature effects, turn out to be equal (ratio=1) in 6 % or even smaller than the reference (ratio<1) in 1 % of the transects. The only way to come to this result is by sampling an erosion factor of about one respectively smaller than one in the Monte Carlo samples that are close to the limit state. Close to the limit state means that a failure event in the reference case can change to non-failure if the minimum erosion factor of 0.9 is applied, or if a non-failure event can be turned into failure when using the maximal erosion factor of 1.55. For samples with relatively mild conditions that for instance erode 20 % of the dune volume above storm surge level, will still not fail if the maximal erosion factor of 1.55 is applied. Similarly, very extreme conditions that virtually erode much more than the volume above storm surge level, will still result in failure if the smallest erosion factor of 0.9 is applied.

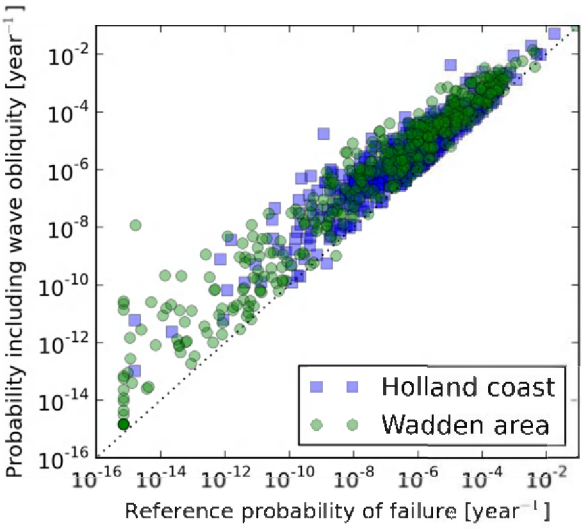

Figure 5.13: Failure probability including effects of wave obliquity and coastal curvature versus reference failure probability.

Half of the transects result in an increase of the probability of failure (>1) with a factor smaller than 10. In this range, mainly the samples that result in non-failure but are close to the limit state are important. Finally, a considerable part of the transects results in failure probabilities that increase with more than a factor 10, up to $\mathcal{O}(1 \times 10^4)$ in a few individual cases. Especially the cases with the larger factors correspond to relatively small probabilities. In these cases, only one or a few samples that lead to failure in the reference case easily changes to a significant number of failures when including wave obliquity and coastal curvature effects.

5.3 Discussion

This chapter describes the estimation of dune failure probability for two different approaches both applied to the major part of the Dutch coast, not including the southern area, hard structures and strongly curved coastal sections. The reference approach does not account for the effects of wave obliquity and coastal curvature. The extended approach, which does account for effects of wave obliquity and coastal curvature, potentially has more spatial coverage. While this chapter is primarily meant as comparison in terms of failure probability and does not focus on the enlarged coverage, a few issues need further discussion.

The 1D cross-shore dune erosion model DUROS+ is applied. Since this model does not account for wave obliquity, the wave boundary conditions are for each transect defined at the local shore normal. Only in case of a normal incident wave direction the waves at this offshore location correspond to the anticipated wave attack at the dune. In case of a spatially (alongshore) varying wave climate, in combination with wave obliquity and/or alongshore non-uniform bathymetry, the waves at the offshore boundary of an arbitrary transect will approach the dune at another alongshore location. To account for this in a proper way, 2DH modelling of extreme waves along the Dutch coast would be required. In this section, this effect is neglected and the related uncertainty is considered acceptable.

The extended approach, including wave obliquity and coastal curvature (Section 5.2), gives a first estimation of these additional phenomena on the dune failure probability. The approach as followed here, uses the existing 1D model as a starting point and adds an extra erosion contribution mainly

related to the alongshore dimension of the processes. Since the extra erosion is based on schematic model simulations, the interaction with other sources of alongshore flow are not taken into account. The horizontal tide is an important source which alternately enhances or dampens the wave generated alongshore current. A better estimation of the dune failure probability could be made if the effects of both wave driven and tide driven alongshore flow are jointly taken into account. Whether the omission of tidal currents leads to an underestimation or overestimation of the failure probabilities basically depends on the combination of the wave/wind direction and the phase of the tide relative to the peak of the surge. More concrete, the question is whether during the period of maximum water level the two sources of alongshore currents need to be added or subtracted. For the Dutch coast, the waves are north north westerly directed during extreme conditions (see Figure 4.16), leading to a southward wave driven current along the Holland coast. The tidal current is directed northward during high tide. Combining these sources, dampens the alongshore current during the period of maximum water level. In conclusion, the failure probabilities regarding wave obliquity as presented in this chapter can be considered as an upper boundary.

Chapter 6

Conclusions and recommendations

6.1 General

The prediction skill of the safety assessment method for dunes, as currently in force in The Netherlands, is limited and the underlying dune erosion model is not valid for the whole dune coast. The main reasons are the omission of the alongshore dimension, the empirical nature of the dune erosion model and the application in the extreme range. The safety of 40 % of the Dutch dune coast cannot be properly assessed. The introduction of the alongshore dimension, crucial for curved coastlines, is a prerequisite for proper safety assessment of the complex dune coasts at the Wadden area and Delta (Zeeland) area. This thesis addresses the role of cross-shore bathymetry, wave obliquity and coastal curvature on dune erosion prediction. Complex dune coasts can potentially be assessed with the improved modelling approach as developed in this thesis. In addition, it is shown that the alongshore dimension is important even for straight coastal stretches with oblique waves, with increased erosion rates of up to about 30 %. However, the application of comprehensive process based dune erosion models requires a tailored probabilistic approach, able to limit the number of simulations and cope with discontinuous limit state functions. As an alternative to the presently applied Monte Carlo and FORM methods, the

Bayesian Network model is introduced. It has advantages in terms of flexibility for extension in a later stage and combination of different data sources.

6.2 Conclusions

Cross-shore bathymetry

Intercomparison of the cross-shore profile influence on dune erosion volumes, simulated with XBEACH in 1D, shows that the upper profile part is much more important than the lower part. The current safety assessment method, which utilizes DUROS+, takes the upper profile part explicitly into account, but the lower part implicitly. Hence, there is no strict need to change the safety assessment model regarding the influence of the cross-shore profile, provided that the offshore part does not influence the forcing significantly.

Wave obliquity

The inclusion of the alongshore dimension is very important for dune erosion modelling in case of oblique incident waves. Simulations with XBEACH in 2DH show that, even in the absence of an alongshore transport gradient, the alongshore current and its interaction with the cross-shore processes are crucial and lead to significantly more dune erosion. The alongshore current leads to additional stirring of sediment, facilitating the cross-shore transport processes. As a result, for an incident wave angle of 40° up to 30 % more erosion is found with respect to the reference situation with shore normal waves.

Coastal curvature

The effect of coastal curvature on dune erosion is not only related to the alongshore transport gradient, but also to the wave obliquity relative to the local shoreline orientation. The alongshore variation in alongshore flow velocity, wave obliquity, wave height and wave set-up as well as their interactions make the dune erosion process much more complex. XBEACH simulations, in 2DH mode, show that the coastal orientation with respect to the (incident) wave angle is of major importance. In the range of investigated coastal radii, between 1900 m and 9500 m, only a marginal dependency on the coastal radius is found

for approximately shore normal waves. Both features are in contradiction with the results of the semi-1D DUROSTA model. At the area along the curved coast where the incident wave angle is 45° w.r.t. the local coastal orientation, XBEACH simulates 30 to 50 % more erosion relative to the reference case with a straight coast and shore normal wave direction.

Probabilistic approach

The introduction of a more advanced and computationally expensive dune erosion model leads to other requirements for the probabilistic approach. The probabilistic methods presently applied require either relatively large numbers of simulations (Monte Carlo) or continuous limit state functions (FORM). These requirements inhibit the comprehensive process-based modelling of complex dune areas as considered in this thesis. The use of a Bayesian Network model provides a flexible way to overcome the limitations of the probabilistic methods and allows model, field and laboratory data to be combined as well as experts' opinions to estimate the dune erosion rate.

Implications for the safety level

In a case study of the major part of the Dutch dune coast the failure probability of the first dune row has been investigated. Failure probabilities have been compared for the reference case, following an approach similar to the current safety assessment method, and the extended case where effects of wave obliquity and coastline curvature have been incorporated. It can be concluded that the inclusion of wave obliquity and coastline curvature effects for the major part of the study area leads to an increase of the failure probability of a factor $\mathcal{O}(10)$.

6.3 Recommendations

The inclusion of the alongshore dimension in dune erosion modelling increases the complexity, especially if alongshore variations are involved. To improve the understanding of the governing mechanisms, this thesis mainly considers simplified cases. This approach is useful to qualitatively understand the mechanisms and to quantitatively estimate the order of magnitude of the

effects. However, for the development of a safety assessment method that includes a proper approach on complex dune areas, further steps have to be taken. The three main components of a probabilistic safety assessment – 1) a hydraulic loading model, 2) a probabilistic method and 3) a dune erosion model – need to fit together. Therefore, the following recommendations focus on these components and the related validation.

Amplification or damping

This thesis solely considers simulations with alongshore uniform bathymetry and excluding ambient flow or vertical tide. Alongshore variation in bathymetry will alter the flow and transport patterns as presented in this thesis. Whether these disturbances are significant and lead to different conclusions for specific configurations needs further investigation. In addition, the combined effect of wave driven alongshore flow and horizontal tide is likely to lead to a sequence of temporary amplification and damping of the alongshore flow. The combined effect is likely to be sensitive to the phase of the tide relative to the storm hydrograph. The sensitivity to this phase and estimation of the resulting most likely erosion rates require further research.

Larger exceedance probabilities

In addition to the ultimate limit state, related to the safety of the hinterland, also the usability limit state for particular coastal functions, like recreation, can be important. This thesis focusses on the extreme conditions, involving water levels that are well above the dune foot. It is recommended to additionally study the coastal response for less extreme conditions. An advantage in this respect is that a relatively short period of measurements easily includes valuable data in this higher frequency regime. The Sand Engine, a mega nourishment at the Holland coast, is considered as a useful case for model validation purposes. The locally strong coastline curvature and the extensive monitoring of the area provide favourable conditions for model validation.

Other configurations

The approach for coastal curvature in this thesis only includes a half circular coastal stretch. The configuration in this model is mainly related to an island

with inlets at both sides. In relation to building with nature initiatives, it is important to know in what way an approximately straight coast with a local (curved) extension, such as the Sand Engine, differs from a curved island head.

Validation of dune erosion model

The models for wave obliquity and coastal curvature effects as described in this thesis give a clear indication of the effects of these phenomena on erosion volumes and patterns. The erosion patterns as found in the results for curved coastlines do qualitatively agree with the circular island experiments of Kamphuis and Nairn (1984). It is recommended to simulate these experiments with XBEACH as a full circular island, using the recently developed possibility to connect the lateral boundaries. In addition, a more detailed inspection of the sediment stirring and transport due to cross-shore and alongshore flow separately is recommended to enhance the insight in the underlying mechanisms and their sensitivity.

Probabilistic approach

This thesis introduces a Bayesian Network model as an alternative to the FORM and Monte Carlo approaches that are applied for the development of the current dune safety assessment method. The Bayesian Network integrates the physical erosion data (laboratory, field and model) with the probabilistic method, where in the FORM and Monte Carlo approaches a clear distinction can be made between dune erosion model and probabilistic method. Hence, a fair comparison in terms of dune erosion volumes (deterministic) and safety levels (probabilistic) is not straightforward. It is recommended to refine the Bayesian Network in order to make a better comparison in terms of dune erosion volumes. In addition, the refined Bayesian Network should also allow to add a comparison in probabilistic terms.

Hydraulic loading

The introduction of the alongshore dimension in dune erosion modelling, does also have consequences for the related boundary conditions. In this thesis, the boundary conditions have been kept relatively simple with no variation in time and space. In the practical application of a 2DH modelling approach for dune

erosion, the required level of detail for the temporal and spatial variation in boundary conditions should be considered.

References

Andrews, D. G. and McIntyre, M. E. (1978). An exact theory of nonlinear waves on a Lagrangian-mean flow. *Journal of Fluid Mechanics*, 89(4):609–646.

Baart, F., Bakker, M., Van Dongeren, A., Den Heijer, C., Van Heteren, S., Smit, M., Van Koningsveld, M., and Pool, A. (2011). Using 18th-century storm-surge data from the Dutch Coast to improve the confidence in flood risk estimates. *Natural Hazards and Earth System Sciences*, 11(10):2791–2801.

Battjes, J. A. and Janssen, J. P. F. M. (1978). Energy loss and set-up due to breaking of random waves. In *16th International Conference on Coastal Engineering*, volume 1, pages 570–587, Hamburg, Germany. ASCE.

Bruun, P. (1962). Sea level rise as a cause of shore erosion. *Journal Waterways and Harbours Division*, 88(1-3):117–130.

Central Intelligence Agency (2008). The World Factbook: Netherlands.

Coastal Engineering Research Center (1984). *Shore Protection Manual*, volume 1. Vicksburg, Miss., U.S.: Dept. of the Army, Waterways Experiment Station, Corps of Engineers, Coastal Engineering Research Center. http://www.biodiversitylibrary.org/bibliography/47829.

Coeveld, E. M. and de Vroeg, J. H. (2004). Model research dune erosion; Measurement report small-scale pilot tests (Modelonderzoek duinafslag; Meetverslag kleinschalige gidsproeven). Technical Report H4265, WL | Delft Hydraulics. In Dutch.

Courage, W. M. G. and Steenbergen, H. M. G. M. (2005). Probox: variables and expressions; Installation and getting started. Technical Report 2005-CI-R0056, TNO Built Environment and Geosciences.

CUR (1997). *Probability in Civil Engineering Part 1: The Theory of Probabilistic Design*. Number 190 in CUR publications. CUR, Gouda, The Netherlands.

de Ronde, J. G., van Marle, J. G. A., Roskam, A. P., and Andorka Gal, J. H. (1995). Wave boundary conditions along the Dutch coast at relatively deep water. Technical Report 95.024, RIKZ. In Dutch.

de Vriend, H. J. (1991). Mathematical modelling and large-scale coastal behaviour. *Journal of Hydraulic Research*, 29(6):727–740.

de Vries, B. B. (2011). Dune erosion near sea walls; XBeach validation. Master's thesis, Delft University of Technology.

Delta Committee (1960). Final report and interim advices of the Delta Committee (Eindrapport en interim adviezen van de Deltacommissie). Technical report, Staatsdrukkerij- en Uitgeverijbedrijf, Den Haag, The Netherlands. In Dutch.

Deltares (2008). Dunes as water defence; Inventarisation of knowledge questions of water boards, provinces and state. (Duinen als Waterkering; Inventarisatie van kennisvragen bij waterschappen, provincies en rijk). Technical Report H5019, Deltares. In Dutch.

Deltares (2010). Development detailed assessment dunes 2011 (D++) (Ontwikkeling detailtoets duinen 2011 (D++)). Interim report SBW-dunes 1202124-003, Deltares. In Dutch.

den Heijer, C. (2005). Effect of wave period on dune erosion. Master's thesis, Delft University of Technology.

den Heijer, C., van de Graaff, J., and van Gelder, P. H. A. J. M. (2008a). Probabilistic sensitivity analysis of dune erosion calculations. In Simonovic, S. P., Bourget, P. G., and Blanchard, S. F., editors, *4th International Symposium on Flood Defence*, Toronto, Ontario, Canada.

den Heijer, C., Reniers, A. J. H. M., van de Graaff, J., and van Gelder, P. H. A. J. M. (2008b). Reducing uncertainty in prediction of dune erosion during extreme conditions. In Smith, J. M., editor, *31th International Conference on Coastal Engineering*, volume 2, pages 1813–1825, Hamburg, Germany. ASCE.

den Heijer, C., Baart, F., and van Koningsveld, M. (2011). Assessment of dune failure along the Dutch coast using a fully probabilistic approach. *Geomorphology*, 143–144:95–103.

den Heijer, C., Knipping, D. T. J. A., Plant, N. G., van Thiel de Vries, J. S. M., Baart, F., and van Gelder, P. H. A. J. M. (2012). Impact assessment of extreme storm events using a bayesian network. In *33rd International Conference on Coastal Engineering*, Santander, Spain.

den Heijer, C. (2012a). Reliability methods in OpenEarthTools. Communications on Hydraulic and Geotechnical Engineering 2012-01, Delft University of Technology.

den Heijer, C. (2012b). Sensitivity of dune erosion prediction during extreme conditions. In Thuy, N. T., editor, *4th International Conference on Estuaries & Coasts*, volume 2, pages 285–291, Hanoi, Vietnam. Water Resources University.

Dillingh, D. and Visser, C. (1984). Calculation model for extra dune erosion due to a gradient in the longshore transport due to a curved coastline. (Rekenmodel voor extra duinafslag ten gevolge van een gradiënt in het langstransport als gevolg van een kromming van de kustlijn). Technical report, Rijkswaterstaat. In Dutch.

ENW (2007). Technical report Dune erosion; Safety assessment of dunes as water defence for the Regulation on Safety Assessment (Technisch Rapport Duinafslag; Beoordeling van de veiligheid van duinen als waterkering ten behoeve van Voorschrift Toetsing op Veiligheid 2006). Technical report, Expertisenetwerk Waterveiligheid. In Dutch.

Falqués, A. (2006). Wave driven alongshore sediment transport and stability of the Dutch coastline. *Coastal Engineering*, 53(2–3):243–254.

Fishman, G. S. (1996). *Monte Carlo: concepts, algorithms, and applications*. Springer, New York. 698 pp.

Galappatti, R. and Vreugdenhil, C. B. (1985). A depth-intregrated model for suspended sediment transport. *Journal of Hydraulic Research*, 23(4):359–377.

Grooteman, F. (2011). An adaptive directional importance sampling method for structural reliability. *Probabilistic Engineering Mechanics*, 26(2):134–141.

Hasofer, A. M. and Lind, N. C. (1974). Exact and invariant second-moment code format. *Journal of the Engineering Mechanics Division, ASCE*, 100(EM1):111–121.

Holthuijsen, L. H., Booij, N., and Herbers, T. H. C. (1989). A prediction model for stationary, short-crested waves in shallow water with ambient currents. *Coastal Engineering*, 13(1):23–54.

Hoonhout, B. M. (2009). Dune erosion along curved coastlines; The influence of coastal curvatures and oblique wave attack on the probability of failure of dunes along the Dutch coast. Master's thesis, Delft University of Technology.

Hoonhout, B. M., van Geer, P. F. C., McCall, R. T., and Boers, M. (2011). Dune erosion and overwash at wide beaches; Part A: applicability DUROS at transects with a wide beach (Duinafslag en -overslag bij brede stranden; Deel A: toepasbaarheid DUROS bij kustprofielen met een breed strand). Technical Report 120124-007, Deltares. In Dutch.

HR2006 (2007). *Hydraulische Randvoorwaarden primaire waterkeringen; voor de derde toetsronde 2006-2011 (HR 2006) (Hydraulic Boundary conditions for primary water defences; for the third evaluation 2006-2011 (HR2006))*. Ministerie van Verkeer en Waterstaat. In Dutch.

Kamphuis, J. W. and Nairn, R. B. (1984). Scale effects in large coastal mobile bed models. In *19th International Conference on Coastal Engineering*, number 19, pages 2322–2338.

Knipping, D. T. J. A. (2012). Impact Assessment of Extreme Storm Events Using a Bayesian Network. Master's thesis, Delft University of Technology.

Korb, K. B. and Nicholson, A. E. (2004). *Bayesian artificial intelligence*, volume 1. Chapman & Hall/CRC.

Min V&W (1989). Technical report 0; overview technical underpinning discussion document coastal defense (technisch rapport 0; overzicht technische onderbouwing discussienota kustverdediging). Technical report, Ministry of Transport and Public Works, Rijkswaterstaat. In Dutch.

Ministeries VROM, LNV, V & W, and EZ (2006). Note space: space for development (Nota ruimte: ruimte voor ontwikkeling). Technical report, Ministeries VROM, LNV, V & W and EZ. In Dutch.

Palmsten, M. L. and Holman, R. A. (2012). Laboratory investigation of dune erosion using stereo video. *Coastal Engineering*, 60:123–135.

Plant, N. G. and Stockdon, H. F. (2012). Probabilistic prediction of barrier-island response to hurricanes. *Journal of Geophysical Research*.

Reniers, A. J. H. M., Roelvink, J. A., and Thornton, E. B. (2002). Morphodynamic modeling of an embayed beach under wave group forcing. *Journal of Geophysical Research*, 109.

Rijkswaterstaat and KNMI (1961). Report on the 1953 storm surge (Verslag van de stormvloed van 1953). Technical report, Rijkswaterstaat and Koninklijk Nederlands Meteorologisch Instituut.

Rijkswaterstaat (2008). The yearly coastal measurements (De JAaRlijkse KUStmetingen (JARKUS)). In Dutch.

Roelvink, D., Reniers, A., van Dongeren, A., van Thiel de Vries, J., McCall, R., and Lescinski, J. (2009). Modelling storm impacts on beaches, dunes and barrier islands. *Coastal Engineering*, 56(11-12):1133–1152.

Roelvink, J. A. (1993). *Surf beat and its effect on cross-shore profiles*. PhD thesis, Delft University of Technology.

Roskam, A. P. and Hoekema, J. (1996). Boundary conditions for wave periods along the Dutch coast (Randvoorwaarden voor golfperioden langs de Nederlandse kust). Technical Report 96.019, RIKZ. In Dutch.

Ross, S. M. (1987). *Introduction to probability and statistics for engineers and scientists*. Elsevier, third edition edition.

Ruessink, B. G. and Jeuken, M. C. J. L. (2002). Dunefoot dynamics along the Dutch coast. *Earth Surface Processes and Landforms*, 27(10):1043–1056.

Sallenger, A. H. (2000). Storm Impact Scale for Barrier Islands. *Journal of Coastal Research*, 16(3):890–895.

Soulsby, R. L. (1997). *Dynamics of Marine Sands*. Thomas Telford, London.

Starr, C. (1969). Social benefit versus technological risk. *Science*, 165(3899):1232–1238.

Steetzel, H. J. (1993). *Cross-shore Transport during Storm Surges*. PhD thesis, Delft University of Technology, Delft, The Netherlands. Also published as: Delft Hydraulics communication, no. 476.

Stijnen, J. W., Duits, M. T., and Thonus, B. I. (2005). Deep water boundary conditions (ELD, EUR, YM6, SCW and SON). (Diepwater randvoorwaarden (ELD, EUR, YM6, SCW en SON)). Technical Report Pr841.40, HKV consultants, Lelystad, The Netherlands. In Dutch.

TAW (1984). Guide on the assessment of dune safety as water defence (Leidraad voor de beoordeling van de veiligheid van duinen als waterkering). Technical report, Technical Advisory Committee on Water Defences, 's-Gravenhage, The Netherlands. In Dutch.

van Baaren, P. F. J. (2007). Influence of the wave period in the dune erosion model DUROSTA. Master's thesis, Delft University of Technology.

van Dantzig, D. (1956). Economic decision problems for flood prevention. *Econometrica*, 24(3):276–287.

van de Graaff, J. (1986). Probabilistic design of dunes; an example from The Netherlands. *Coastal Engineering*, 9(5):479–500.

van der Weele, P. I. (1971). The history of NAP (De geschiedenis van het NAP). Technical report, The Netherlands Geodetic Commission. in Dutch.

van Dongeren, A., Bolle, A., Roelvink, J., Vousdoukas, M. I., Plomaritis, T., Williams, J., Armaroli, C., Idier, D., van Geer, P., van Thiel de Vries, J., et al. (2009). MICORE: Dune erosion and overwash model validation with data from nine European field sites (invited). In *AGU Fall Meeting Abstracts*, volume 1, page 6.

van Gelder, P. H. A. J. M. (2000). *Statistical methods for the risk-based design of civil structures*. PhD thesis, Delft University of Technology, Delft, The Netherlands.

van Gent, M. R. A., van Thiel de Vries, J. S. M., Coeveld, E. M., de Vroeg, J. H., and van de Graaff, J. (2008). Large-scale dune erosion tests to study the influence of wave periods. *Coastal Engineering*, 55(12):1041–1051.

van Koningsveld, M., de Boer, G. J., Baart, F., Damsma, T., den Heijer, C., van Geer, P., and de Sonneville, B. (2010). OpenEarth - Inter-Company Management of: Data, Models, Tools & Knowledge. In *Proceedings WODCON XIX Conference*, Beijing, China.

van Rijn, L. C. (2007). Unified View of Sediment Transport by Currents and Waves II: Suspended Transport. *Journal of Hydraulic Engineering*, 133(6):668–689.

van Santen, R. B., Steetzel, H. J., van Thiel de Vries, J. S. M., and van Dongeren, A. R. (2012). Modelling storm impact on complex coastlines: West-Kapelle, The Netherlands. In *33rd International Conference on Coastal Engineering*.

van Thiel de Vries, J. S. M., van de Graaff, J., Raubenheimer, B., Reniers, A. J. H. M., and Stive, M. J. F. (2006). Modeling inner surf hydrodynamics during storm surges. In Smith, J. M., editor, *30th International Conference on Coastal Engineering*, volume 1, pages 896–908, San Diego, California, USA. ASCE.

van Thiel de Vries, J. S. M., van Gent, M. R. A., Walstra, D. J. R., and Reniers, A. J. H. M. (2008). Analysis of dune erosion processes in large-scale flume experiments. *Coastal Engineering*, 55(12):1028–1040.

van Thiel de Vries, J. S. M. (2009). *Dune erosion during storm surges*. PhD thesis, Delft University of Technology, Delft, The Netherlands.

Vellinga, P. (1984). Beach and Dune Erosion during Storm Surges - Reply. *Coastal Engineering*, 8(2):191–192.

Vellinga, P. (1986). *Beach and Dune Erosion during Storm Surges*. PhD thesis, Delft University of Technology, Delft, The Netherlands. Also published as: Delft Hydraulics communications, no. 372, 1986.

Vrijling, J. K. (2001). Probabilistic design of water defense systems in The Netherlands. *Reliability Engineering & System Safety*, 74(3):337–344.

VTV2006 (2007). Guidelines for safety assessment of primary water defences. Technical report, Ministry of Transport, Public Works and Water Management. In Dutch.

Walstra, D. J. R., Roelvink, J. A., and Groeneweg, J. (2000). Calculation of wave-driven currents in a 3D mean flow model. In Edge, B. L., editor, *27th International Conference on Coastal Engineering*, volume 2, pages 1050–1063, Sydney, Australia. ASCE.

WL | Delft Hydraulics (1981). Investigation of dune erosion during extreme storm surges; evaluation of the results of the two-dimensional model investigation by means of experiments in a three-dimensional model (onderzoek naar duinafslag tijdens superstormvloed; toetsing van de resultaten van het twee-dimensionale modelonderzoek door middel van onderzoek in een drie-dimensionaal model). Report model study M1653, WL | Delft Hydraulics. In Dutch.

WL | Delft Hydraulics (1982). Rekenmodel voor de verwachting van duinafslag tijdens stormvloed (Calculation model for the predition of dune erosion during storm surge). Technical Report M 1263 part IV, WL | Delft Hydraulics. In Dutch.

WL | Delft Hydraulics (1983). Valsnelheid van zand in zeewater van 5 °C (Settling velocity of sand in sea water of 5 °C). Technical Report M 1263 part IV-b, WL | Delft Hydraulics. In Dutch.

WL | Delft Hydraulics (2007). Dune erosion; Product 3: Probabilistic dune erosion prediction method. Technical Report H4357 / A1414, Alkyon Hydraulic Consultancy & Research / WL | Delft Hydraulics / Delft University of Technology.

Working Group 10; Delta Committee (1953-1954). Reports and drawings concerning model investigations at Delft Hydraulics laboratory (Rapporten, verslagen en tekeningen betreffende modelonderzoekingen in het Waterloopkundig Laboratorium te Delft). Technical report, Delta Committee, "Program committee Delft". In Dutch.

Zweig, G. and Russell, S. (1998). Probabilistic Modeling with Bayesian Networks for Automatic Speech Recognition. In Mannell, R. H. and Robert-Ribes, J., editors, *International Conference on Spoken Language Processing*, volume 7, page 3011, Sydney, Australia. Australian Speech Science and Technology Association, Incorporated (ASSTA).

Appendix A

XBEACH model settings

The XBEACH simulations as presented in Chapter 3 were carried out with a Linux build of the version of April 2012 (revision 2898[1]). Below, a sample is included of the model configuration (`params.txt` and `jonswap.txt`) as used for the curved coastline simulations Section 3.4. The configurations for the other simulations, concerning cross-shore bathymetry influence and wave obliquity, are nearly the same.

```
params.txt
----------
%%% Bed composition parameters %%%%%%%%%%%%%%%%%%%
D50           = 0.000225
D90           = 0.000338
%%% Flow boundary condition parameters %%%%%%%%%%%%
epsi          = -1
%%% General %%%%%%%%%%%%%%%%%%%%%%%%%%%%%%%%%%%%%
gridform      = delft3d
nc            = 20
rotate        = 0
xyfile        = xy.grd
%%% Grid parameters %%%%%%%%%%%%%%%%%%%%%%%%%%%%%
depfile       = bed.dep
posdwn        = -1
```

[1] https://svn.oss.deltares.nl/repos/xbeach/tags/2012-04-06-XBeach-V19-easter/src/xbeachlibrary

```
alfa         = 0
xori         = -4830.000000
yori         = -4830.000000
thetamin     = 182.500000
thetamax     = 357.500000
dtheta       = 5
thetanaut    = 1
%%% Initial conditions %%%%%%%%%%%%%%%%%%%%%%%%%%
zs0          = 5
%%% Model time %%%%%%%%%%%%%%%%%%%%%%%%%%%%%%%%%
tstop        = 20000
%%% Morphology parameters %%%%%%%%%%%%%%%%%%%%%%%
morfac       = 5
morstart     = 2000
%%% Physical constants %%%%%%%%%%%%%%%%%%%%%%%%%%
depthscale   = 0.166667
%%% Sediment transport parameters %%%%%%%%%%%%%%%%
Tsmin        = 3
%%% Wave boundary condition parameters %%%%%%%%%%%
instat       = jons
%%% Wave-spectrum boundary condition parameters %%%
bcfile       = jonswap.txt
random       = 0
rt           = 7200
dtbc         = 2
%%% Output variables %%%%%%%%%%%%%%%%%%%%%%%%%%%%
outputformat = netcdf
tintm        = 1000
tintg        = 200
tstart       = 2000
```

```
jonswap.txt
-----------
Hm0        =     9.0000
fp         =     0.0833
mainang    =   270.0000
gammajsp   =     3.3000
s          =    20.0000
fnyq       =     0.3333
```

Acronyms

dag	directed acyclic graph
FORM	First Order Reliability Method
MC	Monte Carlo
JARKUS	yearly Dutch coastal bathymetry survey *"JAaRlijkse KUStmeting"*
NAP	Amsterdam Ordnance Datum *"Normaal Amsterdams Peil"* approximately equal to mean sea level; see Van der Weele (1971) for detailed information
morfac	morphological acceleration factor
SSL	storm surge level
MSL	mean sea level

List of Figures

List of Tables

Acknowledgements

The Dutch Technology Foundation STW and Rijkswaterstaat Waterdienst are gratefully acknowledged for their financial support for this research. The members of the users committee, as established by STW, are acknowledged for the time they spent and the input they provided as a contribution to this research.

At the end of my period as PhD candidate, time has come to reflect on the past years and acknowledge the people that enabled me to carry out the research and write this thesis.

First of all, I would like to sincerely thank my promotors, Marcel Stive and Ad Reniers. Marcel, thanks to you, I got the opportunity to spend my spare time in 2007 on writing my research proposal. Moreover, even before the proposal was accepted, you took the risk and employed me in 2008 based on your vision that in the end there will be ample funding. You gave me the freedom to find my way in the research and always encouraged and supported me unconditionally.
Ad, your contributions to my research proposal were of great value and have most probably largely contributed to the favourable result of being funded. After you left to Miami, you were literally and figuratively far away from my research. Still, during your visits to Delft, we had fruitful discussions and you always asked the right questions. Last but not least, I appreciate your thorough review of the manuscript.

Next I would like to thank my copromotor, Pieter van Gelder and the other committee members. Pieter, your door was always open for a chat, but especially for technical questions on probabilistics, statistics and mathematics. I highly appreciate your involvement, guidance and support to my research.

It is my pleaure to have prof.dr.ir. A.W. Heemink, prof.dr.ir. J.A. Roelvink, prof.dr. P. Hoekstra, dr.ir. J.S.M. van Thiel de Vries and prof.dr.ir. M. Kok in my committee and I appreciate their review and feedback on the manuscript.

My position as PhD candidate allowed me to work with a number of MSc students and guide them in doing their research and writing their theses. Bas and Dirk, I enjoyed working with you and I appreciate your contributions to my thesis. It was my pleasure to also be involved in the supervision of William, Johannes, Patrick, Michiel and Matthijs, albeit that your topics were beyond the scope of my thesis.

During my PhD research I got the opportunity to be part-time employed at Deltares to primarily work on projects that were closely related to my research. This position did not only stimulate me to pay attention to the professional world beyond my research, but also provided me with a large number of additional colleagues, experienced in my field or in adjacent fields. Some of them implicitly or explicitly took part in the guidance and support of my research. I would like to thank Mark van Koningsveld for recruiting me at Deltares, in hindsight just before he left. It was always a pleasure to spend the Tuesdays at Deltares thanks to the nice people I have shared the room with: Ankie, Bert, Carola, Laura, Jamie, Christophe and Jebbe. I appreciate the freedom I got from the (sub)project leaders – Marien, Ferdinand, Dirk-Jan and Ap – in the SBW project to contribute to those subjects that best fitted my own research. I would like to thank Marcel van Gent for his support and constructive feedback from his position in my users committee. Without providing a long but never complete list of names, I would like to thank all my colleagues that together make our institute a nice working environment.

Since my MSc graduation, Delft University has felt like a professional home base to me, being a suitable environment to perform my research. First of all, I have to thank the people I shared the room with: Hoan, Lam, Mark, Poonam, Fedor, Jaap, Arjen, Dongju and Quirijn. Thanks to you, room 3.81 will never be what is used to be. Hoan, I still look back to the years we shared the office, with great pleasure. I learned a lot about Vietnam and Vietnamese-style jokes. You kept on pursuing me to switch to LaTeX; at that time, you didn't manage to convince me, but the layout of this thesis should make you happy. It was an honour for me to have you and Viet as private tour guides for a day, during my visit to Hanoi, last year. Also thanks to you, we had a lot of fun with a number of Vietnamese fellow PhD students – Viet, Tung and Lam – as well as our Japanese friend dr. Tomo, among others during our international

diners. Thanks to you all for the fun we had. Fedor, thanks for the nice time we spent together in our office. You always took the time for a chat or to educate me in computer related topics, or I have to say in virtually anything. Jaap, I still remember that I showed you the Scheldt Flume when I was involved as a student in the dune erosion experiments, at the time that you just started your PhD research. Later on, we became colleagues and you moved to our room to enhance the scientific activity as well as the fun in there. Thanks a lot for your support, encouragement and valuable feedback on the manuscript; I am happy that you participate in my committee. Poonam, thanks for your contribution to the pleasant working environment in our room. Quirijn, I appreciate your cooperative attitude from your position in my users committee and the effort you have put in the proper dissemination of the main message from my thesis.

I have to thank Howard for the nice discussions we had on various topics, over the past years, and for reviewing some parts of my thesis. Dirk-Jan, thanks for accompanying me to the coffee machine so many times on Thursdays and Fridays, for always being available for questions and discussion, among others on the structure of my thesis, and for always encouraging me. Many thanks go to the supporting staff of the Hydraulic Engineering Section: Chantal, Mark, Inge, Judith, and Agnes. Also I would like to thank all my TU Delft colleagues for their role in providing a wonderful working environment, without providing a long but never complete list of names.

Finally, I would like to thank my family and friends for their support and interest in my research. Most special thanks go to Jozine, who unconditionally supported me.

Kees den Heijer

March, 2013

Curriculum Vitae

Cornelis (Kees) den Heijer was born on 23rd December, 1979 in The Hague and grew up in Wassenaar. He graduated in 1998 from secondary school (VWO), Driestar College in Gouda. In 1998, he started studying Civil Engineering at Delft University of Technology. Since 2003, his interest for the topic of this thesis has developed, when he was involved, as a trainee, in dune erosion experiments that were performed at WL | Delft Hydraulics (later on merged into Deltares). Early 2005, he received the MSc degree after finalising his thesis entitled "Effect of wave period on dune erosion". Since late 2004, even before he graduated, he was employed at Delft University of Technology (Civil Engineering Faculty, department of Hydraulic Engineering) to work on the European NEW! Delta project. The project involved competing port authorities and related institutions to work closely together on both scientific and practical problems related to port developments in a vulnerable environment. Towards the end of the project, in 2007, Kees started to write a research proposal for his PhD research. In January 2008, he started to carry out the proposed research, which was later that year funded by Dutch Technology Foundation STW and finally resulted in this thesis. From March 2008 through 2012, he was part-time (0.2 FTE) employed at the research institute Deltares as a researcher/advisor, in addition to his PhD candidate position. Since January 2013, he is working 0.8 FTE at Deltares and is also affiliated to TU Delft.

This page intentionally left blank

Deltares Select Series
Volume 12
ISSN 1877-5608 (print)
ISSN 1879-8055 (online)

Deltares is an independent Dutch research institute for water, subsurface and infrastructure issues. Its mission is to develop and apply top-level expertise on these issues for people, planet and prosperity. Worldwide, around 900 staff are working to find innovative solutions that make living in the world's deltas, coastal areas and river basins safe, clean and sustainable. Since 2009 Deltares has been publishing the Deltares Select Series. Alongside peer reviewed proceedings of symposia organized by Deltares, this series publishes dissertations, edited volumes and monographs by Deltares employees. The editor-in-chief of the series is Dr. Jaap Kwadijk, Chief Scientist of Deltares. For more information, see www.deltares.nl.

Previously published in this series:
Volume 11. C. Harteveld, Making Sense of Virtual Risks – A Quasi-Experimental Investigation into Game-Based Training
Volume 10. G. Hoffmans, The influence of Turbulence on Soil Erosion
Volume 9. A. te Linde, Rhine at Risk? Impact of Climate Change on Low-Probability Floods in the Rhine Basin and the Effectiveness of Flood Management Measures
Volume 8. I. Pothof, Co-current Air-Water Flow in Downward Sloping Pipes
Volume 7. M.A. Van, E.J. den Haan & J.K. van Deen (Eds.), A Feeling for Soil and Water, a Tribute to Prof. Frans Barends
Volume 6. C. Schipper, Assessment of Effects of Chemical Contaminants in Dredged Material on Marine Ecosystems and Human Health
Volume 5. M. Marchand, Modelling Coastal Vulnerability – Design and Evaluation of a Vulnerability Model for Tropical Storms and Floods
Volume 4. S.A.M. Karstens, Bridging boundaries. Making Choices in Multi-actor Policy Analysis on Water Management
Volume 3. J.S.M. van Thiel de Vries, Dune Erosion During Storm Surges
Volume 2. P.M.S. Monteiro & M. Marchand (Eds.), Catchment2Coast, a Systems Approach to Coupled River-Coastal Ecosystem Science and Management
Volume 1. F.J. Los, Eco-Hydrodynamic Modelling of Primary Production in Coastal Waters and Lakes Using BLOOM

This page intentionally left blank